NASA/TP-2006-214295

RFID Transponders' Radio Frequency Emissions in Aircraft Communication and Navigation Radio Bands

Truong X. Nguyen, Jay J. Ely, Reuben A. Williams, and Sandra V. Koppen
Langley Research Center, Hampton, Virginia

Maria Theresa P. Salud
Lockheed Martin, Hampton, Virginia

March 2006

The NASA STI Program Office . . . in Profile

Since its founding, NASA has been dedicated to the advancement of aeronautics and space science. The NASA Scientific and Technical Information (STI) Program Office plays a key part in helping NASA maintain this important role.

The NASA STI Program Office is operated by Langley Research Center, the lead center for NASA's scientific and technical information. The NASA STI Program Office provides access to the NASA STI Database, the largest collection of aeronautical and space science STI in the world. The Program Office is also NASA's institutional mechanism for disseminating the results of its research and development activities. These results are published by NASA in the NASA STI Report Series, which includes the following report types:

- TECHNICAL PUBLICATION. Reports of completed research or a major significant phase of research that present the results of NASA programs and include extensive data or theoretical analysis. Includes compilations of significant scientific and technical data and information deemed to be of continuing reference value. NASA counterpart of peer-reviewed formal professional papers, but having less stringent limitations on manuscript length and extent of graphic presentations.

- TECHNICAL MEMORANDUM. Scientific and technical findings that are preliminary or of specialized interest, e.g., quick release reports, working papers, and bibliographies that contain minimal annotation. Does not contain extensive analysis.

- CONTRACTOR REPORT. Scientific and technical findings by NASA-sponsored contractors and grantees.

- CONFERENCE PUBLICATION. Collected papers from scientific and technical conferences, symposia, seminars, or other meetings sponsored or co-sponsored by NASA.

- SPECIAL PUBLICATION. Scientific, technical, or historical information from NASA programs, projects, and missions, often concerned with subjects having substantial public interest.

- TECHNICAL TRANSLATION. English-language translations of foreign scientific and technical material pertinent to NASA's mission.

Specialized services that complement the STI Program Office's diverse offerings include creating custom thesauri, building customized databases, organizing and publishing research results ... even providing videos.

For more information about the NASA STI Program Office, see the following:

- Access the NASA STI Program Home Page at ***http://www.sti.nasa.gov***

- E-mail your question via the Internet to help@sti.nasa.gov

- Fax your question to the NASA STI Help Desk at (301) 621-0134

- Phone the NASA STI Help Desk at (301) 621-0390

- Write to:
  NASA STI Help Desk
  NASA Center for AeroSpace Information
  7121 Standard Drive
  Hanover, MD 21076-1320

NASA/TP-2006-214295

RFID Transponders' Radio Frequency Emissions in Aircraft Communication and Navigation Radio Bands

Truong X. Nguyen, Jay J. Ely, Reuben A. Williams, and Sandra V. Koppen
Langley Research Center, Hampton, Virginia

Maria Theresa P. Salud
Lockheed Martin, Hampton, Virginia

National Aeronautics and
Space Administration

Langley Research Center
Hampton, Virginia 23681-2199

March 2006

Acknowledgements

This work was funded by the Federal Aviation Administration as part of FAA/NASA Interagency Agreement DFTA03-96-X-90001, Revision 9, as well as the NASA Aviation Safety Program (Single Aircraft Accident Prevention Project).

Aircraft electromagnetic coupling (path loss) data were obtained under NASA Grants NCC3-1043 and NCC3-1078 with United Airlines and Eagle Wings Inc.

Available from:

NASA Center for AeroSpace Information (CASI)
7121 Standard Drive
Hanover, MD 21076-1320
(301) 621-0390

National Technical Information Service (NTIS)
5285 Port Royal Road
Springfield, VA 22161-2171
(703) 605-6000

Table of Contents

List of Tables

List of Figures

Acronyms

A320	Airbus A320 Aircraft
AM	Amplitude Modulation
ANSI	The American National Standards Institute
ASK	Amplitude Shift Keying (modulation)
ATCRBS	Air Traffic Control Radar Beacon System
Atten	Attenuation level
Auto-ID	Automatic identification
B747	Boeing 747 Aircraft
BPSK	Binary phase-shift keying
CW	Continuous-wave
dB	Decibel
dBi	Decibel relative to isotropic reference pattern
dBm	Decibel relative to one milliwatt power
dBμV/m	Field strength unit in dB relative to one μV/m
DME	Distance Measuring Equipment
DSSS	Direct Sequence Spread Spectrum
DUT	Device-Under-Test
EC	European Commission
EIRP	Effective Isotropic Radiated Power
ERP	Effective Radiated Power
EWI	Eagle Wings Inc.
FAA	Federal Aviation Administration
FCC	Federal Communications Commission
FSK	Frequency Shift Keying (modulation)
GHz	Gigahertz
GPS	Global Positioning System
GS	Glideslope
IPL	Interference Path Loss
LAN	Local Area Network
LaRC	Langley Research Center
LOC	Localizer
Max	Maximum
meas.	measured
MEF	Multiple Equipment Factor
MHz	Megahertz

Min	Minimum
MLS	Microwave Landing Systems
msec	milliseconds
mW	milliwatt
NA	North America
NASA	National Aeronautics and Space Administration
OOK	On/Off Key modulation
PDA	Personal Digital Assistant
PED(s)	Portable Electronic Device(s)
RBW	Resolution Bandwidth
Recv	Receive
RF	Radio Frequency
RFID	Radio Frequency Identification
RL	Reference Level
RTCA	RTCA, Inc.
RTLS	Real Time Locating Systems
secs	seconds
SwpTime	Sweep Time
TCAS	Traffic Collision Avoidance System
TRP	Total Radiated Power
UAL	United Airlines
UWB	Ultra-wideband
VHF	Very High Frequency
VHF-1,2,3	VHF-Com radio no. 1, 2, 3
VHF-Com	Very High Frequency Voice Communication
VOR	VHF Omnidirectional Range
Xmit	Transmit

List of Symbols

π	Universal constant = 3.141592654
η_{Tx}	Transmit antenna efficiency factor
A	Device emission power
B	Interference coupling factor, negative of interference path loss in dB
C	Receiver susceptibility threshold
CF	Chamber Calibration Factor (dB)
CLF	Chamber Loading Factor
D_G	Directivity
E	Electric Field Intensity (V/m)
$EIRP$	Effective Isotropic Radiated Power (W)
IL	Empty chamber Insertion Loss
$L_{Chmbr(dB)}$	Chamber loss (dB), or = $-10log_{10}(CLF * IL)$
$L_{RecCable(dB)}$	Receive cable loss (dB)
$L_{XmitCable(dB)}$	Transmit cable loss (dB)
P_{input}	Input power
P_{MaxRec}	Maximum received power measured over one paddle rotation
$P^R(2), P^R(3)$	Power received at points (2) and (3), respectively, in dBm
$P_{SAMeas(dBm)}$	Maximum receive power measured at the spectrum analyzer (dBm) over one stirrer revolution
$P^T(1),$	Power transmitted at point (1), in dBm
P_{TotRad}	Total radiated power within measurement resolution bandwidth
$P_{Xmit(dBm)}$	Power transmitted from source (dBm)
R	Distance (m)
Rx	Receive
TRP	Total Radiated Power (within measurement resolution bandwidth)

Abstract

Radiated emissions in aircraft communication and navigation bands are measured from several active radio frequency identification (RFID) tags. The individual tags are different in design and operations. They may also operate in different frequency bands. The process for measuring the emissions is discussed, and includes tag interrogation, reverberation chamber testing, and instrument settings selection. The measurement results are described and compared against aircraft emission limits. In addition, interference path loss for the cargo bays of passenger aircraft is measured. Cargo bay path loss is more appropriate for RFID tags than passenger cabin path loss. The path loss data are reported for several aircraft radio systems on a Boeing 747 and an Airbus A320 aircraft.

1 Executive Summary

Radio frequency identification (RFID) usage experienced an explosive growth in recent years. The Department of Defense's (DoD's) and major retailers' mandated use in many automatic identification and tracking applications jumpstarted the public interest and awareness of the technology's potential. Initial applications include area monitoring, spot-level locating, cargo security, data storage and logging among many others.

RFID generally can be categorized into passive and active transponders, or tags. Passive tags utilize the power received from the interrogator to power the tags for data transmission. These tags can be produced at very low cost. However, their range is limited due to their low power reflected back from the tags.

Active tags, on the other hand, are powered with internal batteries. As a result, range is better than tags in most cases. However, an active tag cannot function and respond to an interrogation without the batteries as a passive device could.

Passive tags are considered less of an interference concern for aircraft since they do not transmit a response without an interrogator, whose electromagnetic fields power the tags. Active tags can be of higher interference risk since many can operate and transmit on their own without an interrogator. The actual interference risks depend on several factors, including the tags' intentional and unintentional emission level, the propagation path loss factor, and the victim system's susceptibility threshold to the emissions type.

With the support of the Federal Aviation Administration (FAA) Aircraft Safety Organization and the National Aeronautics and Space Administration (NASA) - Aviation Safety Program (AvSP) - Single Aircraft Accident Prevention (SAAP) Project, this report documents the emission measurements of active tags and their interference potential on aircraft sensitive radio receivers. In specific, this work measures the unintentional emissions from several popular RFID tags used for cargo tracking. Personnel tags are not included in this report. In addition, passenger aircraft cargo bay path losses are also measured for several radio systems on a Boeing 747 and an Airbus A320 aircraft. These path losses represent the attenuation between the tags in the aircraft front or aft cargo bay compartments, and the victim receiver's antenna port. The following sections describe the effort to measure the RFID tags emissions and the cargo bay path loss of passenger aircraft.

Aircraft receiver's interference thresholds are not addressed in this report. This element is being addressed by a special committee SC-202 of the RTCA Inc. specifically dealing with electromagnetic compatibility of transmitting portable electronic devices on aircraft [1]. The preliminary data on the subject from the committee's effort can be found in [2]. Furthermore, an extension to the committee effort is being considered to address the effects of "bursty" signals, such as RFID signals, on receiver interference thresholds. This extension work is currently in progress. In this report, "bursty" refers to data transmitted in short, uneven spurts, as opposed to steady-stream data.

RFID Active Tag Emissions Measurement

Spurious emissions from the tags were measured in five measurement bands, covering many important aircraft radio bands. Aircraft radio bands near one another are grouped together into a measurement band to simplify testing. The aircraft bands include Localizer (LOC), Glideslope (GS), Very-High-Frequency Omnidirectional Range (VOR), Very-High-Frequency (VHF) Voice Communication (VHF-Com), Global Positioning Systems (GPS), Traffic Collision Avoidance System (TCAS), Air Traffic Control Radar Beacon System (ATCRBS), Distance Measuring Equipment (DME), Microwave Landing Systems (MLS), and others.

The tags considered are from several major active tags vendors specializing in cargo tracking technology. The vendors include Savi Technology, Identec Solutions, Sovereign Tracking Systems LLC, WhereNet and RF Code. The individual tag's relevant operational characteristics and test modes are discussed. The laboratory measurement techniques are described. Details concerning filter selections for equipment overload prevention, fundamental and harmonic emissions rejection, and measurement trade-offs are specified.

The measurements were performed in two reverberation chambers. The larger chamber was used for the 100 to 350 Megahertz (MHz) range, and the smaller chamber covered 960 MHz – 5100 MHz range. The smaller chamber has lower chamber loss and results in more sensitive measurements. However, operation is limited to approximately 300 MHz and above due to its intrinsic reverberation chamber characteristics.

The measurement data show that the emissions from one tag can be as high as -17.2 dBm. Based on past studies [3], this level could be of great interference concern if the transmitter is located in the passenger cabin and the transmission is continuous. The tag emission results were also compared against RTCA/DO160 aircraft emission limits, and in many cases, the tags' peak emissions far exceeded them. However, the interference effects of bursty RFID transmissions on aircraft radio receivers are not known and merit additional investigations.

The results also indicated that there are significant variations in tags' emissions, even for those of the same design. Simultaneous measurement of multiple tags can increase the likelihood of capturing the bounds of the transmissions, while having significant speed advantage over testing multiple individual tags. In this case, multiple-equipment-factor (MEF) is not expected to be a major concern due to the low likelihood of simultaneous transmissions of two or more tags. Furthermore, the MEF for two tags is only 3 dB at the worst case. This measurement uncertainty is far out weighted by the importance of capturing the bound of all emissions.

Aircraft Cargo Bay Path Loss Measurement

Interference path loss (IPL) measurements were conducted in cargo-bays on Boeing 747 and Airbus A320 aircraft. A transmit antenna was placed in the cargo bay to simulate emitting sources and propagation losses were measured for multiple aircraft radio systems. The radio systems include LOC, VHF-Com, GS, DME, ATCRBS and GPS. Many of these systems include multiple antennas at the top and bottom of the aircraft fuselage. On both aircraft, the forward and aft-cargo bays were measured. This work was part of a larger collaborative effort between United Airlines (UAL), Eagle Wings Inc. (EWI), NASA and FAA personnel to address multiple topics related to Portable Electronic Devices (PEDs) and aircraft interference.

The process and the equipment used were similar to those in the past studies [3]. A tracking spectrum analyzer was used, which has a built-in radio frequency (RF) generator that can perform synchronized frequency sweeps. In previous measurements in the passenger cabin, the transmit antenna was positioned to radiate toward each of the cabin windows. In this measurement, the cargo bay doors were scanned. In addition, the cargo bays were scanned volumetrically, with the transmit antenna physically moved continuously until the entire cargo bay volume and all polarizations were included. The spectrum analyzer recorded the peak coupling into the radio systems via outside antennas and cables.

Only the peak coupling measurements (or the minimum IPLs) are reported. The data were normalized as if a dipole antenna was used as the transmit antenna. The results show that many aircraft antennas couple strongly with the cargo bay due to their close proximity.

Interference analysis is not performed due to lack of interference threshold data for bursty signals. Interference threshold analysis for bursty signals is being conducted independent of this effort.

(This page was intentionally left blank)

2 Introduction

In the recent years, the use of RFID has grown exponentially in many industries such as service, distribution logistics, manufacturing and countless other applications. RFID is an automatic identification (Auto-ID) technology that provides information about and allows tracking of cargo, people, animal and products in transit. RFID joins an array of technologies that were developed over many years to allow Auto-ID in many applications. These other technologies include bar-code system, smart cards, optical character recognition and biometric procedures (voice identification, finger printing, etc.). Each has advantages as well as limitations in many areas concerning costs, data capacity, security, flexibility, and reliability.

In RFID technologies, radio frequency is used to communicate between a data storage device (a tag) and a reader/scanner. RFID is fast, reliable, and does not require line-of-sight or contact between the reader and the tags. Non-contact read and non-line-of-sight communication allow data read through many containers, fog or other visual obstructions. RFID tags can have large data storage capacity and be field-programmable, providing great flexibility in many applications.

At the minimum, a RFID system must have at least a reader and one tag. A tag contains data to be read, and is typically attached to goods and personnel that are mobile or in transit. A tag may also contain sensors for various environmental sensing and logging functions. A reader decodes the information from the tags and communicates with the rest of the systems for interpretation. A reader usually also functions as an interrogator to cause the tag to respond. However, there are systems with the interrogators separated from the readers for more precise location tracking.

There are two main groups of RFID systems classified according to power supply in the tag: passive and active. Passive tags do not have an integrated power supply and must draw all required power from the field of the reader. The field can be electric, magnetic, or electromagnetic. A passive tag can have very long life since its operations do not depend on a battery. On the contrary, an active tag uses a battery to power part or all functions. Thus, the usefulness of an active RFID tag is closely related to battery life, cost and serviceability. To maintain battery life, the transmission power from the tags should be the minimum for achieving desirable read range.

Both active and passive tags may be attached to goods and cargo onboard an aircraft. Passive tags may even be installed with aircraft parts to provide information about their history and service records. Currently, operation of these tags onboard an aircraft is still prohibited. However, it is widely known that RFID tags have been shipped with cargo on many commercial cargo aircraft.

Without a reader onboard, passive tags are considered less of an interference risk since they require a strong encoded field from the reader for activation. Active tags have higher risk because they have built-in batteries and many can beacon without being interrogated. Extreme low-cost designs may not suppress spurious emissions beyond the regulatory requirements and may result in high peak spurious emissions near aircraft radio bands.

2.1 Objective

The primary objective of this study is to develop a process for measuring spurious emissions from various RFID tags. In addition, the measurement and results of aircraft interference path loss (IPL) for sources in the cargo bays of passenger aircraft are reported. The emission and path loss measurements are essential in assessing interference risks to aircraft radio receivers.

2.2 Scope

In this report the RFID tags emission measurements are restricted to unintentional (spurious) emission in and near the aircraft radio spectrum. Intentional transmissions from the tags are typically known, or are easily determined, and are excluded from the measurements.

The tags considered are limited to the active tag designs, with built-in batteries to power the data transmissions. The emphasis will be on tags suitable for cargo tracking. Personnel tags are not considered in this report.

2.3 Approach

Assessment of aircraft radio receiver interference is typically accomplished by addressing the source – path loss – victim elements of the equation:

$$A + B \geq C, \qquad \text{(Eq. 2.3-1)}$$

at any frequency in the aircraft radio communication and navigation bands, where

"*A*" is the maximum RF emission from a PED in dBm,

"*B*" is the maximum interference coupling factor in dB, and is usually a negative value. "*-B*", a positive dB value, is referred to as the minimum IPL,

"*C*" is the receiver's minimum in-band, on-channel interference threshold in dBm.

If the minimum interference threshold, "*C*", is lower than the maximum interference signal level at the receiver's antenna port, "(*A* + *B*)", there is a potential for interference.

A primary focus was to measure the maximum RF emission, "*A*", from the RFID tags. Reverberation chambers and methods are used due to their accuracy and repeatability as compared to the standard semi-anechoic chamber method. This method was used in previous studies [3][4][5], and show good result comparability with semi-anechoic method [4]. Further details are described in a later section.

The minimum IPL, "*-B*", were previously reported [3] for devices located in the passenger cabin. However, RFID tags are typically affixed to cargos located in cargo bays; thus, cargo bay IPL data are also needed. In this report, cargo bay IPL measurement data are reported for radio systems on two aircraft. These cargo-bay IPL data are relevant for conducting interference risk analysis.

Receiver interference thresholds "C" for *bursty* interference signals are not considered. Rather, the subject is being addressed in a separate study. "Bursty" refers to signals that are transmitted in short spurts, as opposed to steady-stream data. RFID signals are bursty in that their "on" time is in the order of one to hundreds of milliseconds (msec) while their "off" time can be seconds or longer. Earlier data reported in [6][7][2] are only for continuous-wave like, or noise-like interference signal, and are not appropriate. Many aircraft radio receivers may not be susceptible to short interference burst. For those systems, using the thresholds for CW-like interference may be overly conservative.

2.3.1 Emission Measurements of RFID Tags

Similar to the earlier efforts [3][4][5], various aircraft radio bands were grouped into five measurement bands to reduce the number of measurements and test time. Aircraft radio bands that overlapped, or were near one another were grouped together, and emissions were measured across the entire combined band simultaneously. Five frequency groups, designated as measurement Band 1 to Band 5, covered many aircraft radio bands, including LOC, VOR, GS, VHF-Com, TCAS, ATCRBS, DME, GPS, and MLS. Table 2.3-1 shows the relationship between the measurement and aircraft radio bands.

Table 2.3-1: Emission Measurement Band Designations and Corresponding Aircraft Radio Bands.

Measurement Band Designation	Measurement Freq. Range (MHz)	Aircraft Systems Covered	Spectrum (MHz)
Band 1	105 – 140	LOC	108.1 – 111.95
		VOR	108 – 117.95
		VHF-Com	118 - 138
Band 2	325 – 340	GS	328.6 – 335.4
Band 3	960 – 1250	TCAS	1090
		ATCRBS	1030
		DME	962 - 1213
		GPS L2	1227.60
		GPS L5	1176.45
Band 4	1565 – 1585	GPS L1	1575.42 ± 2
Band 5	5020 - 5100	MLS	5031 – 5090.7

It is implied that high emissions anywhere in a measurement band potentially affect all systems grouped in that band. No effort is made to distinguish whether the emissions were on any specific radio band or channel.

Two reverberation chambers were used to conduct the measurements, producing results in *total radiated power* (TRP) [8]. This method differed from the approach used in RTCA/DO-199 [6], where radiated power was estimated from the electric field measured at a distance from a device-under-test (DUT). Further details about conducting emission measurements in a reverberation chamber are found in Section 3.

The tag models were tested individually. Methods to "blink" the tags depended on the tag capability, and whether the tag could be made to beacon at a fast rate. Typically a special utility was required. In addition, for tags triggered upon sensing motion/movement, a "shaker" apparatus was built using a shielded motor assembly and cables to avoid undesirable motor noise in the test chamber.

Many tags blinked upon receiving a command from an interrogator. In these cases filters were used between the interrogator and its antenna to prevent any unwanted interrogator noise from entering the chamber.

In most cases, there were no options to allow changing the tags' operating frequency and data rates, as it was the case for testing cellular phones and wireless local-area-network (LAN) devices [3][4][5]. However, the blink rate of the beacon tags may be changed. Emission characteristics are expected to be the same, regardless of the method to blink the tags.

It is difficult to compare the tags' emissions to that of other PEDs currently allowed onboard an aircraft. The emission modulation characteristics, the use locations, and the receiver interference thresholds are vastly different between the two problems.

2.3.2 Cargo Bay Path Loss Measurement

As a part of a separate effort IPL data were measured in the cargo bays a Boeing 747 (B747) and an Airbus A320 aircraft. The minimum IPL between locations in the cargo bays and the aircraft radio receivers' antenna ports were measured and reported for LOC, GS, VHF, DME, ATCRBS and GPS systems. The IPL data are reported in this report due to the relevancy to the RFID interference analysis.

In the IPL measurement a small antenna was used to simulate a transmitting source, such as a RFID tag, in the cargo bay. The antenna was attached to a tracking source delivering a fixed known power. A spectrum analyzer captures the magnitude of the simulated signal coupled into aircraft antennas and its cabling. The attenuation level between the transmitted signal and the measured signal is recorded as the IPL.

The transmitting source was used to scan along the cargo door seam in linear polarizations perpendicular and parallel to the direction of the seam. It also scans the cargo bay volumetrically in three linear polarizations. Further details and summarized results are reported in Section 4.

2.4 Report Organization

Section 3 describes the measurement of RFID tag emissions in the aircraft radio bands. Section 3.1 briefly discusses relevant characteristics of tags from various vendors. Section 3.2 describes the measurement process, the test technique and the test facility. Section 3.3 reports the measurement results.

Section 4 describes the measurement of cargo bay path loss of two passenger aircraft. Section 4.1 describes the measurement process. Section 4.2 summarizes the cargo-bay IPL for various systems on a B747 and an A320 aircraft.

Section 5 briefly discusses the aircraft receiver interference thresholds. Summary and conclusions are discussed in Section 6. Appendix A briefly reviews emissions data for laptop computers and personal digital assistant (PDAs) for comparison purposes. These data were measured in a previous study [3].

3 RFID Active Tag Emissions

Active RFID tags come in a variety of forms, shapes and operational characteristics. The tags chosen for the study come from vendors such as Savi Technology Inc., Identec Solutions Inc., Sovereign Tracking Systems LLC, WhereNet Corp. and RF Code, Inc. These vendors represent a large segment of the active tags manufacturers for cargo tracking applications. This section discusses tags operational and test issues associated with the tags from the above vendors. Tag triggering methods for the testing are discussed, and the laboratory measurements and results are presented.

3.1 RFID Technology Overview

This RFID technology overview section briefly describes the operations of various RFID systems with emphasis on RF characteristics relevant to the measurements of spurious emissions from the tags. At the minimum, an operational system consists of tags and a reader, whose function is to receive and decode

the signals from the tags. Discussions regarding the readers' characteristics and their emission profiles are minimized as these devices are not expected to operate within an aircraft during flight. RFID tags are of a greater concern. There is a much higher chance these tags are turned on and transmitting while the aircraft is in flight.

For the tags, there are three popular modes of operations: beacon, interrogated and motion. These modes determine how and when the tags "blink". A blink may consist of one or multiple bursts of transmissions. Often the tags may operate in multiple modes concurrently, such as beacon and motion, or beacon and interrogated.

In beacon mode the RFID tags automatically transmit at a programmable regular interval. This mode allows for continuous monitoring of the conditions and locations of the cargo while the tag is at a fixed location or in motion. Based on laboratory observations, many tags can beacon *reliably* as fast as every two seconds. The tags may be programmed to beacon at a faster rate; however, the transmission may not be reliable at a regular interval.

In motion mode the tags blink whenever encountering abrupt motions such as vibrations, bumps or physical movement. A motion tag can transmit as fast as every 1-2 seconds if experiencing motions continuously. On an aircraft the motion tags may blink in a coordinated manner corresponding to the aircraft abrupt motions. These motions are typically observed during take-off and landing or may be caused by the weather.

In interrogated mode a tag would blink whenever it received an interrogating signal. That signal may be addressable to a specific tag, or non-addressable commanding all the tags within the coverage area to respond. The interrogating signals usually come from the reader for wide range coverage. However, there are implementations in which a separate interrogator with shorter range is positioned near a choke point. As a tag enters the coverage of area of an interrogator, it transmits the stored information as well as the identification of the interrogator. A separate reader receives and interprets the signal from the tags, and to interface with the network. There may be more than one interrogator positioned at one or more choke points such as doors. In addition, the interrogator frequency may be different from the tag transmitting frequency.

The following subsections briefly describe the operations of individual systems from various vendors. Only information relevant to the set-up, measurement, and analysis are included. The information is not intended to be a tutorial or performance comparison. Rather, the information provided is to help justify the reasons for the chosen measurement parameters. In addition, the information may help in future interference analysis related to receiver interference threshold for RFID bursty transmissions.

3.1.1 Savi Technology

Savi Technology implements a multi-frequency, three-element architecture in their designs. In addition to the traditional two-element architecture that includes reader and tags, three-element architecture also incorporates another component – a SignPost. The SignPost is simply an interrogator that communicates with the tags over a short-range 123 kHz frequency link. The maximum range of the interrogator is 2.5 meters or 4 meters depending on the model. The tags, on the other hand, communicate with a reader over a longer-range 433 MHz frequency link. The reader provides long range read, while the interrogator provides spot coverage for more precise tag locations.

In the three-element design, the tags transmit data bursts, or "blinks", as they enter the coverage zone of the interrogator. The interrogator may be strategically positioned near a choke point such as a warehouse door. A reader reads and decodes information transmitted by the tags. A tag's transmission may include its own identification, the interrogator's identification, sensor and imbedded data. In addition, the tags can also beacon at a programmable interval without an interrogator.

Three tags were acquired for this evaluation: SaviTag ST-602, ST-604 and ST-654 models. The three tags have different form factors, ranges and capabilities. Several typical tag operating parameters relevant to this study are listed in Table 3.1-1. Figures 3.1-1 and 3.1-2 show the tags, an interrogator, and a reader forming a complete set-up. A reader was not needed for the testing, however.

Figure 3.1-1: SaviTag ST-602, ST-604 and ST-654 models.

Savi SignPost

Savi Reader

Figure 3.1-2: The Savi interrogator and reader.

For the evaluation, it is desirable to blink the tags continuously at a fast rate while conducting the emissions measurements. The simplest method is to program the tag to beacon at desired interval. This approach was used; however special software from the vendor was required in addition to the basic hardware such as an interrogator and/or a reader. This software programming capability was achieved very late in the planning stage. As a result other back-up methods were explored. Details concerning the alternative methods are described in Appendix B.

3.1.2 Identec Solutions

Several tags are available from the Identec Solutions, including the credit-card style ID series and the I-Q series. The I-Q series includes basic models, as well as models with temperature sensors and models with increased data storage space. For this evaluation, tag models I-Q8 and ID-2 were acquired. Both have minimum built-in storage space, and lack the temperature sensing capabilities. These capabilities were not expected to greatly affect the RF emission characteristics of the tags.

RFID readers are available that communicates with the tags in two formats: PC Card and fixed. The fixed reader can read up to 4 antenna ports simultaneously. The PC Card format is designed for use with a laptop computer and has a single antenna port. For the purpose of making the tags blink, the less expensive PC Card is sufficient. Software is also available that can help to read and to blink the tags sequentially. Each tag also has a light-emitting-diode (LED) indicator that can be set to confirm the interrogator and response. The maximum tag transmission power is 0.75 milliwatt (mW) effective radiated power.

Each tag and reader can be set at the factory to operate at either 868 MHz Europe version or 915 MHz North America version. For this study, the 915 MHz North America versions of tags and readers were acquired. Figure 3.1-3 shows the two tag models acquired for the testing. Other tag data relevant to the testing are shown in Table 3.1-1.

Figure 3.1-3: Identec I-Q8 and ID-2 tags.

The reader outside the test chamber was connected to its antenna inside via a coaxial cable. A bandpass filter was used between the reader and its antenna to block any unwanted emissions while passing the desirable communication signals.

3.1.3 Sovereign Tracking Systems LLC

The tags considered are motion activated. In a typical setting, the tags are activated when they sense motions such as vibration or if the tags are moved. The switch on the back of the tag must be "on" (or depressed when the tag is affixed to the cargo) for activation.

There are also tags available that can be activated through an external electrical "mini-phone" plug. However, the "mini-phone" plug would complicate the testing in ensuring that any emissions from the trigger device are filtered out. As a result only the motion tags are considered in this study. The RF transmission circuitries should be the same between the models with motion activation or with external data input activation.

Two motion tags acquired include the ATS and ATS-3A models (model ATS-3B has an external data input for activation). Either tag can be preset to operate at either 417.8 MHz (United States market) or 433.72 MHz (global market). For this study the acquired ATS tags were set to operate at 417.8 MHz and ATS-3A tags at 433.72 MHz. They have -10 dBm peak transmit power and -40 dBm peak harmonic levels. Figure 3.1-4 shows the tag models acquired from Sovereign Tracking Systems LLC.

There are several conditions that will activate the transmitters on the motion tags once the tags' batteries are installed.

1. Start up. When the tags are mounted (by depressing a switch on the back of the tags), the tag transmits a 6-code signal once. Each code is 70 msec in duration.

2. Tag vibrated or moved. A 3-code signal is transmitted, 210 msec in length. If the motion continues the tag will continue to transmit a 3-code signal with a time interval of 1.5 seconds. However, the tag would stop transmitting if it senses the same continuous motion for 10 minutes, then resume normal operation after about 10-15 seconds of inactivity.

3. Standby mode. 3-code signals are transmitted in every 15 minutes.

4. Emergency mode. When the tag is separated from the attached cargo, the switch in the back of the tag is switched off. The tag transmits 3-code signals five times with 10 seconds interval.

The operating mode of interest occurs when the tag continuously senses motion and transmits a 210 msec burst every 1.5 seconds. In the laboratory testing, the tag shaker should be constructed to avoid continuous motion or continuous vibration to prevent tag shut down after 10 minutes.

Figure 3.1-4: Sovereign ATS3-A and ATS tags (set to operate at 433.72 MHz and 417.8 MHz, respectively)

3.1.4 WhereNet

WhereTag III (Model TFF-1011) RFID tags were acquired from WhereNet for the evaluation. The tags normally operate in beacon mode. The blink rate is user configurable from 5 seconds to 1 hour. The blink rate configuration is performed with a "WherePort" device that communicates with the tags through low frequency magnetic signals. The tags have the 2 mW maximum output power.

The WhereTag III model currently complies with the American National Standard Institute (ANSI) 371.1 Real Time Locating Systems (RTLS) industry standard. The WhereTag III tag transmits spread spectrum signals between 2.4 to 2.483 Gigahertz (GHz), centering around 2.44 GHz. Each transmission, or "blink" consist of several "sub-blinks" of 1.4 msec duration and 125 msec (+/- 15 msec dithering) spacing between the consecutive sub-blinks. The sub-blinks are identical in information content. Multiple sub-blinks were used to overcome data collisions. The number of sub-blinks can be set.

The acquired tags were preset at the factory to blink every 5 seconds, the fastest rate possible for this tag. No special hardware or software was needed. A picture of the WhereTag III tag is shown in Figure 3.1-5.

Figure 3.1-5: WhereTag III tag.

3.1.5 RF Code

Figure 3.1-6 shows the two models acquired from RF Code, Inc. The Mantis model (p/n 05101297-26A) can operate in beacon mode at 12.5 second intervals. It can also blink on motion up to 1 second intervals. The Spider model (p/n 05101677-01C) typically beacons every seven seconds. However, for our evaluation, the tags were preset at the factory to beacon at its fastest rate of every 2 seconds. The tags operated at 303.8 MHz and were measured to have 113 msec burst duration.

Figure 3.1-6: RF Code Tags.

3.1.6 Other Active RFID tags

RFID tags from other vendors that specialized in asset tracking were also considered. Among them were products from ActiveWave Inc. transmitting at 916 MHz or 868 MHz, and receiving at 433 MHz.

Also considered were new products from MultiSpectral Solutions Inc. that would be soon available to the general public. This system operates near 6.3 GHz using ultra-wideband (UWB) technology. These tags did not arrive in time for the testing and their data are not included in this report.

3.1.7 Tag Operational and Test Mode Summary

Table 3.1-1 lists the tag characteristics relevant to the measurement and analysis. These characteristics include operating frequency range, burst duration, maximum transmitted power, modulation, typical tag blink interval, and the fastest blink interval set for the testing.

Table 3.1-1: RFID Tag Operational and Test Modes

Manufac.	Frequency (MHz)	Meas. Burst Duration	Xmit Max Power	Modulation	Typical Blink Interval- (Advertised)	Fastest Blink Interval For Test Purposes
Savi	433.92 MHz (Xmit), 123 kHz (Recv)	5 msec	ST-654: 0.6 mW ST-604 & ST-602: 0.025 mW (EIRP)	FSK +/- 50 KHz	SignPost Interrogated and/or 10 secs Beacon	2 secs Beacon
Identec	915 MHz (NA) (868 MHz EC)	20 msec	I-Q: 0.75mW ERP ID-2: 0.75mW ERP	AM 10%	Interrogated	Interrogated
RF Code	303.8 MHz	113 msec	5 mW	Pulse	Mantis: 1sec Motion 12.5sec Beacon Spider: 7 sec Beacon	Mantis: 1 sec Motion Spider: 2 sec Beacon
WhereNet	2.400 GHz to 2.4835 GHz	1.4 msec (~125 msec sub-blink interval)	2 mW	BPSK DSSS ANSI 371.1 RTLS	WherePort Trigger 6 sec Beacon (5 secs – 1hour User settable)	5 sec beacon
Sovereign Tracking	417.8 MHz (ATS), 433.72 MHz (ATS3-A)	290 msec	ATS3-A: -10 dBm (Harmonic:-40dBm)	ASK OOK	1.5 seconds maximum	1.5 sec Motion
ActiveWave *	916 or 868 MHz (Xmit) 433 MHz (Recv)	20 msec	Xmit: 1mW	ASK OOK	Configurable 2 sec – 6 hours	Not Tested
Multispectral Solutions *	6.3 GHz	nanoseconds	30 mW	UWB	1 second typical – Programmable	Not Tested

***** Tags did not arrive in time for the testing. Data listed for information only
Accronyms used in table are defined on page vi.

3.1.8 FCC Emission Limits

The aircraft radio bands of interest are among the restricted bands listed in Federal Communications Commission (FCC) 15.205. As a result, the field strength of emissions in these frequency bands are required to meet the limits shown in FCC 15.209 regardless of otherwise stated limits in the subpart pertaining to intentional radiators. UWB devices are among the few exceptions.

It is important to note that compliance with the FCC 15.209 limits must be made with instruments employing quasi-peak detector or equivalent for frequencies below 1 GHz. Above 1 GHz the limit

applies to average emissions. In addition, FCC 15.35 specifies the limit for peak emissions to be 20 dB above the limit for average emissions.

Outside of the restricted bands, the individual RFID tags RF emissions conform to different FCC Part 15 provisions [9]. The specific FCC provisions vary with tag operation frequency, use, modulation types, etc... The FCC provisions provide the limits on the transmission characteristics such as power level, transmission length, spurious emission levels and other restrictions.

In general, the tags' emissions are often categorized under "Intermittent" or "Periodic" Transmission and conform to various radiated emission requirements of one or more of the following FCC 15.109, 15.209, 15.231, 15.240, 15.247 and 15.249. FCC 15.250 and 15.252 are also applicable to UWB RFID applications. These provisions provide general as well as specific RF emissions requirements.

3.2 Measurement Process

Reverberation chambers are used for their accuracy and repeatability. Unlike previous testing of wireless LAN [3] devices and wireless phones [4][5], RFID testing is unique in that the RF transmissions are bursty in nature, with short signal duration and very low duty factor. Very low duty factor, wide measurement bandwidth, instrument speed limitation and the high number of samples required for the reverberation chamber test method together can result in very long test. As a result, a modified approach was adopted to reduce test time. Additional details are discussed in a later section.

For high sensitivity measurements, harmonics and high unwanted signals outside of the measurement bands need to be rejected before reaching the measurement systems. This requires using filters designed or tuned specifically for the measurement. Without filters the measurement signals may overload the pre-amplifier or the front-end of the spectrum analyzer, leading to intermodulation products as well as skewed measurements. However, certain high harmonics and spurious emissions were extremely difficult to reject due to their close proximity to the measurement bands. In those cases the measurements were performed with reduced amplification, resulting in reduced sensitivity.

3.2.1 Harmonics Considerations

In selecting filters it is important to compare the aircraft radio bands of interest to the tags' fundamental and harmonic frequencies. Table 3.2-1 shows the fundamental and up to 5th harmonic frequencies from various tags. In addition, the aircraft radio bands are also shown in Table 3.2-2 for comparison.

The comparison shows that none of the fundamentals or harmonics (up to 5th) fall within the aircraft radio bands listed. However, the fourth harmonic of the RF Code tag and third harmonic of the 417.8 MHz tag came very close to the DME band. These may be difficult to filter out in the measurement. These specific harmonic frequencies are underlined in the Table 3.2-1.

It was determined during the testing that many tags also have high spurious emissions outside of the measurement bands, and that filtering the fundamental and harmonic frequencies alone may not be sufficient. Many of those emissions were at frequencies close to the measurement bands and were difficult to filter. Signal amplification was reduced to avoid overloading at the pre-amplifier, effectively reducing measurement sensitivity.

Table 3.2-1: RFID Tags Fundamental and Harmonic Frequencies

Manufacturers	Operating Frequency (MHz)	Harmonic Frequencies (MHz)			
		2nd	3rd	4th	5th
RF Code	303.8	607.6	911.4	1215.2	1519
Savi	433.92	867.84	1301.76	1735.68	2169.6
Sovereign	417.8	835.6	1253.4	1671.2	2089
	433.72	867.44	1301.16	1734.88	2168.6
Identec	915	1830	2745	3660	4575
	868	1736	2604	3472	4340
WhereNet	2400 - 2483	4800 - 4966	7200 - 7449	9600 - 9932	12000 - 12415
Active Wave*	916	1832	2748	3664	4580
	868	1736	2604	3472	4340
Multispectral Solution*	6200	12400	18600	24800	31000

* These tags are for harmonic frequency checking only. They were not available for the testing.

Table 3.2-2: Aircraft Bands Considered and Spectrum

Aircraft Band	Spectrum (MHz)
LOC	108.1-111.95
VOR	108-117.95
GS	328.6-335.4
TCAS	1090
ATCRBS	1030
DME	962-1213
GPS L2	1227.6
GPS L5	1176.45
GPS L1	1575
MLS	5031-5090.7

3.2.2 Measurement Method

Performing antenna port conducted power measurement is typically the most direct and easiest approach to measuring emissions from the antenna port of the device. However, most RFID tags do not have an antenna port accessible from the outside. In addition, conducted power measurement fails to account for radiated emissions from components other than through the antenna port. As a result a radiated emission test chamber is usually required for a more complete measurement.

In this study reverberation chambers are used because of their excellent repeatability, field uniformity, aspect independence, and measurement speed. The results are in the form of total radiated power (TRP), rather than in field strength as in anechoic or semi-anechoic chamber test methods. The measurement and data analysis processes used are similar to those previously documented in [3][4][5], but with modifications to accommodate the RFID types of signals.

Test Facility Description

The NASA Langley Research Center's (LaRC) High Intensity Radiated Fields Laboratory has three separate reverberation chambers located adjacent to one another. This facility is capable of performing radiated susceptibility and emission measurements using either one chamber at a time or in two or three chambers simultaneously. Using multiple chambers allows for distributed testing of systems, creating different electromagnetic environments in each chamber. The National Institute of Standards and Technology (NIST) have characterized these chambers. The NIST results indicated a high degree of electromagnetic field uniformity performance within the stated usable frequencies. Details regarding their performance are located in [10].

A chamber's lowest usable frequency is determined by its construction and geometry, and a sufficient mode density within the chamber to provide a uniform electromagnetic environment [11]. Due to its largest size of the three chambers, "Chamber A" is the only one capable of conducting measurements in Band 1. The lowest usable frequency for Chamber A is approximately 100 MHz with +/-2 dB field uniformity [10]. The smallest chamber, "Chamber C", was also used for testing at higher frequencies. The lowest usable frequency for Chamber C is approximately 350 MHz. Figure 3.2-1 shows the inside of Chamber A.

Due to high chamber quality factors, the reverberation chamber method may not be appropriate for very short pulse durations [12]. The chamber time-constant should not be greater than 0.4 of the pulse-width of the modulated signal. This requirement ensures that once a pulsed signal is turned on, the field environment in the chamber has sufficient time to reach (near) steady-state level before the pulse is turned off.

Figure 3.2-1: Inside reverberation Chamber A.

The chamber time-constants vary with frequency, and are about 0.6 microsecond near 100 MHz for an empty Chamber A. The measurement results are therefore accurate for continuous-wave (CW) signals and pulsed signals of 1.5 microseconds (= 0.6 microseconds / 0.4) or longer. A method for measuring chamber quality factor and time-constant is described in [12]. Additional data concerning the specific test chamber quality factor can be found in [10].

For RFID tags, the shortest transmission burst is 1.4 msec for the WhereTag III tag, measured using a spectrum analyzer. Since most bursts contain far fewer than approximately 1000 data bits, the bit duration should be far longer than the required 1.5 microsecond for accuracy. As a result the test chambers can accommodate all the RFID pulse-widths under consideration.

RF absorber can be added to the chamber to lower the time-constant if needed; however, spurious emission signal characteristics must be known in advance for all devices-under-test in all measurement bands. Measurement sensitivity may also be reduced due to the higher chamber loss. Absorber was not needed in this study.

Tag Interrogation Method for the Testing

Figures 3.2-2, 3.2-3 and 3.2-4 show emission test setups in a reverberation chamber for RFID beacon tags, interrogated tags and motion tags. The figures depict different methods used blink the tags. Beacon tag testing does not need any special hardware as shown in Figure 3.2-2.

For interrogated tags, a special setup for the interrogator is needed as illustrated in Figure 3.2-3. This setup includes a filter network inline with the interrogator's antenna. The filter network pass the interrogator signal, while blocking other unwanted emissions from entering into the test chamber in the measurement bands. An interrogator may come in various formats. It can be a PC card (run on a laptop computer) or a separate fixed unit. The interrogator may also be built into the same unit with a RFID reader.

For motion tags, Figure 3.2-4 shows a tag shaker assembly used to create motion to make them blink. The tag shaker assembly and the power cable are shielded to prevent unwanted RF leakage.

Description of Measurement Method

Tests conducted in reverberation chambers rely on several methods to produce a statistically uniform and isotropic electromagnetic environment (field statistics measured over one stirrer revolution are isotropic and spatially uniform). Two of these methods are mode-stirred and mode-tuned [11]. Stirrers with reflective surfaces are rotated continuously during mode-stirring, or stepped at equal intervals for a complete rotation during mode-tuning.

The mode-stirred method was adopted due to ease of setup, implementation, and significant speed advantage over the mode-tuned method. While the mode-tuned method can be more accurate in immunity testing applications (especially for DUTs with slow response time), the mode-stirred method is superior for most emission measurement applications due to speed. With a spectrum analyzer used for measuring receive power, the emission measurement system can respond very fast to the changing fields caused by the continuously rotating stirrers. Settling-time delays for stirrer stepping in mode-tuned operations are eliminated, resulting in significant speed improvements. In addition, combining mode-stirred operations with continuous frequency sweeping can further expedite the measurements.

In typical reverberation chamber applications, measurement uncertainty levels can be lowered by selecting the number of measurement points in a stirrer revolution approximately equal to the number of calibration points. The number of measurements during one stirrer revolution should be as large as possible within constraints of instrument capabilities and test time. Using the mode-stirred method, several thousand measurements per stirrer revolution are easily achievable using a spectrum analyzer. On

the other hand, the mode-tuned method with the number of measurements exceeding 100 per stirrer revolution is often considered impractical due to excessive test time.

Utilizing the mode-stirred method, the two stirrers located in the corners of the chamber were continuously rotated at 5 rpm during chamber calibrations and emissions testing. Also illustrated is the measurement path. RF filters and a preamplifier are indicated in the receive path.

Reverberation chamber emission measurement and calibration typically involve [13]:

1) Empty chamber insertion loss measurement;

2) Measurement of chamber loading caused by the presence of test devices inside the chamber; and

3) Measurement of maximum receive power over a paddle rotation of the stirrer with the DUT powered on in various test modes.

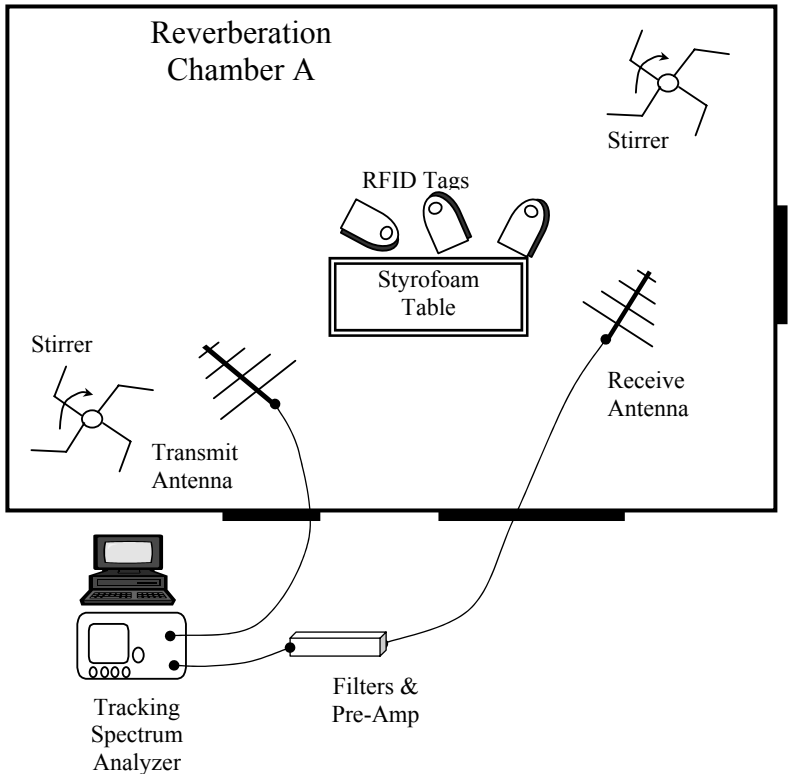

Figure 3.2-2: Testing beacon tags in reverberation chamber.

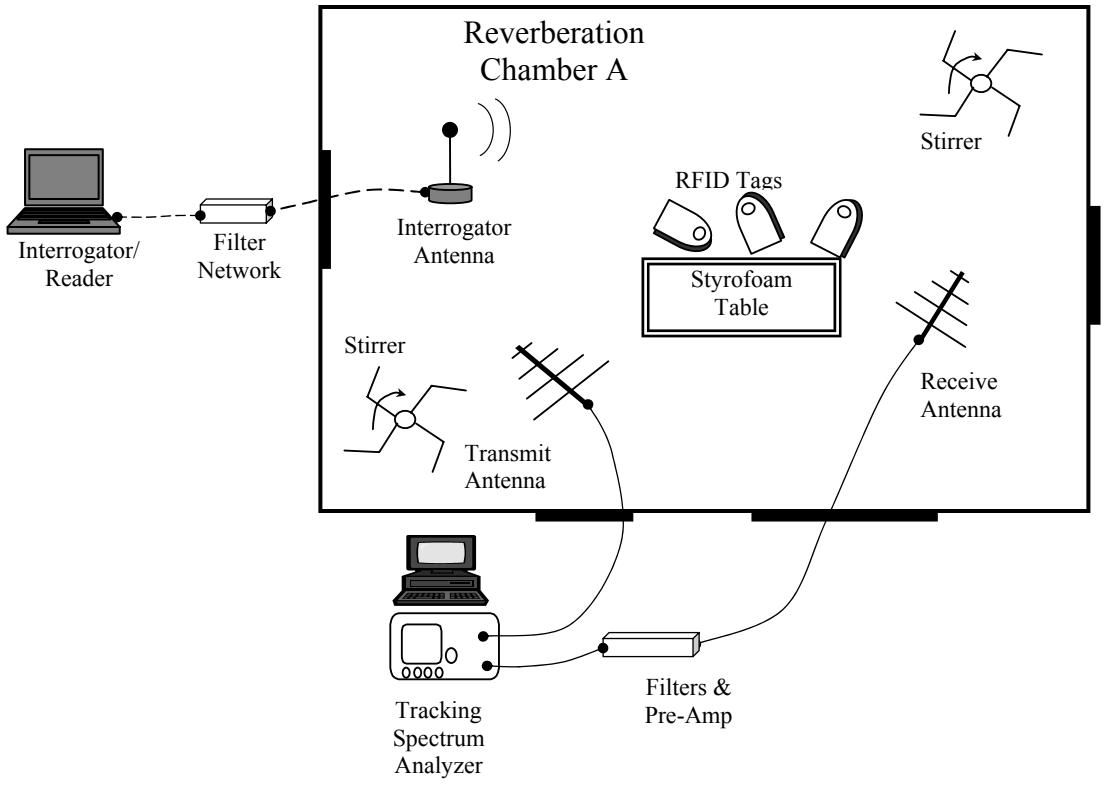

Figure 3.2-3: Testing interrogated RFID tags in a reverberation chamber.

The total radiated power within the measurement resolution bandwidth can be calculated using [13]:

$$P_{TotRad} = (P_{MaxRec} * \eta_{Tx}) / (CLF * IL) \ , \qquad \text{(Eq. 3.2-1)}$$

where P_{TotRad} = total radiated power within the measurement resolution bandwidth,

P_{MaxRec} = maximum received power measured over one complete paddle rotation,

CLF = chamber loading factor, or the additional loading effects caused by the presence of objects in the test chamber,

η_{Tx} = efficiency factor of the transmit antenna used in chamber calibration and assumed to be unity for the antennas used,

IL = empty chamber insertion loss, pre-determined during chamber calibration.

IL is measured during chamber calibration and is defined as the ratio of the maximum receive power and the transmit power in a stirrer revolution [13]:

$$IL = P_{MaxRec} / P_{Input} \ , \qquad \text{(Eq. 3.2-2)}$$

where P_{MaxRec} and P_{Input} are the maximum received power and the transmit power at the antennas, respectively.

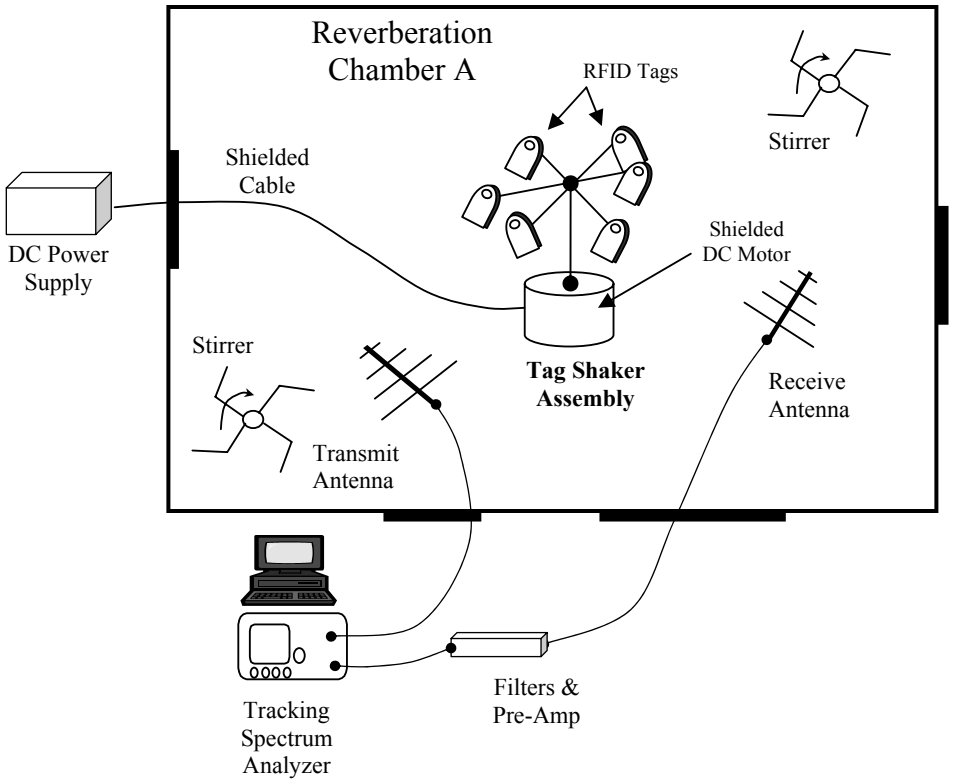

Figure 3.2-4: Testing motion tags in reverberation chamber.

IL is usually first measured and averaged over multiple locations for improved uncertainties. *CLF* is then measured once (one location) when test objects or personnel are introduced into the test chamber. Correction for *CLF* is applied only when the values exceed a given threshold (3 dB is used in [12]).

CLF ≈*1* in this study since the tags are small and have little effect on overall chamber loading. Thus (*CLF*IL*) is simply (*IL*). In addition, *IL* was measured at one location rather than averaged over multiple locations. The effect is an acceptable small increase in uncertainty of about 2 dB or less, based on past measurements and the results of a detailed study reported in [10].

In an actual setup, it is often convenient to include transmit and receive path losses in the chamber calibration measurements. These path losses account for the presence of test cables, in-line amplifiers, attenuators and filters for various purposes. Transmit path losses are associated with components connecting the source and the transmit antenna, whereas receive path losses are associated with components connecting the receive antenna and the spectrum analyzer. As a result, chamber calibration factor (*CF*), in dB, is introduced:

$$\begin{aligned} CF &= (P_{Xmit(dBm)} - P_{SAMeas(dBm)}) \\ &= L_{Chmbr(dB)} + L_{RecCable(dB)} + L_{XmitCable(dB)}, \end{aligned} \qquad \text{(Eq. 3.2-3)}$$

where

CF = chamber Calibration Factor (dB),

$L_{Chmbr(dB)}$ = chamber loss (dB), or

= $-10 * log_{10}(CLF * IL)$,

$L_{RecCable(dB)}$ = receive cable loss (dB),

$L_{XmitCable(dB)}$ = transmit cable loss (dB),

$P_{SAMeas(dBm)}$ = maximum receive power measured at the spectrum analyzer (dBm) over one stirrer revolution,

$P_{Xmit(dBm)}$ = power transmitted from source (dBm).

Passive losses (not to include amplifier gains) are defined to be positive in dB. The total radiated power in dBm can be computed using:

$$P_{TotRad(dBm)} = P_{SAMeas(dBm)} - L_{XmitCable(dB)} + CF . \quad \text{(Eq. 3.2-4)}$$

Measurement instrumentation included a spectrum analyzer with a built-in tracking source (frequency-coupled with the spectrum analyzer), a data acquisition computer, transmit and receive antennas, RF filters and pre-amplifiers. The measurement procedure begins by performing a transmit cable loss measurement. This step can be performed using a RF network analyzer, or a tracking source and spectrum analyzer combination functioning as a scalar network analyzer.

Next, a chamber calibration is performed. A known level of power is delivered from the tracking source into the chamber through the transmit antenna while the stirrer(s) are continuously rotating at a predetermined rate. The spectrum analyzer is used to record the maximum power coupled into the receive antenna (and the receive path) while performing synchronized frequency sweeps with the tracking source across the measurement bands. Eq. 3.2-3 is applied to determine the *CF*.

During the emission measurements, the spectrum analyzer is set in the maximum hold mode while continuously sweeping over the measurement frequency band. The tags are commanded to blink at the fastest rate possible. Eq. 3.2-4 is applied to normalize the measurement data with the calibration data to arrive at the final total radiated power. The source is also disconnected, and the transmit antenna terminated with a 50-ohm load to avoid RF leakage from the tracking source into the test chamber. The measurement noise floor is also measured in each band with the tags powered off or removed from the chamber.

In past studies [3][4][5], establishing and maintaining connectivity with a wireless DUT can be difficult in a reverberation chamber due to severe multipath interference. In this study all tags responded well and there were no difficulties associated with tag interrogation.

Figures 3.2-5, 3.2-6 and 3.2-7 show the testing of interrogated, motion and beacon tags in reverberation chambers.

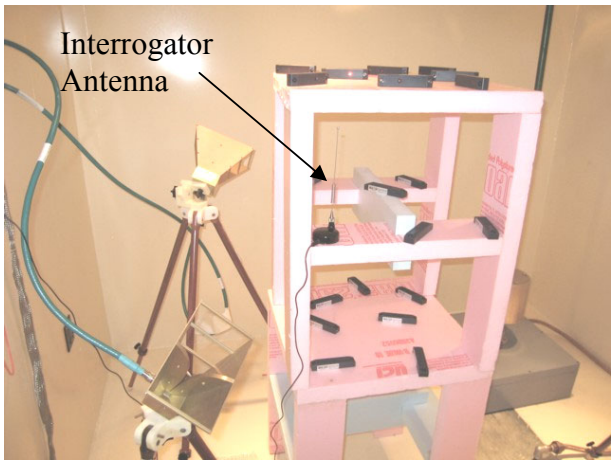

Figure 3.2-5: A test set up for interrogated tags. The interrogator antenna is connected to an interrogator outside the test chamber through an in-line filter.

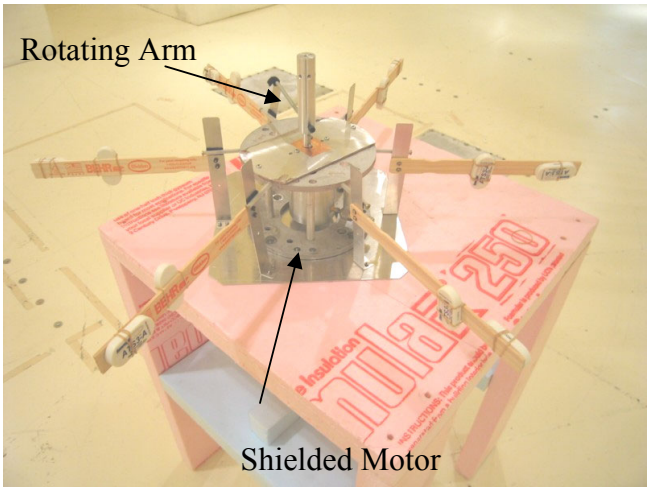

Figure 3.2-6: A test set up for motion tags. The rotating arm bumps the tag holder assemblies to shake the tags.

Figure 3.2-7: Test set-ups for tags in beacon mode.

Instruments and Settings

An Agilent E4407B spectrum analyzer with a built-in tracking source was used for most of the chamber testing and calibration. Since the built-in tracking source operates only up to 3 GHz, a separate set up was used for Band 5 *chamber calibration*. For Band 5, a combination of Hewlett Packard (HP) 8561E spectrum analyzer and a HP 85644 tracking source were used. Both of these systems can operate up to 6.5 GHz. Together they can perform synchronized frequency sweeps, effectively operating as a scalar network analyzer. Once the chamber calibrations were completed, the actual measurements were performed with the Agilent E4407B due to its speed. The E4407 can perform a 601-point sweep in about 6 msec as opposed to 50 msec for the HP 8561E. Faster measurement speed is important for measuring short RFID signal bursts. Section 3.2.3 discusses more on this issue.

A laptop computer with GPIB interface was used to save trace data from the spectrum analyzer. All instrument controls were performed manually.

Table 3.2-3 documents the spectrum analyzer settings. These instrument settings and the filter/pre-amplifier selections were carefully selected for the maximum measurement speed and sensitivity without overloading the measurement equipment. Table 3.2-4 documents various combinations of test chambers and antennas used for the test bands.

Table 3.2-3: Emission Measurement Instrument Settings

	Band 1	**Band 2**	**Band 3**	**Band 4**	**Band 5**
Common Settings	RBW: 100 KHz SwpTime: 6 msec, 601 pts		RBW: 300 KHz SwpTime: 6 msec, 601 pts	RBW: 100 KHz SwpTime: 6 msec, 601 pts	RBW: 100 KHz SwpTime: 10.31 msec, 601 pts
RF Code	Motion Tags: RL 10 dBm Atten: 20 dB Beacon Tags: 0 dBm RL 0 dB Atten		Motion Tags: RL: 10 dBm Atten: 20 dB Beacon Tags: RL: 10 dBm Atten: 20 dB	Motion Tags: RL 10 dBm Atten: 20 dB Beacon Tags: RL 10 dBm Atten: 20 dB	RL: -10 dBm Atten: 0 dB
SAVI	RL: -10 dBm Atten: 0 dB		ST-654: RL: 0 dBm Atten: 10 dB ST-602,-604: RL:10 dBm Atten: 20 dB	ST-654: RL: 0 dBm Atten: 10 dB ST-602,-604: RL:10 dBm Atten: 20 dB	RL: -10 dBm Atten: 0 dB
Sovereign	RL: -10 dBm Atten: 0 dB		RL 10 dBm Atten: 20 dB	RL 10 dBm Atten: 20 dB	RL: -10 dBm Atten: 0 dB
Identec	RL: -10 dBm Atten: 0 dB		RL: -10 dBm Atten: 0 dB	RL:-10 dBm Atten: 0 dB	RL: -10 dBm Atten: 0 dB
WhereNet	RL: -10 dBm Atten: 0 dB		RL: -10 dBm Atten: 0 dB	RL:-10 dBm Atten: 0 dB	RL: -10 dBm Atten: 0 dB

Table 3.2-4: Antennas in the Measurement Path

Test Freq. Band	Test Chamber	Transmit Antenna (for Calibration)	Receive Antenna
1	A	A&H SAS-200/514 Log-Periodic	EMCO 3144HP
2	A		
3	C	A&H SAS-571 Dual Ridge Horn	A&H SAS-571 Dual Ridge Horn
4	C		
5	C		

Proper filtering is required for accurate measurement. Several filters were used for this study. Two separate filters sets were used, one in the RFID interrogation path and the other in the measurement path. These filters are illustrated in the Figure 3.2-3.

For set-ups that require an interrogator, filters are positioned between the interrogator and its antenna. These filters pass the intentional transmissions from the interrogator while blocking any spurious emissions from the same device in the measurement bands. Many combinations of filters were used for different tags operating frequencies and measurement frequencies. In most cases multiple filters were used in combinations to achieve desired specific performance.

Filters in the *measurement path* reject the intentional tag emissions as well as strong spurious emissions outside of the measurement bands from overloading the high gain pre-amplifier or spectrum analyzer, resulting in distortions in the measurements. Different combinations of highpass, bandpass, lowpass and tunable notch filters were tuned specifically for each combination of RFID devices and the measurement bands. Also used are high gain pre-amplifiers. The amplifiers and filters in combination provide desirable measurement sensitivity and selectively. Tables 3.2-5 to 3.2-8 show the filters and amplifiers used in the interrogator path and the measurement path.

Table 3.2-5: Filters Used For Identec Tags (915 MHz)

Measurement Band	Meas. Freq. Range (MHz)	Interrogator Path Filters	Measurement Path Filters
Band 1	105 - 140	1)10 dB attenuator 2) K&L Microwave BP–6B120-860X80 (820-900 MHz) 3)Tunable Bandpass*	1) Low Pass: K&L 8IL40-336/U468 (fc=336 MHz) (x2) 2) Pre-Amplifier: Miteq AU-1291-N-1103-1179-WP 61 dB, 0.01 -500 MHz
Band 2	325 - 340		
Band 3	960 - 1250		1) High Pass K&L 5IH10-960/U1600 (two used) 2) Narda Band Pass Filter (1-2GHz)** 3)Low Pass K&L 7IL10-1600/X1710 *** 4) Pre-Amplifier: MIteq-AMF-4F-00800250-06-13p, 60 dB, 800-2500 MHz
Band 4	1565 -1585		
Band 5	5020 - 5100		1) K&L Band Pass: 4FV30-5050/X100 (2 used) 2) Miteq AMF-5F-02600520-06-10P

* The filter was tuned so that the combination provided greater than 70 dB attenuation at 960 MHz
** To provide additional 15 dB rejection at 915 MHz to avoid overloading
*** Pass up to GPS band, while rejecting harmonics at 1830 MHz

Table 3.2-6: Filters Used For RF Code Tags (303.8 MHz)

Measurement Band	Meas. Freq. Range (MHz)	Motion Tags & Beacon Tags
Band 1	105 - 140	1) Mini Circuit NLP-150; Fc=150 MHz (2 used) 2) Pre-Amplifier: Miteq AU-1310-N-1103-1179-WP 31 dB, 0.01 -500 MHz (see Note 1)
Band 2	325 - 340	1) Tunable Notch Filter set at 303.8 MHz to reject fundamental emissions, 40 dB rejection ratio (see Note 1) 2) Low Pass: K&L 8IL40-336/U468 (fc=336 MHz) to reject harmonics (2 used) 3) Pre-Amplifier: Miteq AU-1310-N-1103-1179-WP 31 dB, 0.01 -500 MHz
Band 3	960 - 1250	1) 20 dB Attenuator- Agilent 2) K&L LP, 1600 MHz, 7IL10-1600/X1710 3) K&L HP, 960-1600 MHz, 5IH10-960/U1600 (2 used) 4) Pre-Amplifier: MIteq-AMF-4F-00800250-06-13p, 60 dB, 800-2500 MHz
Band 4	1565 -1585	
Band 5	5020 - 5100	1) K&L Band Pass: 4FV30-5050/X100 (2 used) 2) Miteq AMF-5F-02600520-06-10P ; 60 dB; 2.6-5.2 GHz

*Note 1: Notch filter was used due to good rejection ratio between the closely spaced pass-band and stop-band. However, strong spurious emission between 313 and 320 MHz were not filtered due to the signal being too wide for a notch filter and the frequency too close to the measurement bands.

Table 3.2-7: Filters Used For Sovereign Tags (417.8 MHz & 433.72 MHz) and Savi's Tags (433.92 MHz)

Measurement Band	Meas. Freq. Range (MHz)	Interrogator Path Filters	Measurement Path Filters
Band 1	105 - 140	Beacon or Motion Tags No Filters needed	1) K&L LP 336 MHz 8IL40-336/U468 2) Pre-Amplifier: 31 dB Miteq AU-1310-N-1103-1179-WP, 0.01 -500 MHz
Band 2	325 - 340		
Band 3	960 - 1250		1) Tunable Notch filter (Savi-602 and -604 only) 2) 10 dB attenuator (Savi-602 and -604 tags only due to high noise) 3) K&L LP, 1600 MHz, 7IL10-1600/X1710 4) K&L HP, 960-1600 MHz, 5IH10-960/U1600 (2 used) 5) Pre-Amplifier: 60 dB MIteq-AMF-4F-00800250-06-13p, 800-2500 MHz
Band 4	1565 -1585		
Band 5	5020 - 5100		1) K&L BP 5.0-5.1 GHz: 4FV30-5050/X100 (2 used) 2) Pre-Amplifier, 60 dB Miteq AMF-5F-02600520-06-10P; 60 dB; 2.6-5.2 GHz

Table 3.2-8: Filters Used For WhereTag III Tag (2.4 – 2.4835 GHz)

(MHz) Band	Meas. Freq. Range (MHz)	Interrogator Path Filters	Measurement Path Filters
Band 1	105 - 140	No Filters needed. Beacon Tags	1) K&L LP 336 MHz 8IL40-336/U468 2) Pre-Amplifier: 31 dB Miteq AU-1310-N-1103-1179-WP, 0.01 -500 MHz
Band 2	325 - 340		
Band 3	960 - 1250		1) K&L LP, 1600 MHz, 6IL30-1600/U2497 3) Pre-Amplifier: 60 dB, MIteq-AMF-4F-00800250-06-13p, 800-2500 MHz
Band 4	1565 -1585		
Band 5	5020 - 5100		1) K&L BP 5.0-5.1 GHz: 4FV30-5050/X100 (2 used) 2) Pre-Amplifier, 60 dB Miteq AMF-5F-02600520-06-10P; 60 dB; 2.6-5.2 GHz

3.2.3 Emission Measurement Issues

Short burst-length RFID signals (presumably the same for the spurious emission during the burst transmission) require careful selection of equipment and settings for a balanced measurement speed and sensitivity. It is desirable that during a single burst transmission, the measurement instrument is able to sweep over the entire measurement band. It is also desirable that the instrument frequency sweeps and the burst signals are synchronized to ensure that all frequencies in the measurement bands are covered.

One approach is to sweep at rate low enough so that the sweep time to complete one sample (there are 601 samples per trace) is longer than the blink period of the tags. This approach ensures at least one tag transmission during the time it takes for the frequency to sweep across one frequency bin (of the 601 frequency bins per trace). However, for a 5 second blink rate, a frequency sweep would take nearly 1 hour, resulting in one sample at each frequency. 100 samples or more for each frequency is desired for the mode-stir method, resulting in a rather excessive 100 hours per tag (4 days), per measurement band. As a result this approach was tried and abandoned in favor of a more speedy approach, but possibly not as rigorous.

Several approaches were tried. The approach adopted was to put the spectrum analyzer trace display on maximum hold, while observing the results for convergence. The data are recorded at regular intervals, approximately every 15-30 minutes, and the results compared. Over a period of time, which may vary with different tags, the peak emissions converge to an envelope. The envelope data are chosen as the final results once the last several measurement traces are nearly identical.

Experimentations using the slow sweeps versus fast sweeps also did not show significant differences in a few test cases. However, measurements using fast sweeps reduced test time significantly. In many cases, the measurements converged within as short as 1 hour or less, especially for signals with longer duty factor.

Using this approach, the results were shown to be very repeatable, and the measurements could easily be repeated for verification purposes. More attention from the tester was required, however.

In addition to selecting the fast sweep rate, testing many tags at the same time can reduce test time significantly. Testing 20 tags concurrently can increase the burst transmission rate by factor of 20. However, there is a small possibility of having multiple tags transmit at the same time, resulting in cumulative effects at the receive antenna. The cumulative effects were previously defined as MEF.

MEF is not a major concern with RFID tags. The tag transmissions are very short relative to the blink period, and the chance of both signals transmitted at the same time is small. The probability of having three or more tags blink at the same time is even more remote. At the worst case, two tags contributing equally at the receive antenna would result in a 3 dB MEF. This small error is considered acceptable for the much reduced test time. However, it is highly unlikely that any two tags would blink at the same time while contributing *equally* at the receive antenna. Thus the MEF is expected to be lower than 3 dB. Table 3.2-9 shows the number of tags tested simultaneously to speed up the testing.

Table 3.2-9: RFID Tag Operation and Test Modes

Tag Models	Typical Operation Mode/ Test Mode	No. of tags Tested Concurrently
RF Code		
Motion Tags	Motion/ Motion	20
Beacon Tags	Beacon/ Beacon	20
Savi		
ST-654	Interrogated and Beacon/	25
ST-604	Beacon	30
ST-602		30
Sovereign		
ATS	Motion/ Motion	12
ATS-3A		12
Identec		
I-D2	Interrogated/ Interrogated	20
IQ-8		20
WhereTag III	Beacon/ Beacon	10

3.2.4 Data Reduction

Raw data were downloaded from the spectrum analyzer using SoftPlot, a commercial software package for interfacing with test instruments [14]. Using SoftPlot, up to 16 measurement traces can be compared in a single plot. This feature is highly desirable for monitoring convergence of the emission data. Once measurement traces converged, the data were exported to Microsoft Excel for additional processing. The data were processed according to Eq. 3.2-3 and 3.2-4. The emission results are show in Section 3.3.

3.3 RFID Measurement Results

The emission data were measured according to the process described. The peak emission envelopes for the tags are reported in Figures 3.3-1 to 3.3-25. They are organized according to the measurement Bands 1 to 5, and in the order according to the tags' operating frequencies.

It is not advisable to directly compare the tags' *peak* emissions for effects on aircraft radio receivers. The individual tag modulation characteristics, such as duty factor and pulse length, may affect aircraft radios differently. The effects of individual RFID tag's low duty factor on receiver interference thresholds should be considered in the interference analysis.

While emissions from other PEDs can be used as baselines for allowable devices as shown in Appendix A, they should not be compared directly with the tags emissions. The devices have very different duty factors, and their effects on radio receivers could be different. In addition, these PEDs are typically used in the passenger cabin, while the RFID tags are typically used on cargo containers in the cargo bay. The IPL data are different for the two locations.

3.3.1 Band 1

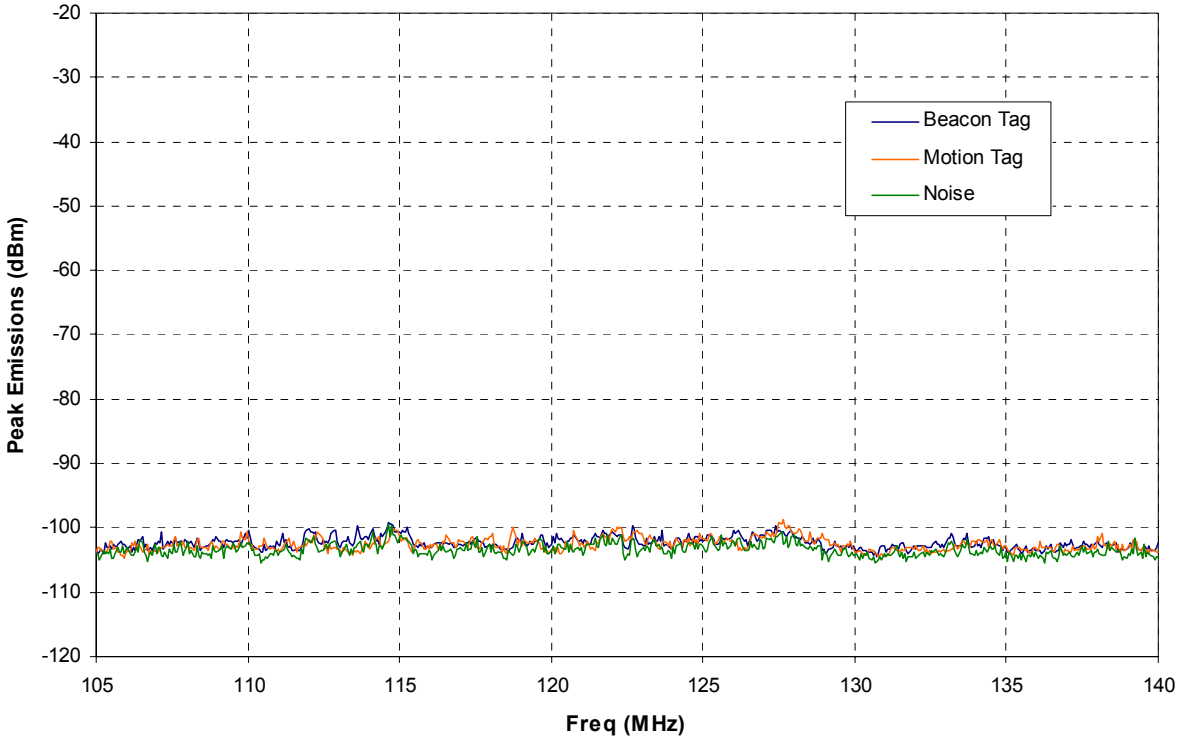

Figure 3.3-1: RF Code Tag Emissions, Band 1.

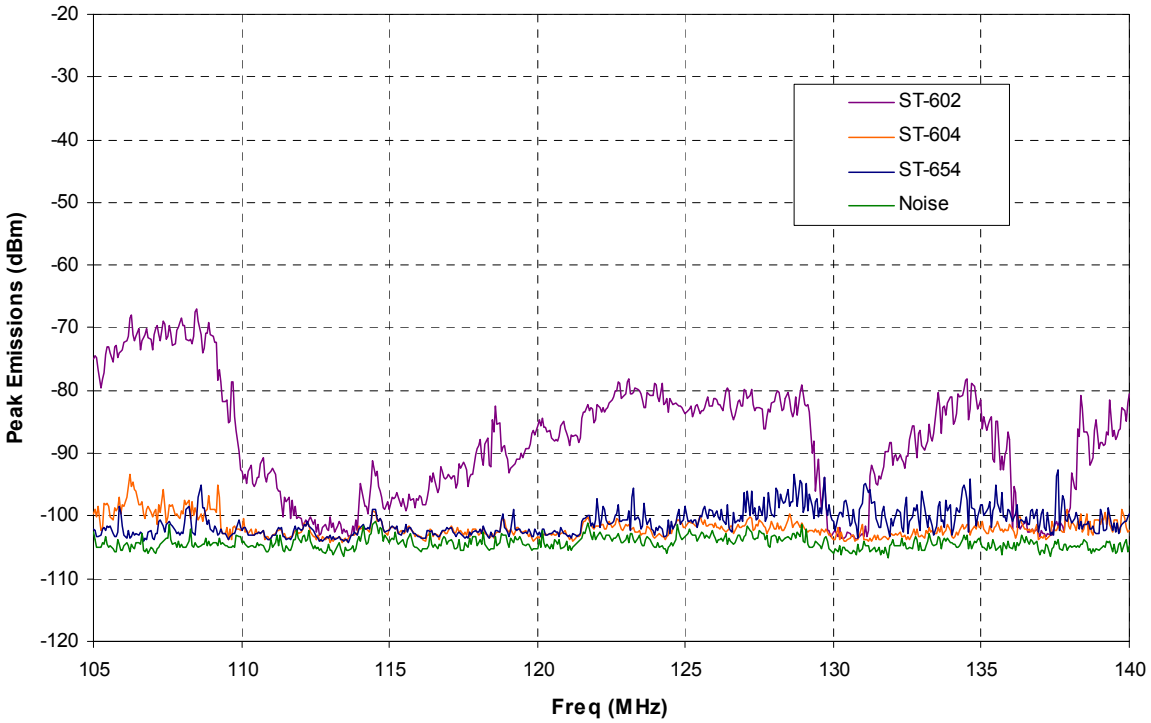

Figure 3.3-2: Savi Tag Emissions, Band 1.

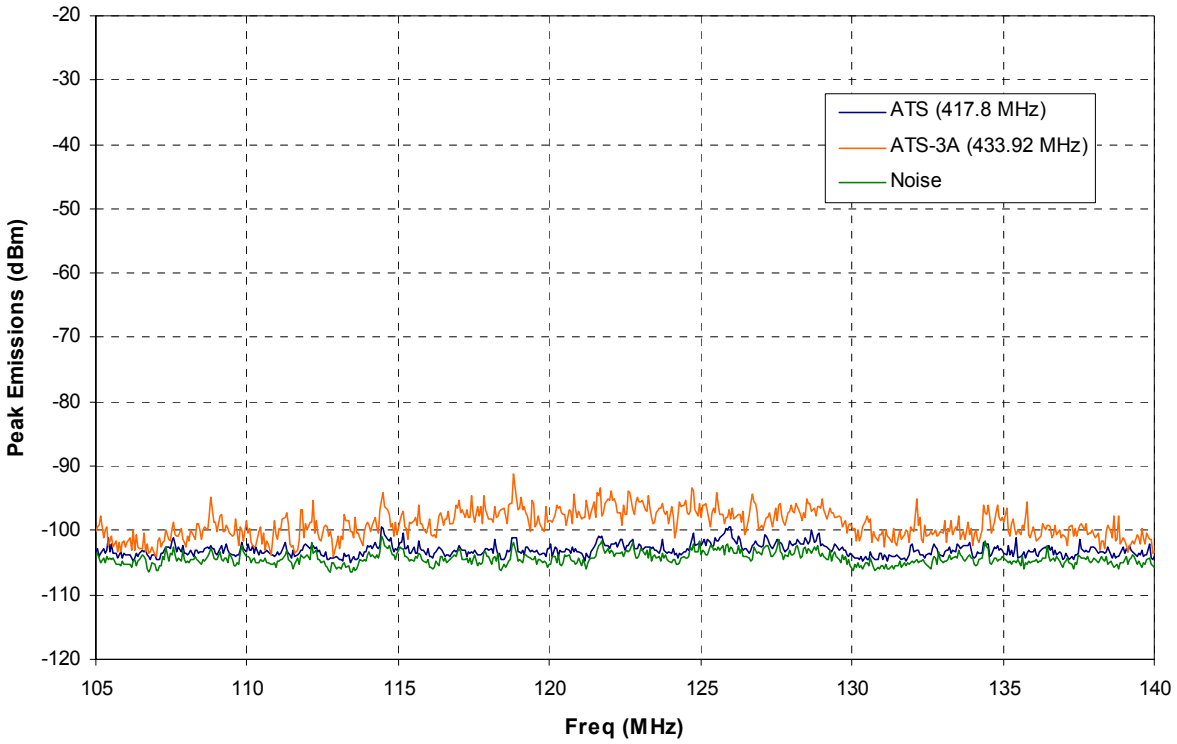

Figure 3.3-3: Sovereign Tag Emissions, Band 1.

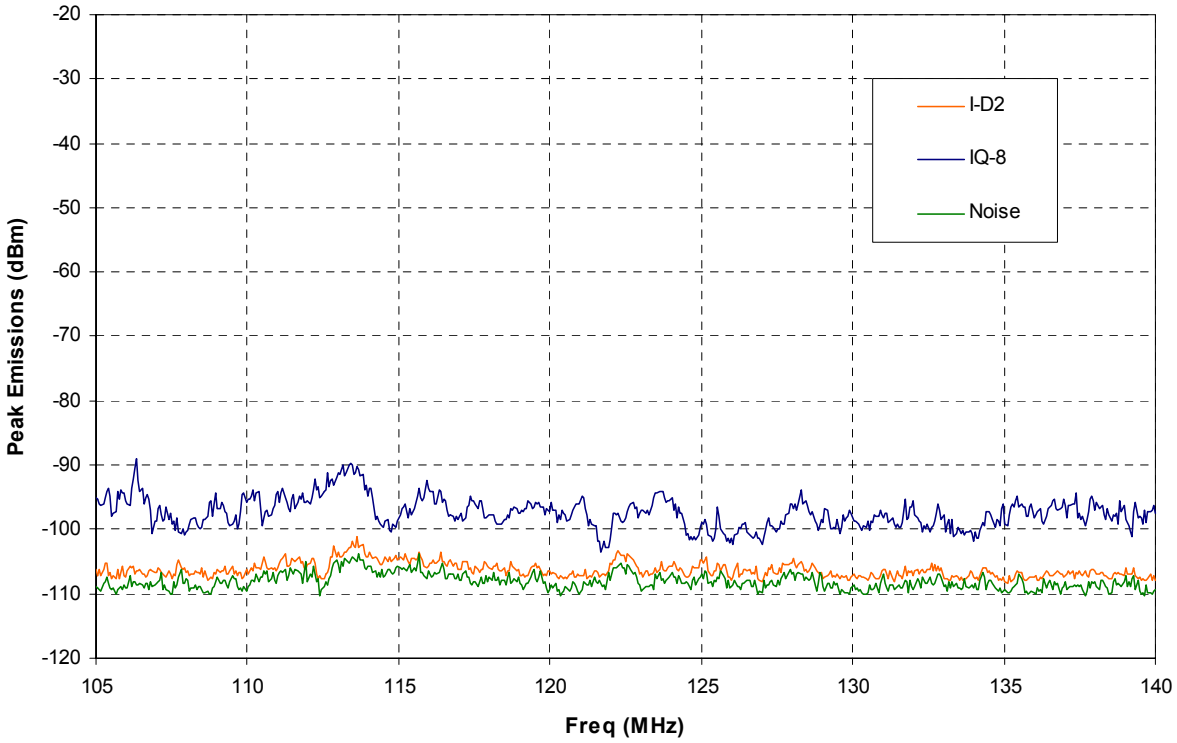

Figure 3.3-4: Identec Tag Emissions, Band 1.

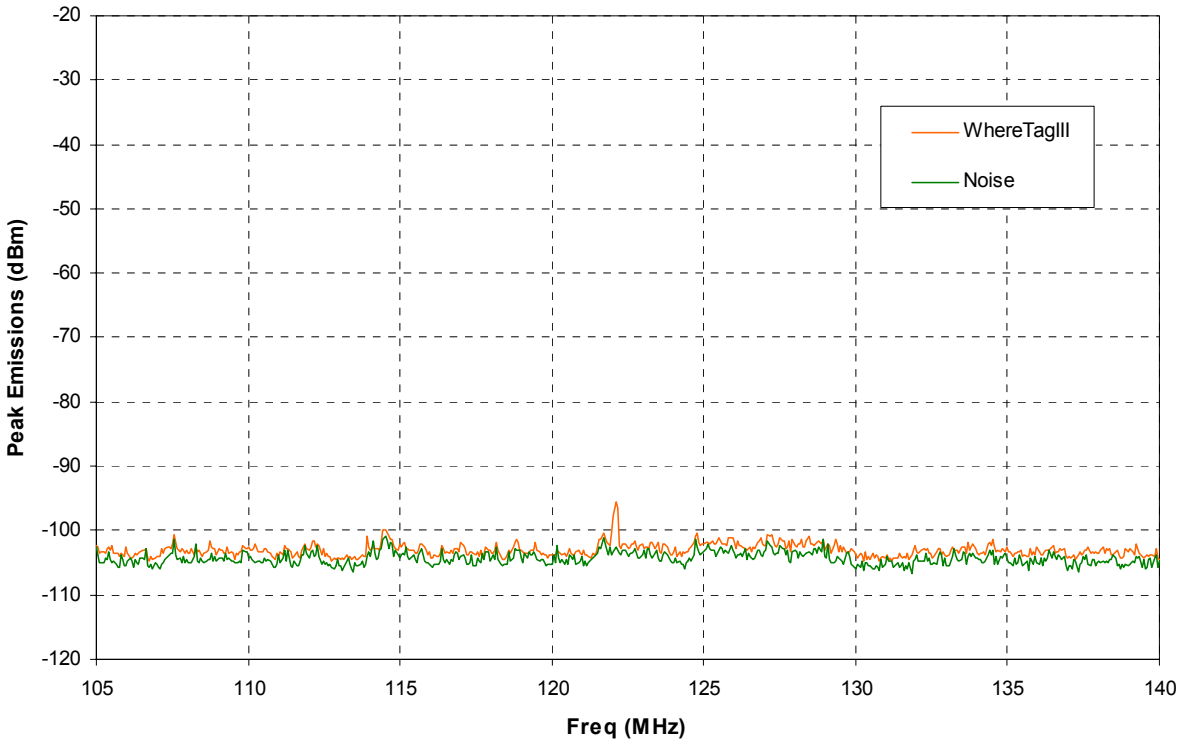

Figure 3.3-5: WhereNet Tag Emissions, Band 1.

3.3.2 Band 2

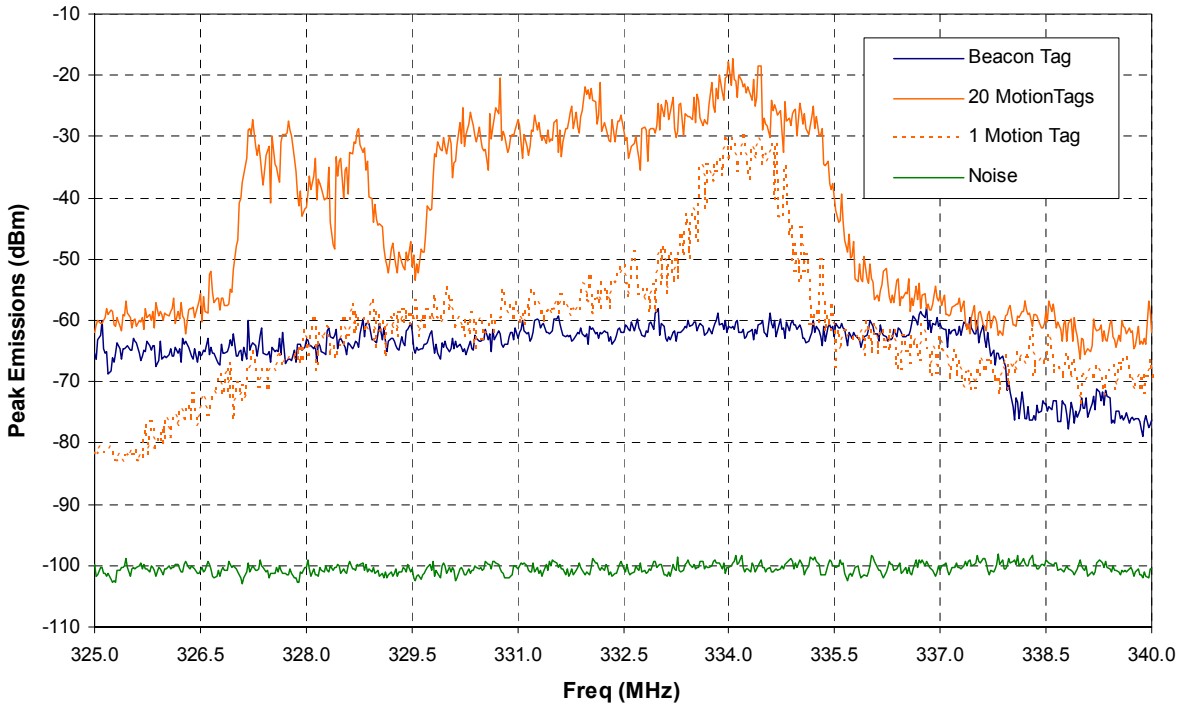

Figure 3.3-6: RF Code Tag Emissions, Band 2.

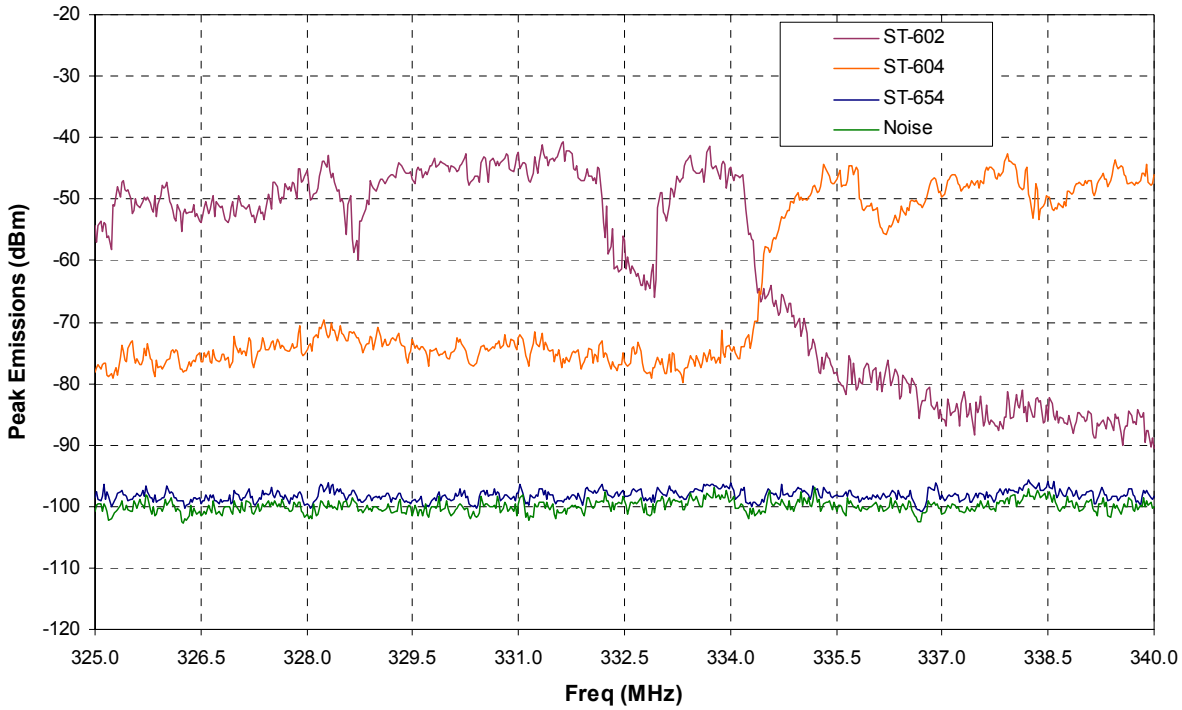

Figure 3.3-7: Savi Tag Emissions, Band 2.

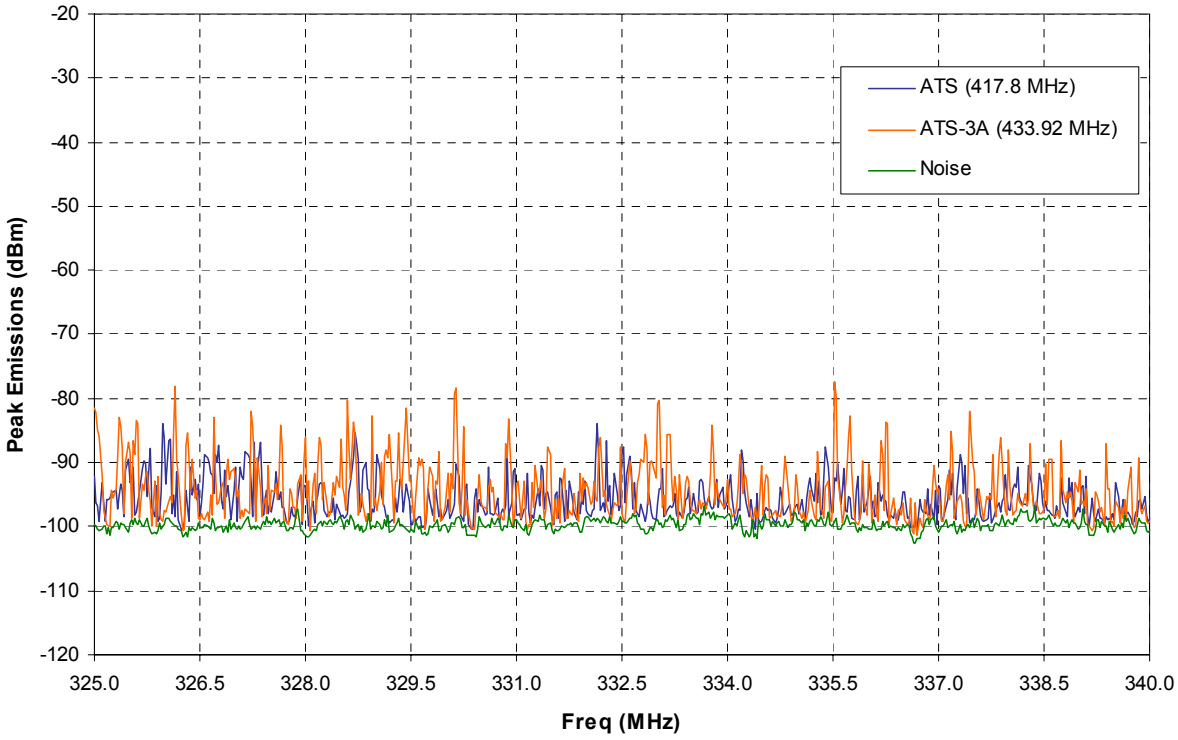

Figure 3.3-8: Sovereign Tag Emissions, Band 2.

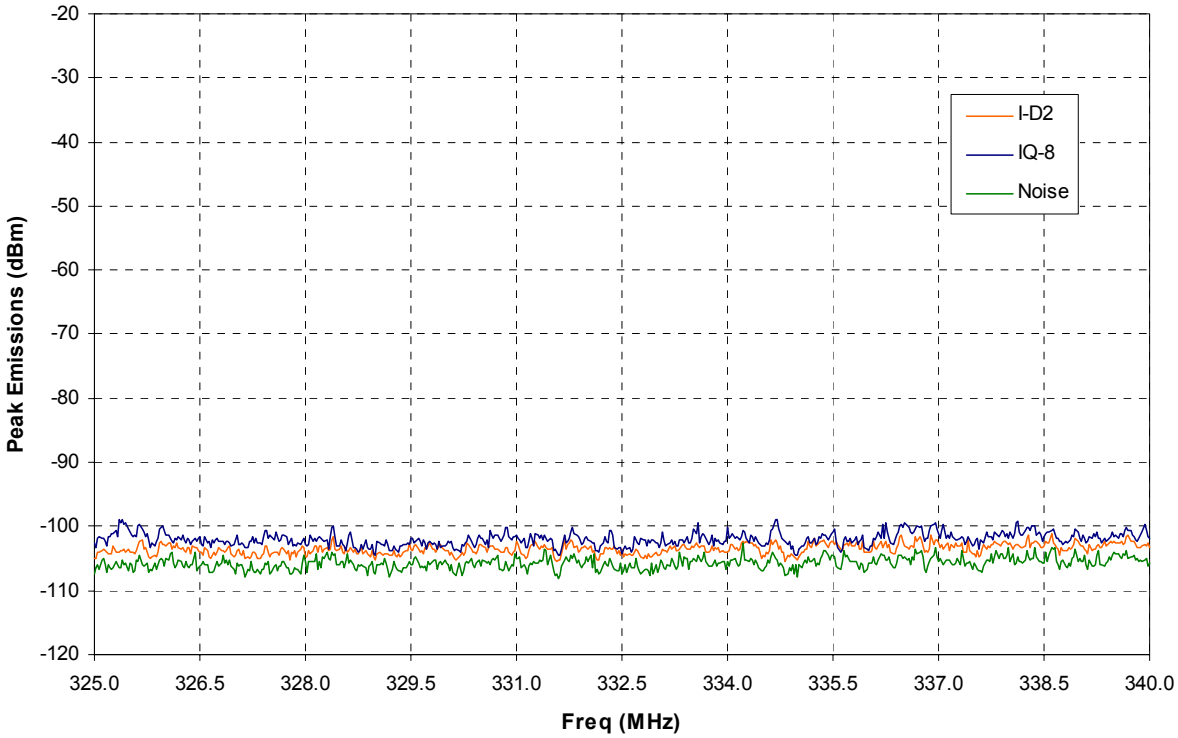

Figure 3.3-9: Identec Tag Emissions, Band 2.

Figure 3.3-10: WhereNet Tag Emissions, Band 2.

3.3.3 Band 3

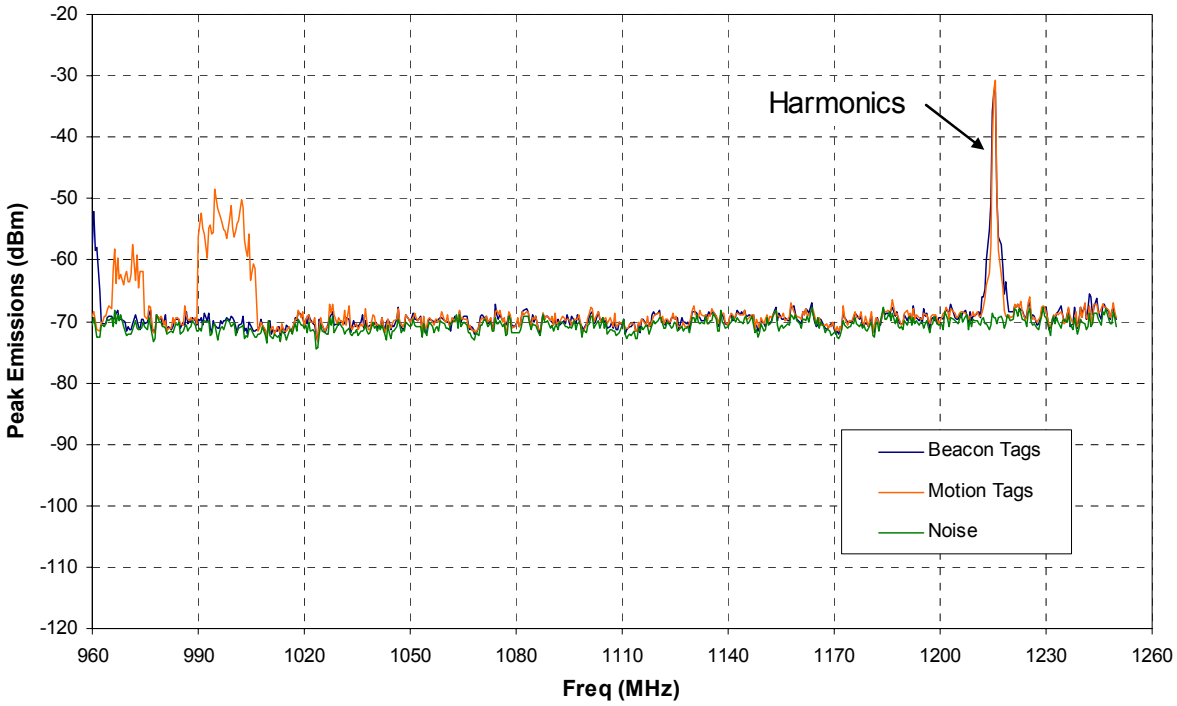

Figure 3.3-11: RF Code Tag Emissions, Band 3.

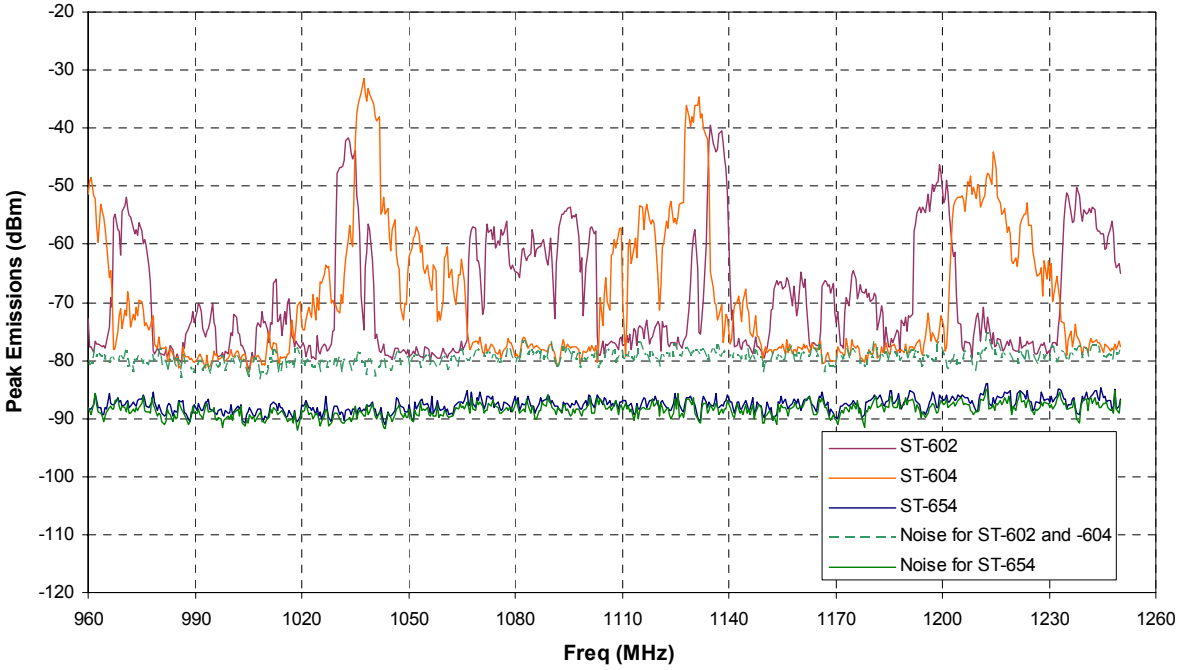

Figure 3.3-12: Savi Tag Emissions, Band 3.

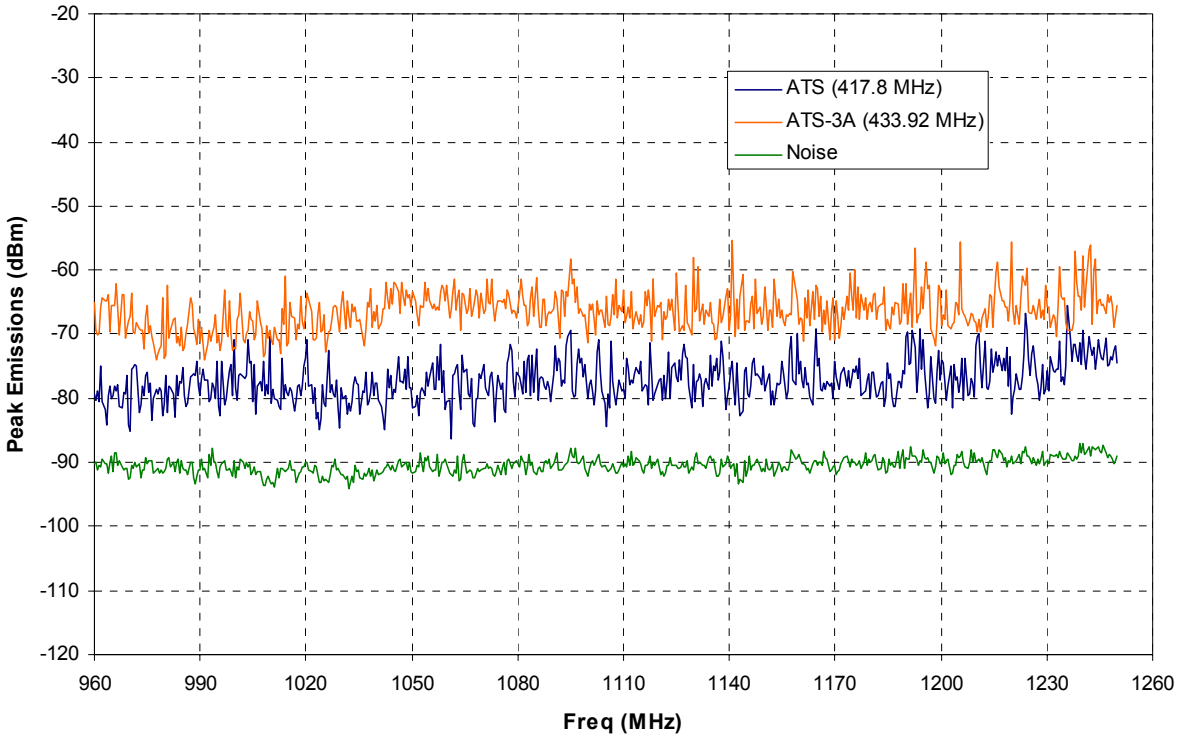

Figure 3.3-13: Sovereign Tag Emissions, Band 3.

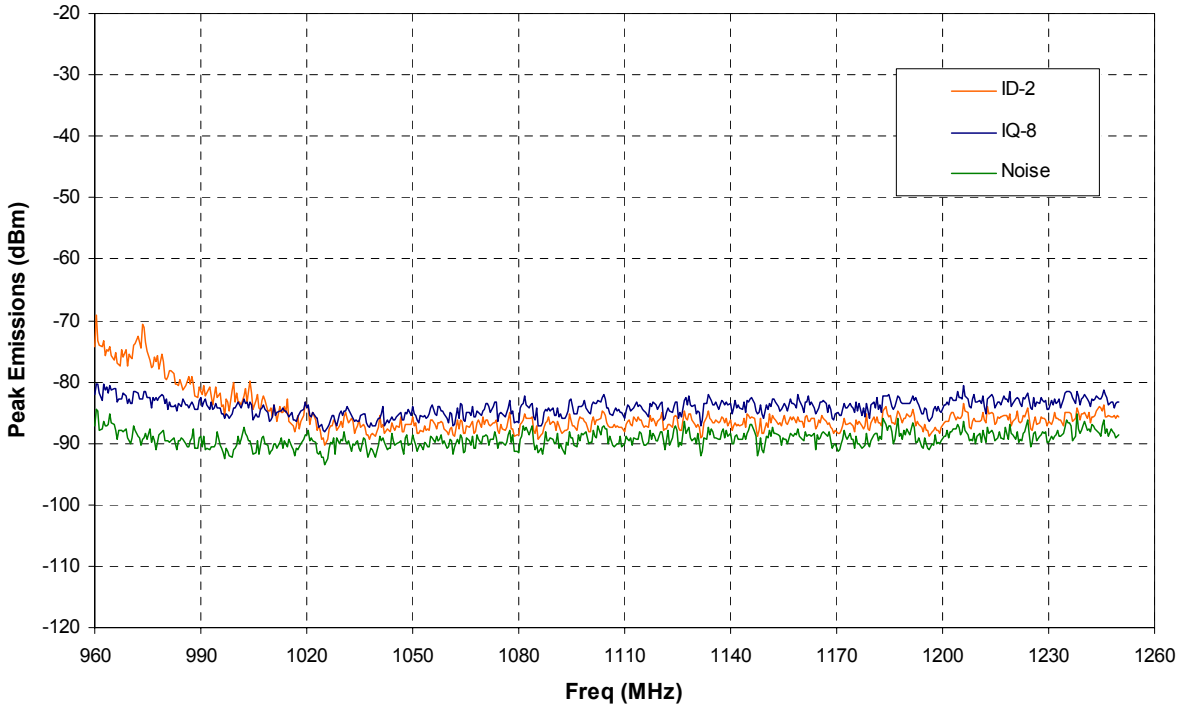

Figure 3.3-14: Identec Tag Emissions, Band 3.

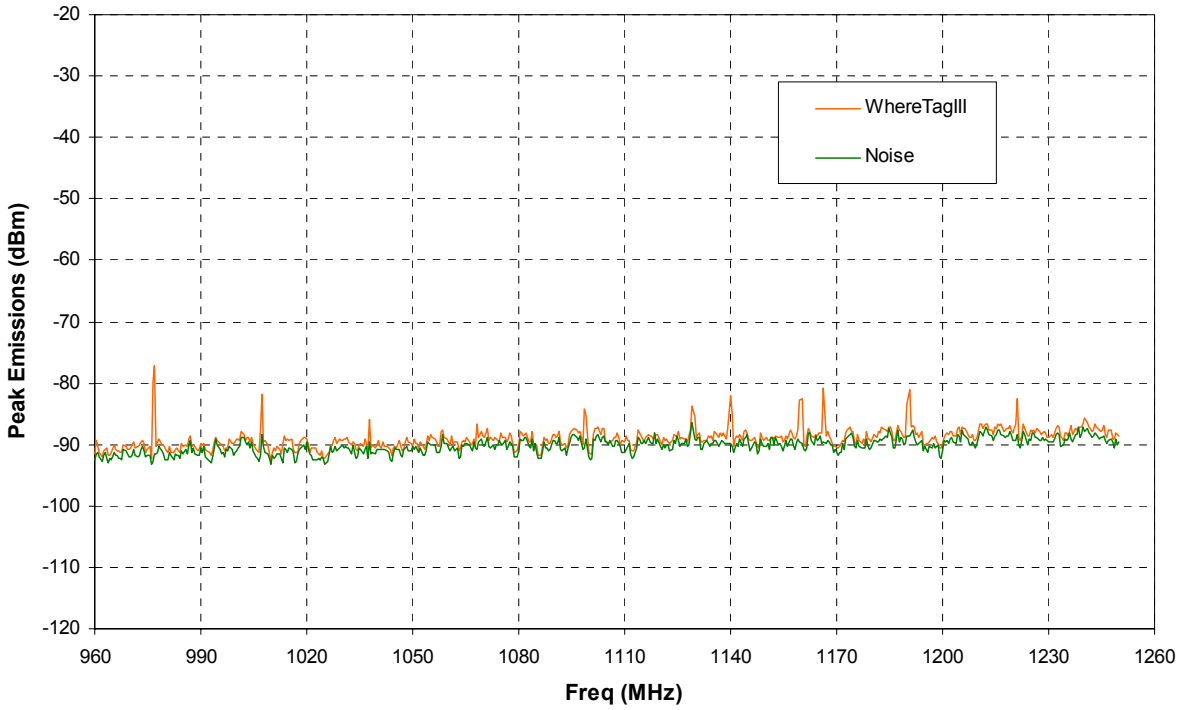

Figure 3.3-15: WhereNet Tag Emissions, Band 3.

3.3.4 Band 4

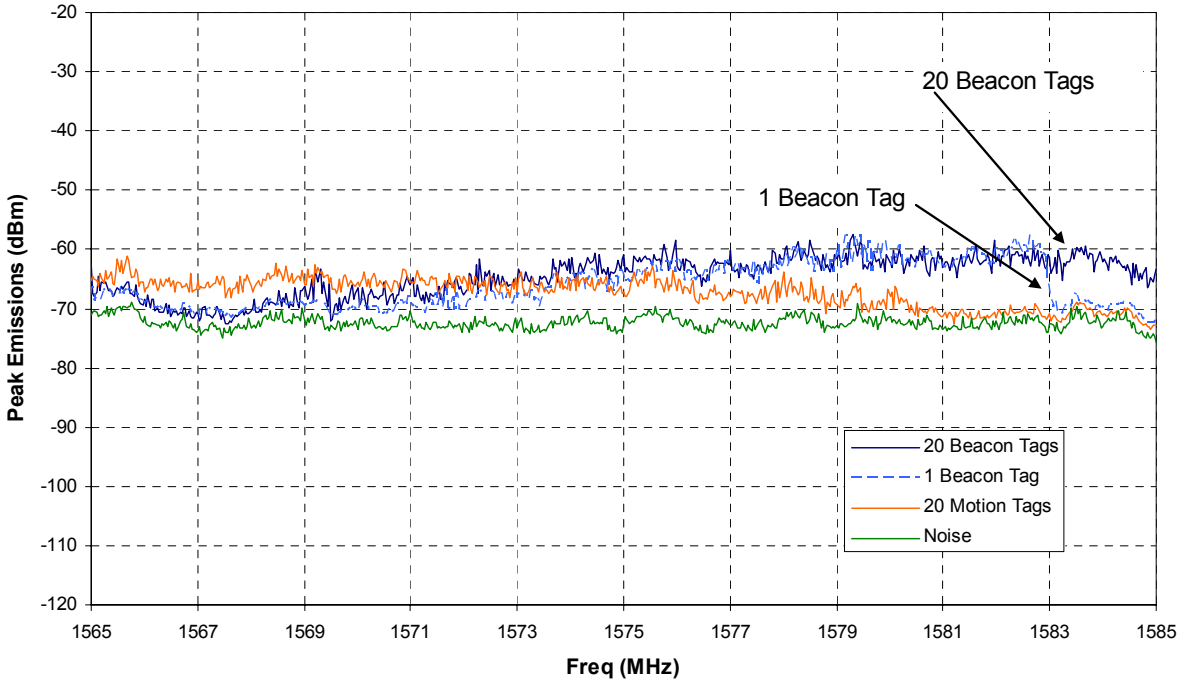

Figure 3.3-16: RF Code Tag Emissions, Band 4.

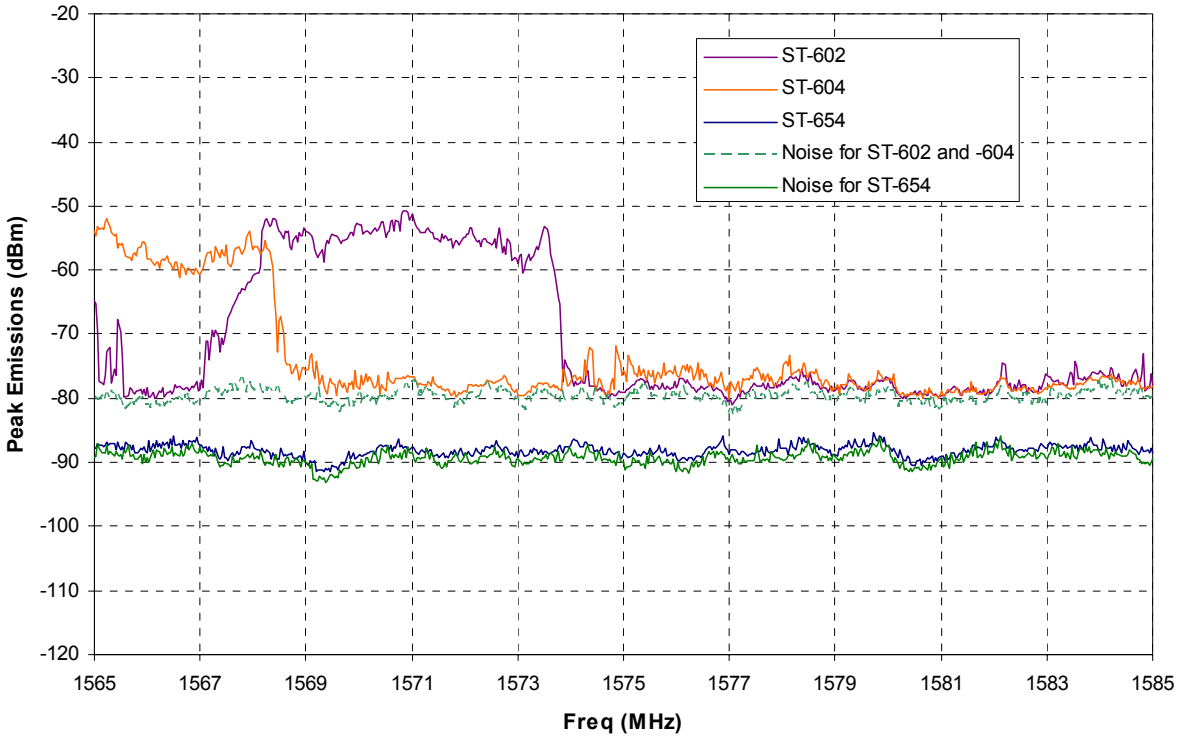

Figure 3.3-17: Savi Tag Emissions, Band 4.

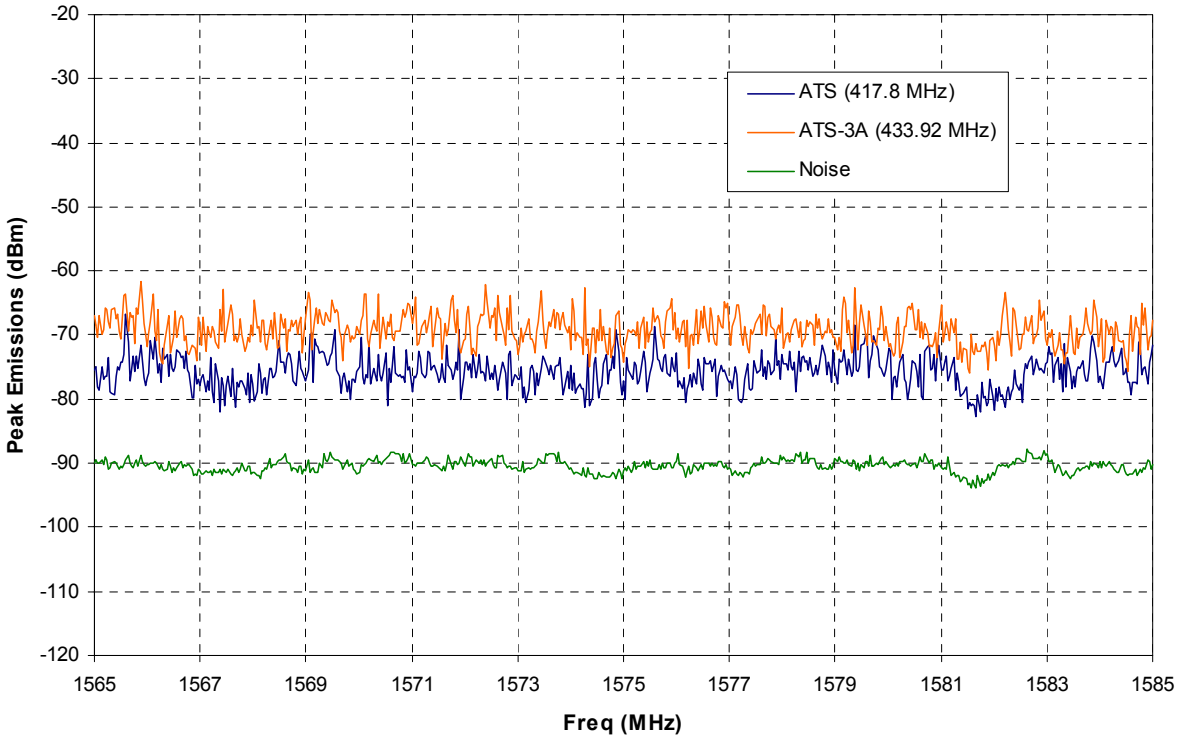

Figure 3.3-18: Sovereign Tag Emissions, Band 4.

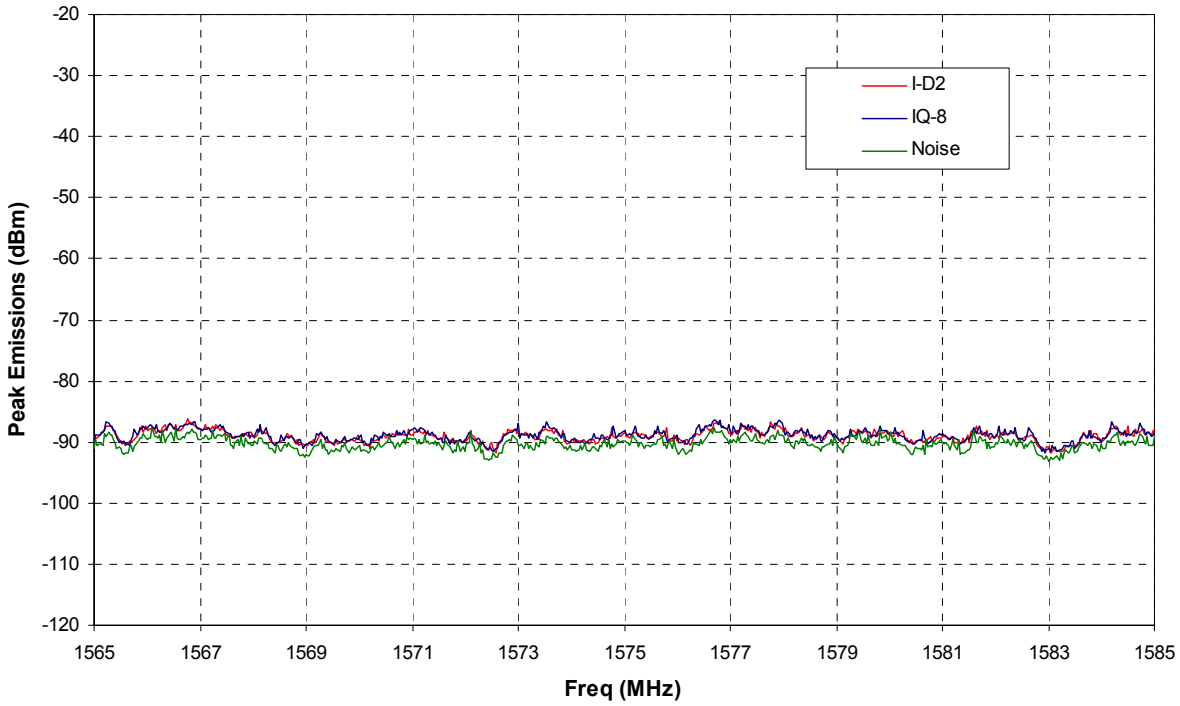

Figure 3.3-19: Identec Tag Emissions, Band 4.

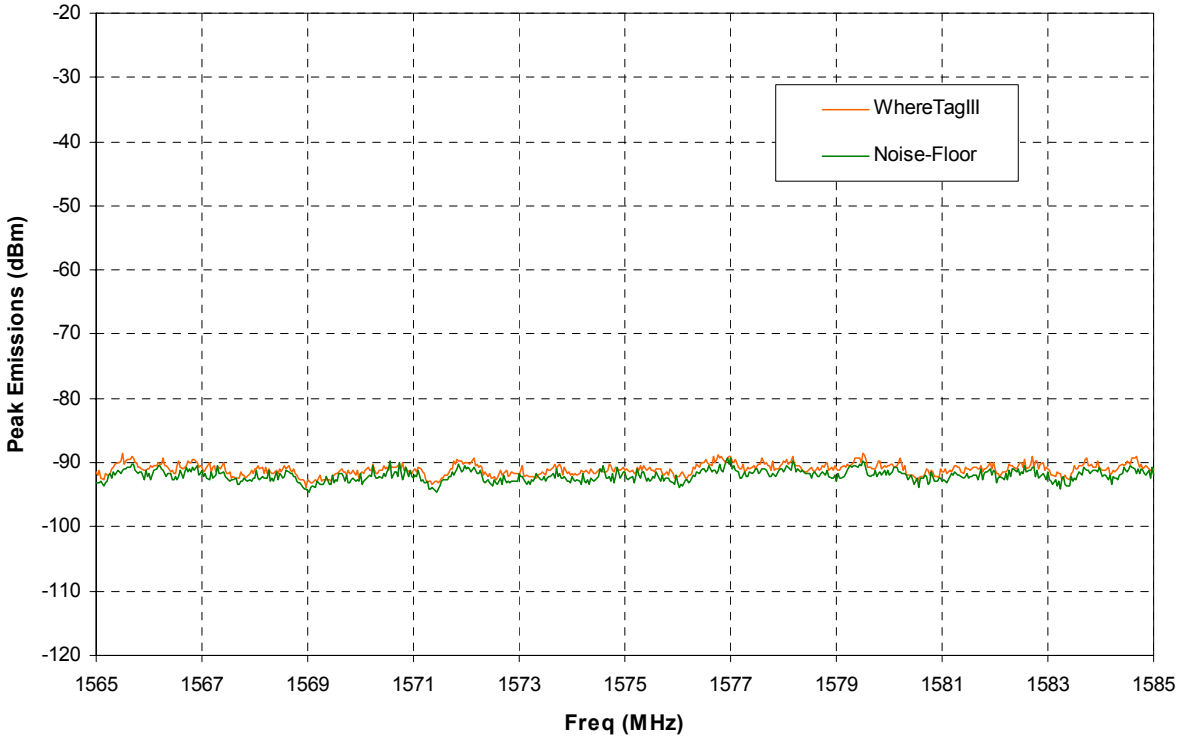

Figure 3.3-20: WhereNet Tag Emissions, Band 4.

3.3.5 Band 5

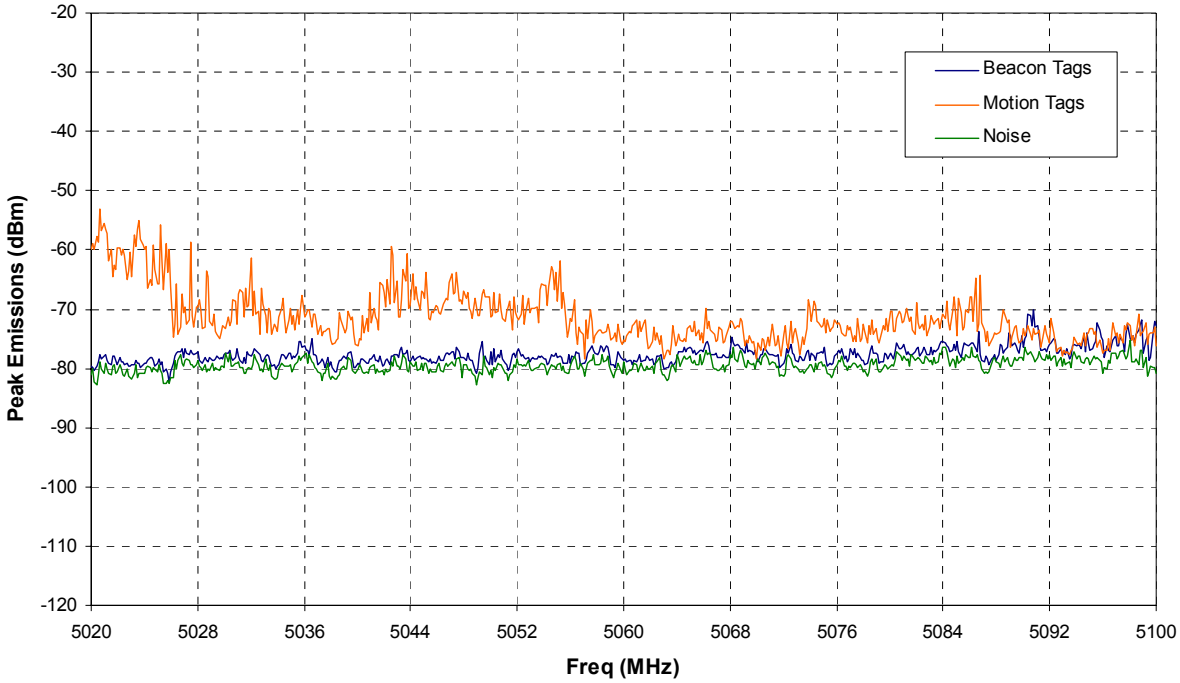

Figure 3.3-21: RF Code Tag Emissions, Band 5.

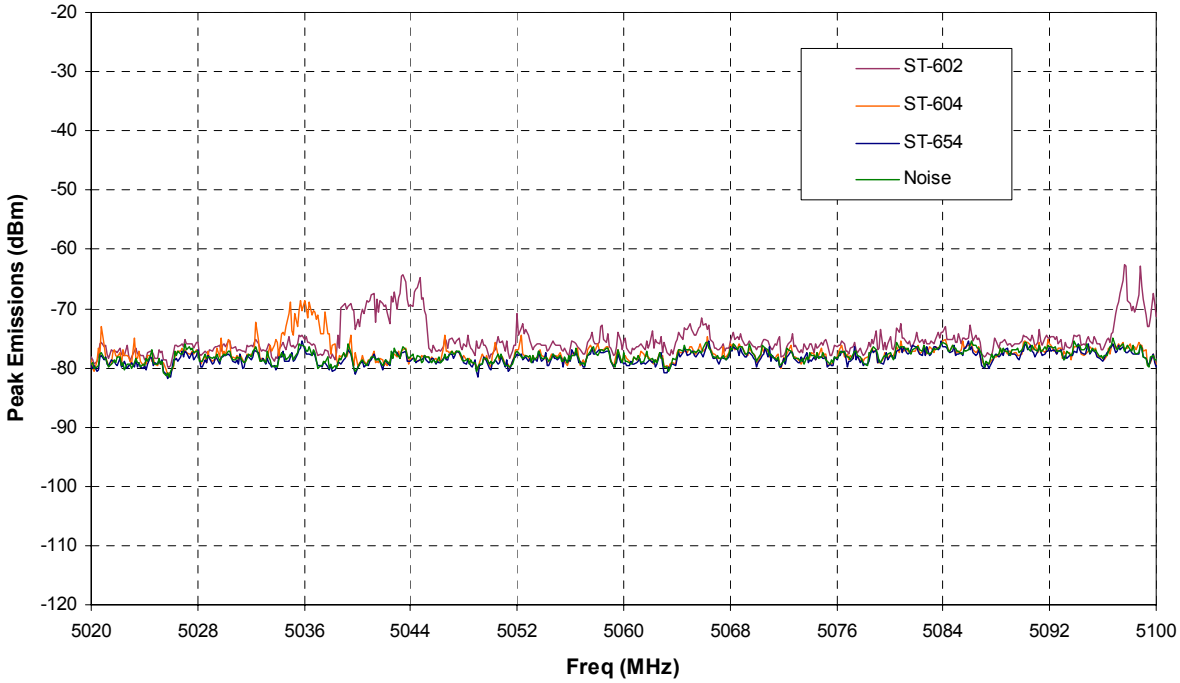

Figure 3.3-22: Savi Tag Emissions, Band 5.

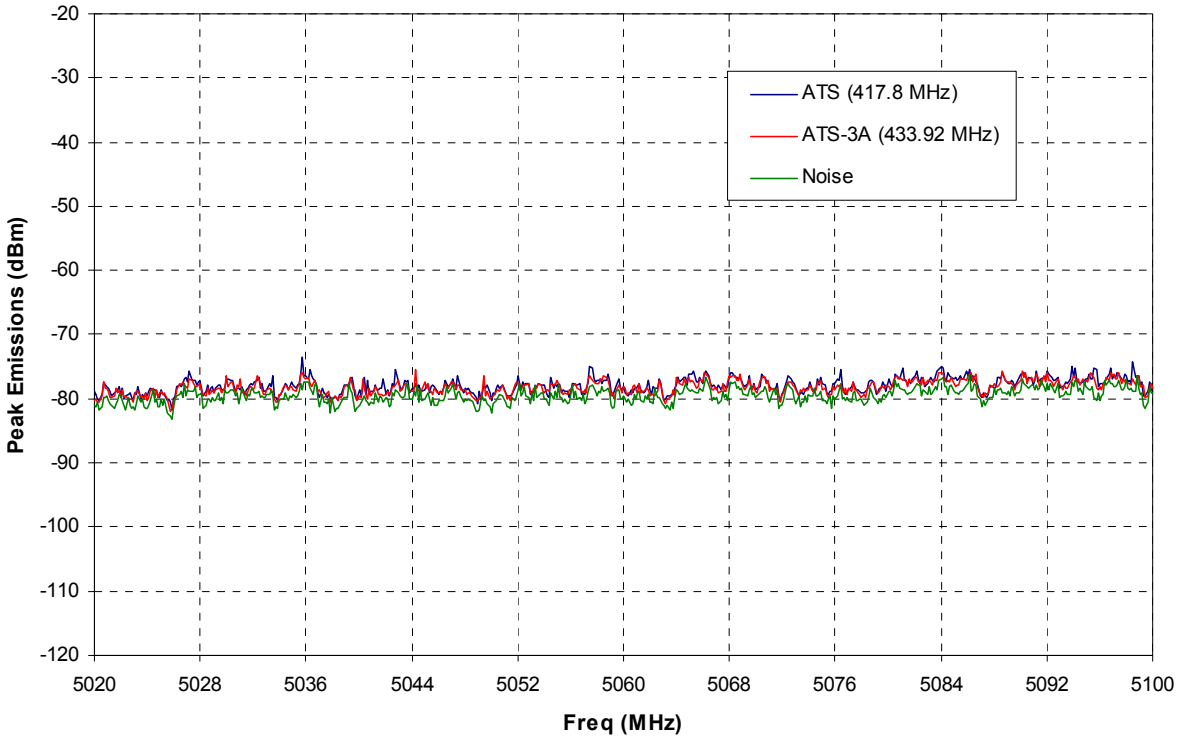

Figure 3.3-23: Sovereign Tag Emissions, Band 5.

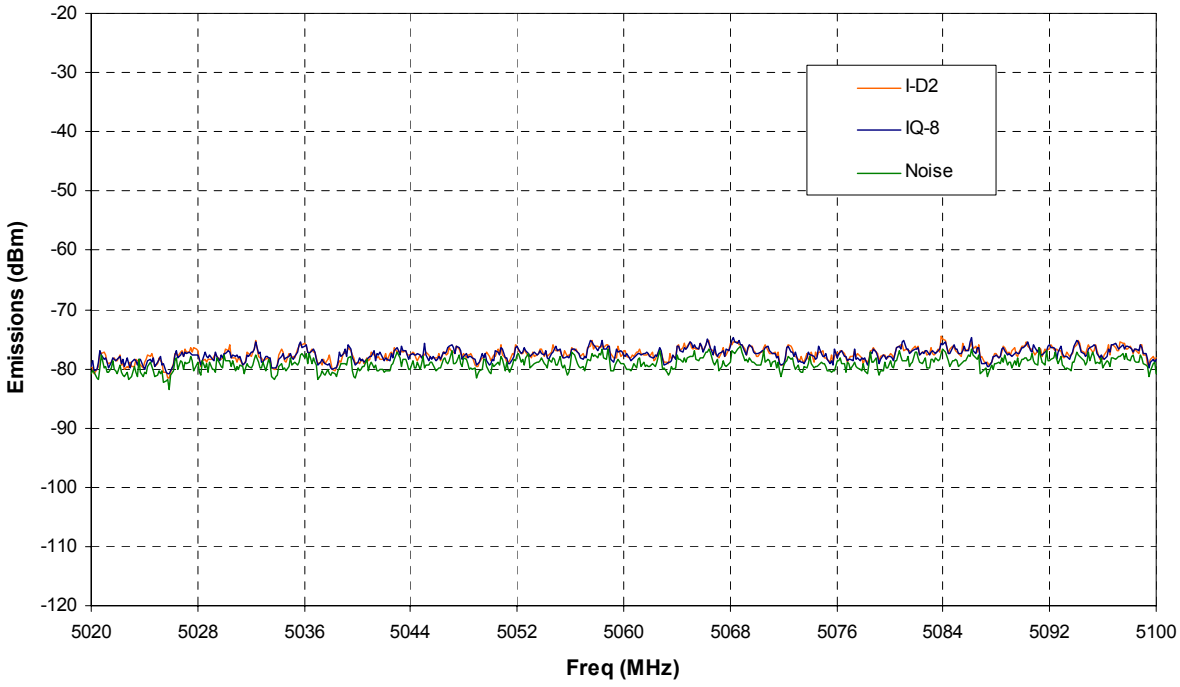

Figure 3.3-24: Identec Tag Emissions, Band 5.

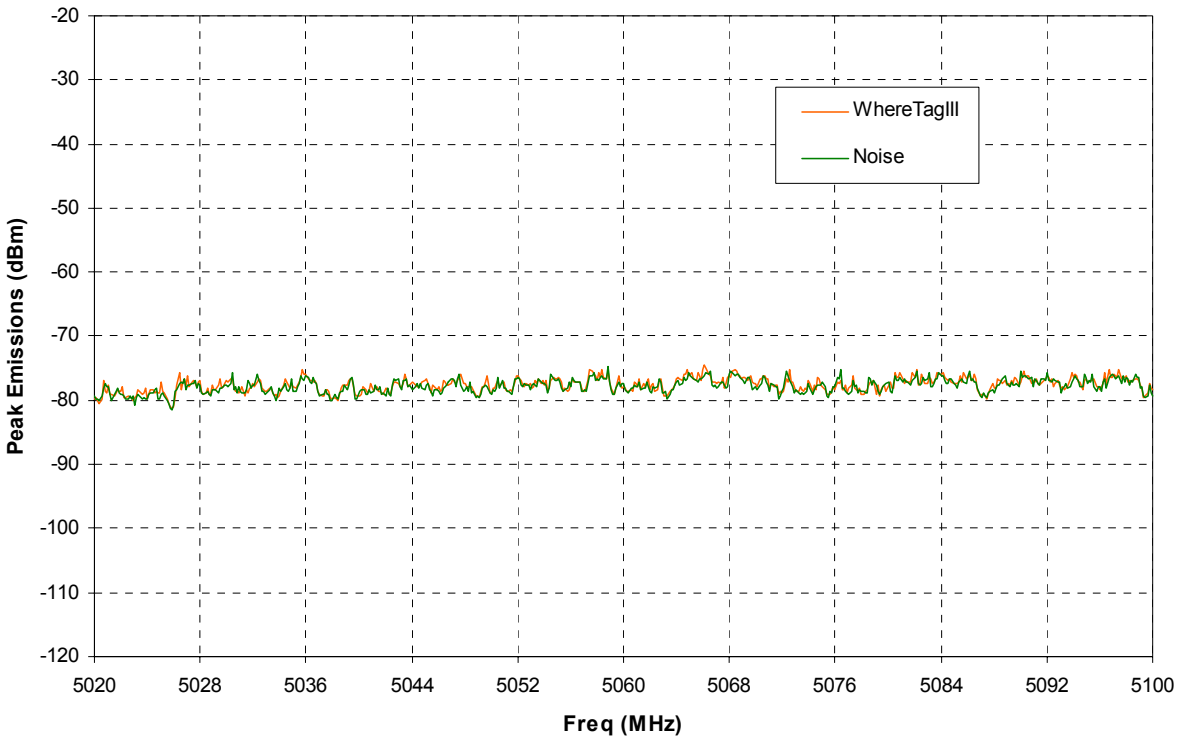

Figure 3.3-25: WhereNet Tag Emissions, Band 5.

3.3.6 Further Measurement Discussions

Multiple Tags Measurement

Figure 3.3-26 illustrates the benefits of testing multiple tags. It shows the peak emissions results for 20 RF Code's motion tags versus 1 motion tag. It is clear that there are large differences in the peak emission levels between the two measurements that can be as much as 35 dB at some frequencies. MEF or age of batteries cannot explain the difference. Pre-measurement scans, proper filtering and attenuations ensured that pre-amplifier overloading was not an issue. One possible explanation is that variability in manufacturing may result in different emissions. By simultaneously measuring the emissions of multiple tags, the emission envelope of each individual tags were captured.

Testing multiple tags may introduce small uncertainties due to MEF. However, it ensures that the emission envelopes of all the tags are captured. This benefit far outweighs the small extra uncertainty.

Without additional sources of uncertainties, the MEF effect typically appears as uniform offset between the emission levels for a single and multiple devices. Figure 3.3-16 compares the emissions of 20 RF Code's beacon tag versus 1 beacon tag in the GPS band. Both measurements show similar emission levels across most of the band, from 1565 to 1583 MHz, confirming MEF not being a significant concern in the measurement accuracy. Above 1583 MHz the data for 1 tag dropped to the noise level. While the cause for this drop is not determined, it is consistent that the multiple tags measurement establishes a bound for single device measurements.

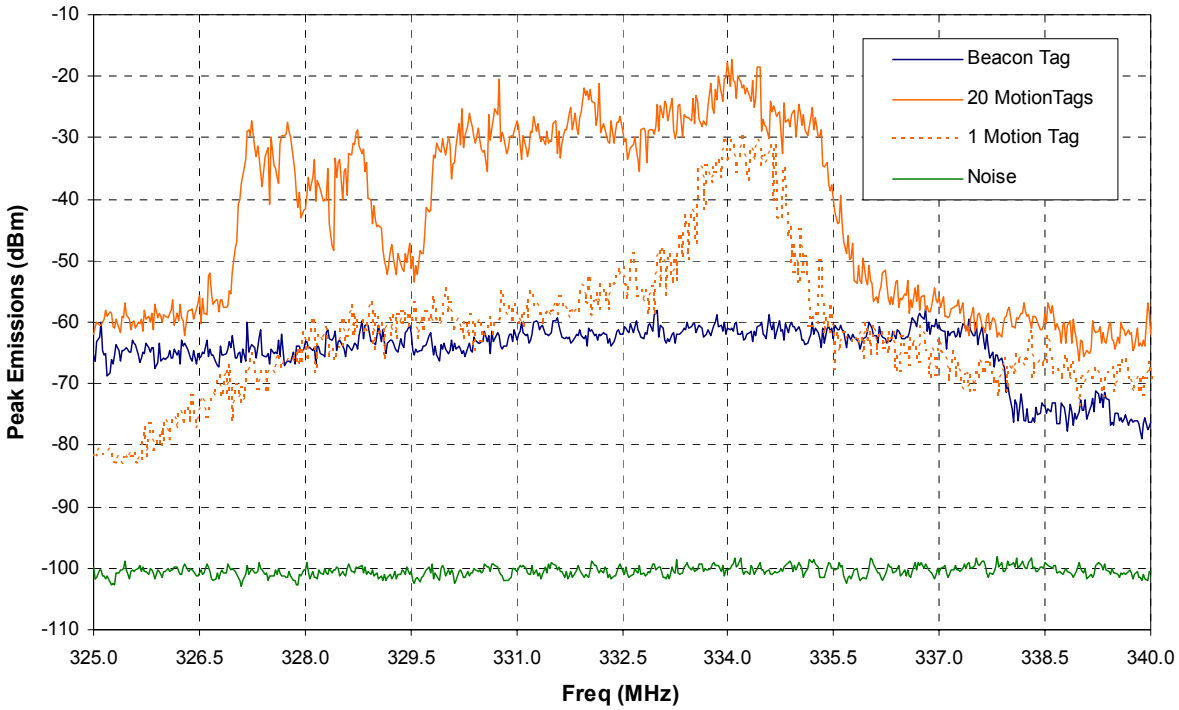

Figure 3.3-26: Comparison of emissions from RF Code's 20 motion tags versus 1 motion tag (repeat of Figure 3.3-6).

Performing Pre-measurement Scan

It is important to perform a pre-scan over the bandwidth of the components and of the set-up to identify any high emissions that could result in erroneous measurements. Once the high emissions are identified, it is preferable that they be filtered out for the best measurement sensitivity. However, not all emissions can be filtered. Proper pre-amplification and instrument attenuation should be selected such that the total power does not overload the pre-amplifier or the measurement instrument.

Figure 3.3-27 illustrates high emissions near the measurement bands. These high emissions were difficult to filter out. In this chart the data were downloaded from the spectrum analyzer and are unprocessed.

Figure 3.3-28 shows the final measurement after high emissions were identified with the fundamental emissions filtered out and a 30 dB (nominal) pre-amplifier added. The measurement also shows a response to a -40 dBm calibration signal. This figure illustrates better measurement sensitivity than the previous figure.

Figure 3.3-29 provides another illustration of high emissions outside the measurement Bands 1 and 2 that were not filtered out. As a result the measurements were performed with reduced amplification, resulting in reduced sensitivity.

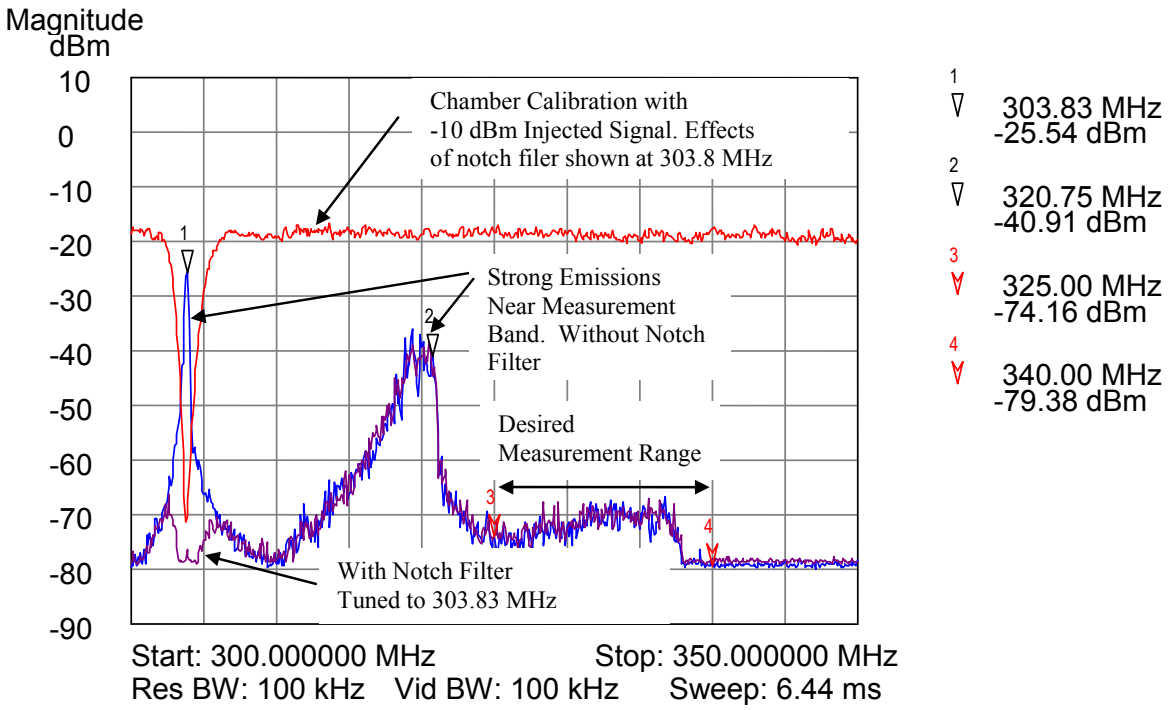

Figure 3.3-27: Illustrations of strong emissions at locations (1) and (2) near the measurement range (3)-(4) for RF Code's beacon tags. Emissions at (1) were filtered using a notch filter. Notch filter is not effective for broadband emissions at (2). Pre-amplifier was not used.

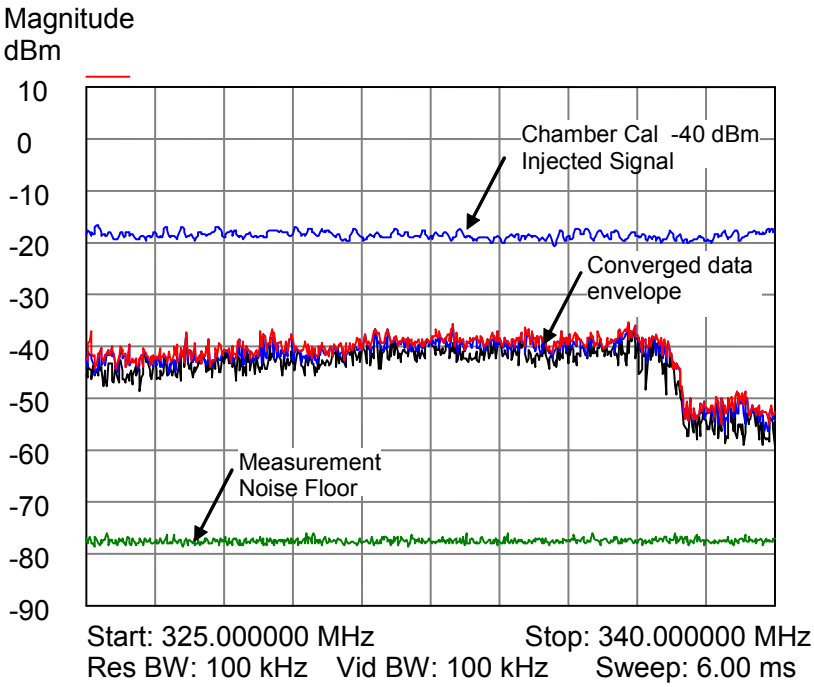

Figure 3.3-28: Raw emission data from spectrum analyzer for RF-Code's beacon tags. Measurements were performed over desirable frequency range with 30 dB pre-amplifier. Multiple traces show the data converged to the final trace label in red.

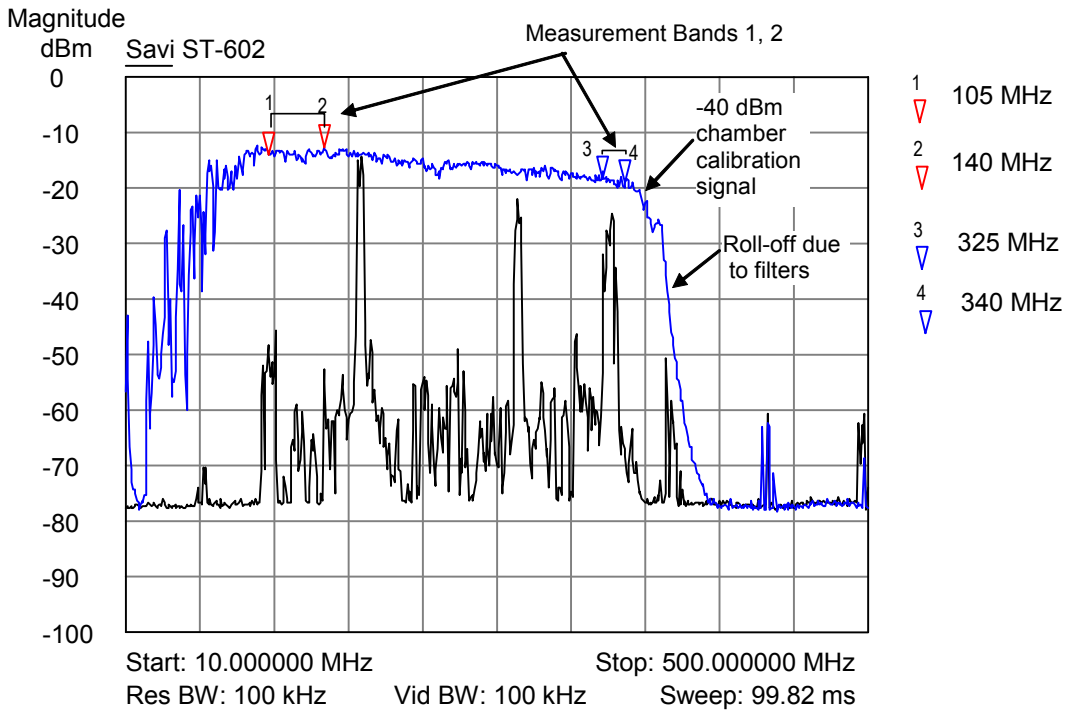

Figure 3.3-29: A pre-measurement sweep of Savi ST-602 tag to confirm filter selection and amplification level. A -40 dBm signal resulted in the "calibration signal" trace as labeled. Data not calibrated.

3.4 Result Summary and Spurious Emission Limit Comparison

This section summarizes the measurement results and compares them against the RTCA/DO-160E Section 21 spurious emission limits. Section 3.4.1 summarizes the results in table and graph formats. Section 3.4.2 compares the tags from each manufacturer against the aircraft emission limits.

3.4.1 Result Summary

Table 3.4-1 summarizes the measured emissions levels from all the tags measured. The table summarizes the peak emission data reported earlier in the figures. Data that were near or below the measurement noise-floor are shown in parenthesis. These data may not be a real representation of the actual device emission, which could be lower. Rather, they represent the sensitivity limit for the particular set-up.

Table 3.4-1: Peak Emission Level in the Measurement Bands

Tag Models	Peak Emission Level (dBm)				
	Band 1	**Band 2**	**Band 3**	**Band 4**	**Band 5**
RF Code					
Mantis 2s Beacon	(-99.1)	**-57.7**	**-52.0 ***	**-57.4**	**-70.8**
Motion Activated	(-98.8)	**-17.2**	**-48.4 ***	**-61.2**	**-53.1**
Savi					
ST-602	**-67.0**	**-40.7**	**-39.5**	**-50.7**	**-62.5**
ST-604	**-93.4**	**-42.6**	**-31.6**	**-51.9**	**-68.7**
ST-654	**-92.7**	(-95.6)	(-84.0)	(-85.5)	(-75.4)
Sovereign (12 tags)					
ATS (417.8 MHz)	(-99.3)	**-83.9**	**-65.4**	**-66.8**	(-73.4)
ATS-3A (433.92 MHz)	**-91.1**	**-77.3**	**-55.3**	**-61.6**	(-75.4)
Identec					
I-D2	(-101.2)	**-101**	**-69.2**	(-86.2)	(-74.6)
IQ-8	**-89.0**	**-98.8**	**-80.4**	(-86.4)	(-74.6)
WhereTag III	**-95.6**	**-86.8**	**-77.3**	(-88.6)	(-74.5)

***** Third Harmonic frequency is outside of DME band. Therefore, the harmonic emission levels are not included in this table. It is thought that the fundamental frequencies are unlikely to vary sufficiently to cause the harmonics to fall within DME to be of concerns.

( ) Data indicate peak emissions below or close to measurement noise floor

Figure 3.4-1 plots the data in Table 3.4-1. Data for tags from the same vendor were grouped and have similar trace colors and marker shapes. The individual tags are separated from one another with different trace patterns. It is also important to note that the lines are used in linking the data points at the markers for visual effects. Their magnitudes *between* the markers have no intrinsic values.

In addition, the data points that are at or below the measurement noise floor are labeled with hollow markers. At these markers, the emissions were too low to be measured with the current set-up. Thus, the values simply represent the measurement sensitivity.

It is also important to note that measurement noise floors may be different for different tags. The tags were measured with different set-ups to maximize sensitivity and accommodate individual tag operating and emission characteristics. The setup differences may include variations in pre-amplification level, filter selection, and spectrum analyzer attenuation level. These variations resulted in different measurement noise floors. In fact, the measurement data for one tag may be below the noise-floor for another measurement.

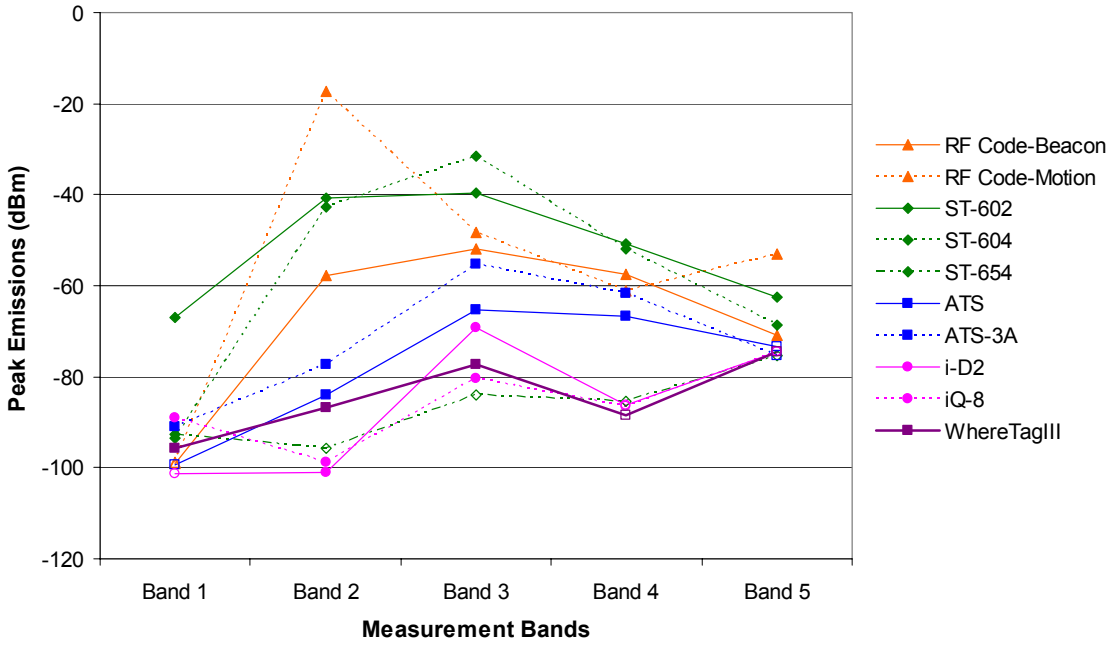

Figure 3.4-1: RFID tags emission summary.

3.4.2 RTCA/DO-160E Emission Limit

Category L is the most appropriate for equipment located in the cargo bay of an aircraft. According to RTCA/DO-160E Section 21 [15]:

"Category L: *This category is defined for equipment and interconnected wiring located in areas far from apertures of the aircraft (such as windows) and far from radio receiver's antenna. This category may be suitable for equipment and associated interconnecting wiring located in the electronic bay of an aircraft.*"

In many cases an aircraft cargo bay is located adjacent to the electronic bay without additional shielding between the two bays. Thus the emission limits used for the electronic bay should be appropriate for the cargo bay.

Category M may also be appropriate for cargos that are in the passenger cabin, close to windows or near large apertures. Past studies also indicate strong RF leakage at aircraft doors at low frequencies [3], thus locations near the cargo doors may also fit under Category M. According to RTCA/DO-160E Section 21 [15]:

"Category M: *This category is defined for equipment and interconnected wiring located in areas where apertures are EM (electro-magnetically) significant and not directly in view of radio receiver's antenna. This category may be suitable for equipment and associated interconnecting wiring located in the passenger cabin or in the cockpit of a transport aircraft.*"

To compare with measured emission data in dBm, the field emission limits in RTCA/DO-160E Categories L and M are converted to the equivalent *effective isotropic radiated power* (*EIRP*) using Eq. 3.4-1. In addition, *Effective Radiated Power (ERP)* can be computed from *EIRP* using Eq. 3.4-2.

$$EIRP = \frac{E^2 \cdot 4\pi R^2}{120\pi} \text{ (watts)} \qquad \text{(Eq. 3.4-1)}$$

$$ERP\ (dBm) = EIRP(dBm) - 2.15\ (dB) \qquad \text{(Eq. 3.4-2)}$$

where E = Electric Field Intensity at distance R (*V/m*)

R = Distance (*m*)

Ideally, *E* field measurement is taken in the direction of maximum radiation from the test device. To convert power, *EIRP,* from watts to dBm, the expression *10 * log(1000*EIRP)* should be used. For the RTCA/DO-160E limit given in *dBμV/m*, the unit is converted to *V/m* before applying Eq. 3.4-1.

Table 3.4-2 details the categories L and M emission limits in dBμV/m measured at 1 meter distance. The minimum limit value within each of the measurement bands is chosen for that band. The values are converted to EIRP in dBm assuming unity device directivity.

Table 3.4-2: Band Minimum RTCA/DO-160E Section 21 Spurious Radiated Emission Limits

	Emission Limits at 1 m (dBμV/m)		**Equivalent EIRP Limits (dBm)**	
	Category L	**Category M**	**Category L**	**Category M**
Band 1	45.0	35.0	**-59.8**	**-69.8**
Band 2	52.8	52.8	**-52.0**	**-52.0**
Band 3	60.3	50.0	**-44.5**	**-54.8**
Band 4	63.7	53.7	**-41.1**	**-51.1**
Band 5	71.8	71.8	**-33.0**	**-33.0**

3.4.3 Spurious Emission Limit Comparison

Radiated emissions measured using a reverberation chamber provide results in "total radiated power" (*TRP*) within the measurement resolution bandwidth. *TRP* is different from *EIRP* and *ERP* except for antennas or devices with an isotropic radiation pattern. Rather,

$$EIRP\ (\text{dBm}) = TRP\ (\text{dBm}) + D_G\ (\text{dB}), \qquad \text{(Eq. 3.4-3)}$$

where D_G is *directivity,* or maximum *directive gain* of the test device. Directive gain of any device is a measure of radiated power as a function of aspect angle referenced to the isotropic value. For spurious emissions, D_G is the directivity at the spurious emission frequency of interest. D_G is usually difficult to measure or calculate since maximum radiation angles and radiation mechanisms for *spurious* emissions are often not known. Maximum theoretical estimation of D_G based on device size tends to significantly over-estimate the real directivity, especially at high frequency, because the device geometry is typically not designed to radiate efficiently as an antenna as assumed in the theoretical estimation. However, there

are recent theoretical statistical developments to estimate the "expected" directivity for non-intentional radiators [16]. Additional details on expected directivity are discussed in Section 3.5.

For simplicity, the tested devices (RFID tags) are assumed to have unity D_G for spurious emissions. Thus, *TRP* is assumed to be the same as *EIRP* at all spurious frequencies of interest. This assumption introduces an uncertainty level equal to D_G, according to Eq. 3.4-3. For a dipole antenna with small electrical length, D_G is close to 1.76 dBi (or dB relative to isotropic). For a half-wave dipole, D_G is close to 2.15 dBi. This level of uncertainty is considered acceptable for a first order comparison.

In comparing the emission levels (shown in TRP) against the emission limits (shown in EIRP), the data representing the tag emissions should be raised by the same dB level as the device's directive gain, if known. The *expected* directive gains for the devices are discussed in section 3.5, which were derived from [16]. Since the expected directive gain is not the actual directivity of the device, they are not added in the following charts.

Figure 3.4-2 compares the actual measured emissions from the tags and the DO-160E Section 21 emission limits for the measurement bands. The relevant DO-160E spurious emission limits are summarized in Table 3.4-2. Separately, Figures 3.4-3 to 3.4-7 compare to the DO-160E limits against the *individual* emissions results for tags from RF Code, Savi, Sovereign, Identec, and WhereNet. The hollow markers in the figures represent the data that were at the measurement noise floor. As a result, the data points may not represent the actual emission level, which could be lower than the values shown. It is also important to note that the lines are used in linking the data points at the markers for visual effects. Their magnitudes *between* the markers have no intrinsic values. In this first order comparison, the tags' directivities are assumed to be unity. Thus EIRP is the same as TRP.

It is noted that emissions higher than the DO-160E limits may not necessarily represent a threat to aircraft systems. Bursty emissions with very low duty cycle may present a much reduced risks compared to the continuous emissions assumed in the DO-160E limits. The amount of risk reduction may vary with the duty factor, length of transmission, modulation characteristic, and receiver designs.

It can be viewed that a device is acceptable, with respect to aircraft radio system front door interference, if its emissions levels are below the DO-160E emission limits (after considering the uncertainty associated with its directivity). Failing to meet the DO-160E emission limit, the effects of bursty transmissions on the individual system's interference thresholds should be evaluated. Operational characteristics may make many systems inherently less susceptible to the RFID type of transmission.

As an alternative to using the DO-160E emission limits, all elements of Eq. 2.3-1 may be addressed. The elements include peak emission data as reported earlier in this section, the interference path loss data of the aircraft areas where the devices are expected to be used, and the interference thresholds of the aircraft radio systems to the type of signals emitted by the device under consideration.

It is seen that many RFID tags' peak emission levels far exceed the Category L or M limits. The largest margin is 35 dB RF Code motion tags. However, it is not known if they pose interference risks without knowing the effects of bursty behaviors on the interference threshold levels.

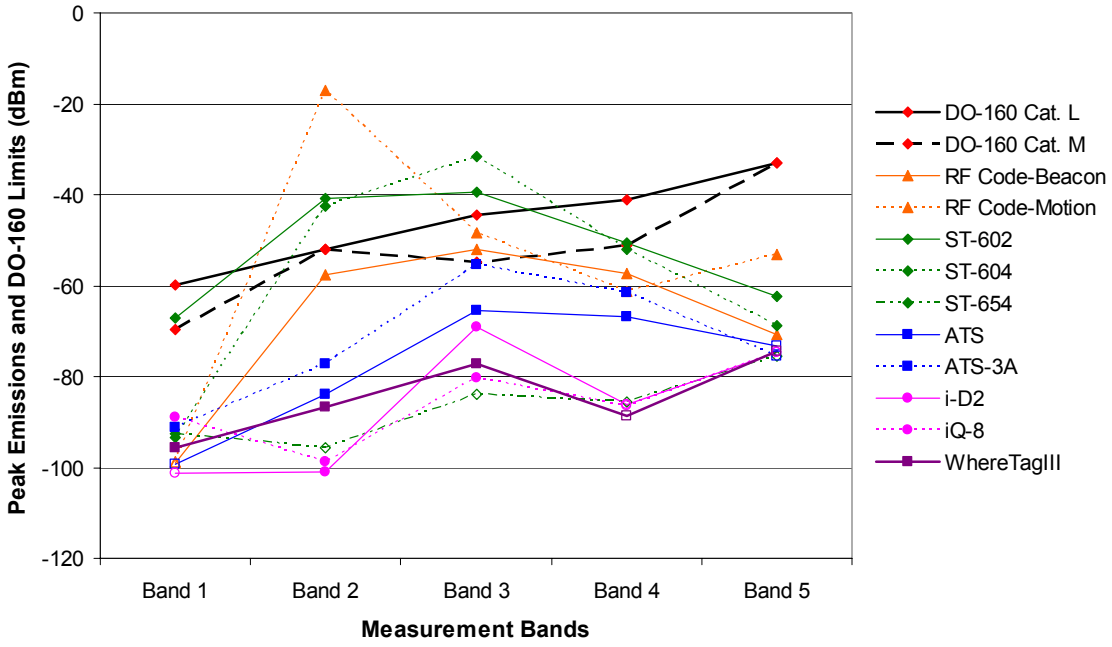

Figure 3.4-2: RFID tags emissions and comparison with RTCA/DO-160E Section 21 limits.

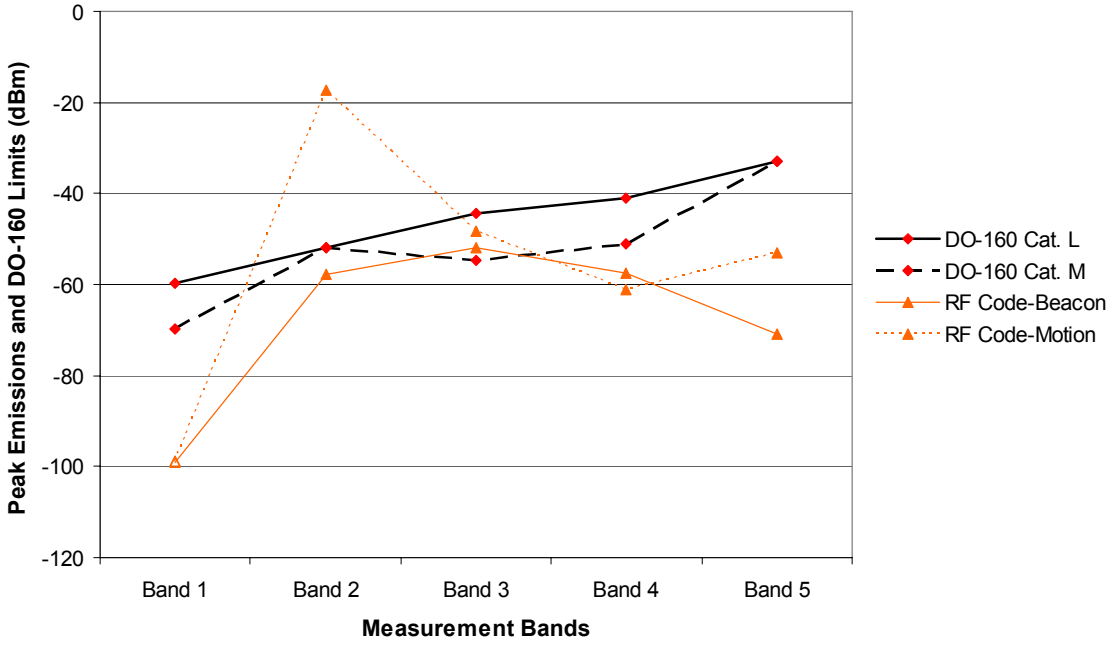

Figure 3.4-3: RF Code's beacon and motion tags peak spurious emissions.

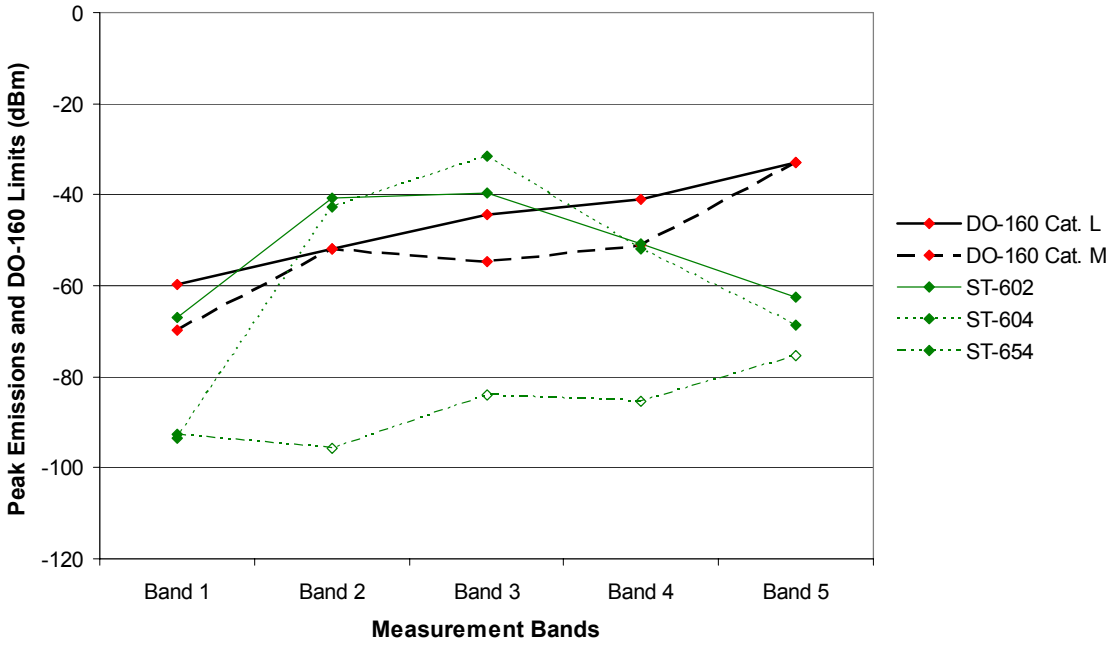

Figure 3.4-4: Savi's tags peak spurious emissions.

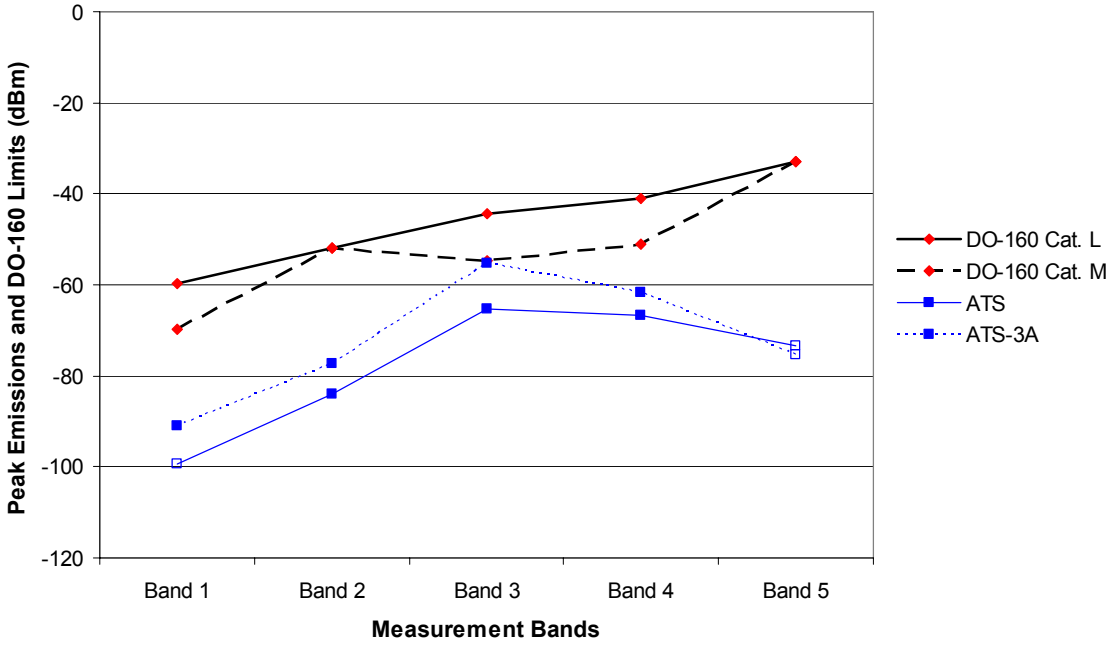

Figure 3.4-5: Sovereign's tags peak spurious emissions.

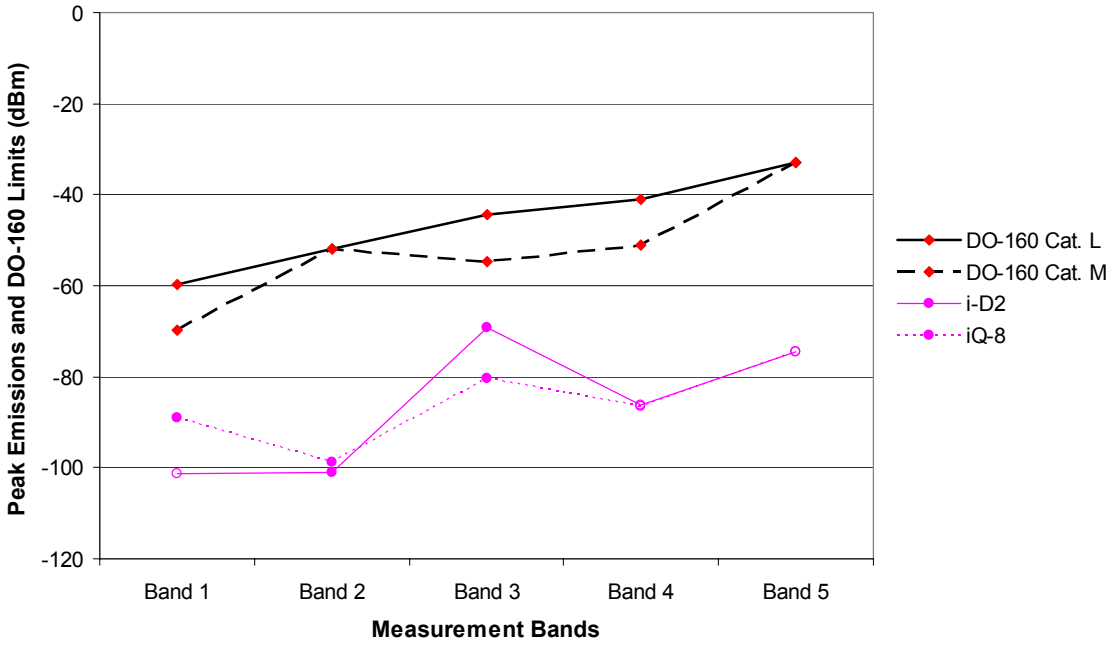

Figure 3.4-6: Identec's tags peak spurious emissions.

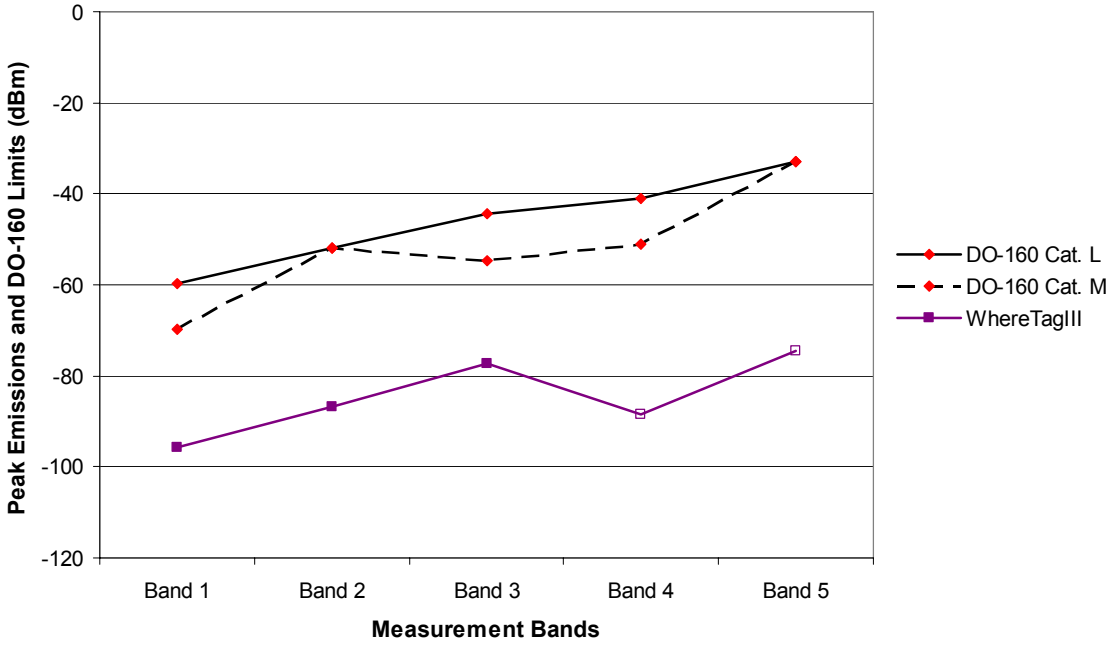

Figure 3.4-7: WhereNet's tags peak spurious emissions.

Baseline Comparison with Allowable Devices

For baseline purposes, Figure 3.4-8 shows the PEDs emissions in comparison with the DO-160E Section 21 spurious emissions limits. The PEDs include eight laptop computers and PDAs that are normally allowed during certain parts of flight. These PEDs are typically used in the passenger cabin rather than the cargo bay for the RFID tags, thus direct comparison may be inappropriate. However, for aircraft with RFID tags positioned in the passenger cabin, the comparison is more suitable. In such cases tags with lower peak emissions than PEDs' should not be of greater risk to aircraft radio receivers. In addition, the tags' intermittent transmissions may further reduce the interference risks compared to steady interference signals.

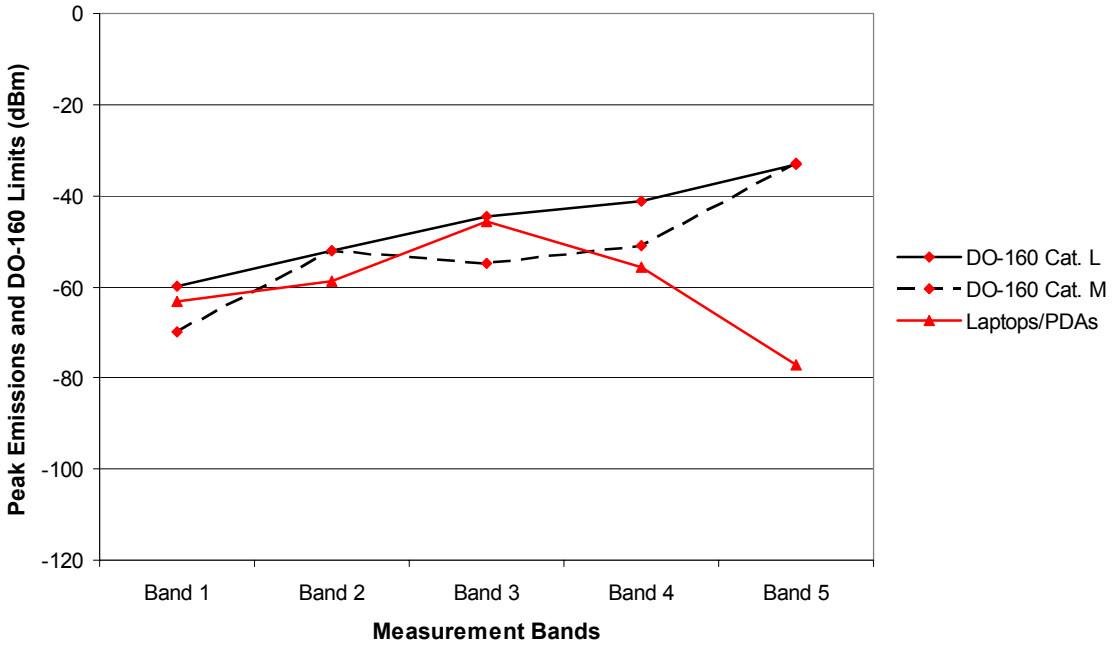

Figure 3.4-8: Laptop/PDA Emissions in comparison with RTCA/DO-160E Category L and M limits.

3.5 Device's Expected Directivity Uncertainty

The comparisons in the previous section were between the device's TRP and RTCA/DO-160E equivalent EIRP limits, assuming unity directivity. For most devices directivity is different than unity. Thus, to convert to EIRP, the device's TRP must be adjusted upward by the amount equal to the directivity of each individual device. This value can vary with frequency, device size and geometry. It is also difficult to estimate for spurious emissions due to wide frequency coverage and since the specific radiation mechanisms are often not known.

Reference [16] provides a method to estimate the expected directivity from a statistical approach. This approach was intended for estimating the directivity of non-transmitting (intentionally) devices, or directivity at spurious frequencies. It is not intended for intentional transmitters such as antennas. In the approach, the expected directivity of a device can be estimated if its maximum dimension is known.

RFID tags come in various sizes and configurations. The tested RFID tags can vary from 4 cm (about 1.6 inches) in size to the maximum of 15 cm (about 6 inches). Figures 3.5-1 and 3.5-2 show the expected directivity for devices 4 and 15 cm in the maximum dimension, using the equations developed in [16]. These figures show the results of three calculations: 1) the theoretical maximum directivity for a high gain antenna of the same size, 2) the expected directivity for a 1-planar cut measurement, and 3) expected directivity for a 3-planar cut measurement. In general, the charts show directivity is between 5 dB near 100 MHz to 6-8 dB near 5 GHz.

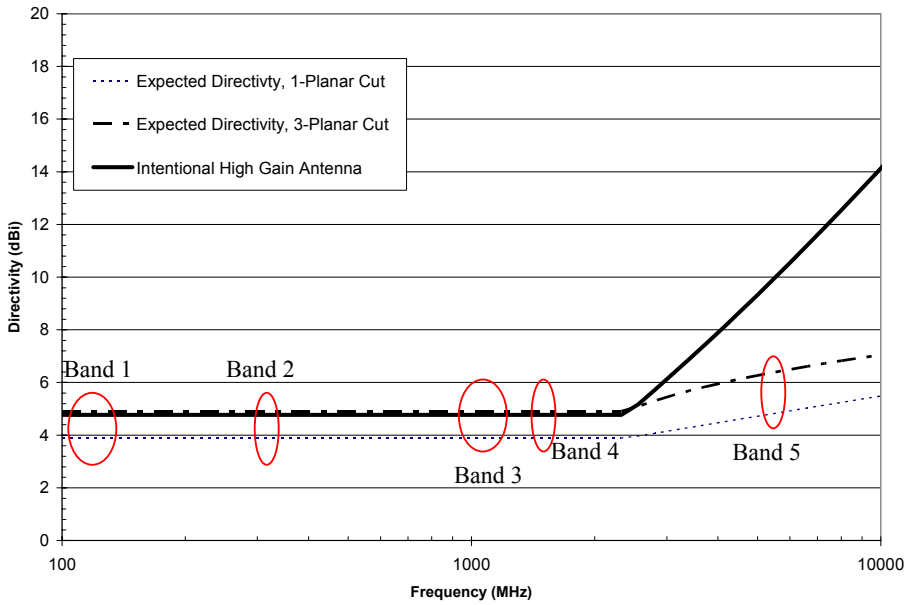

Figure 3.5-1: Expected directivity for a 4 cm (approximately 1.6 inches) unintentional transmitter.

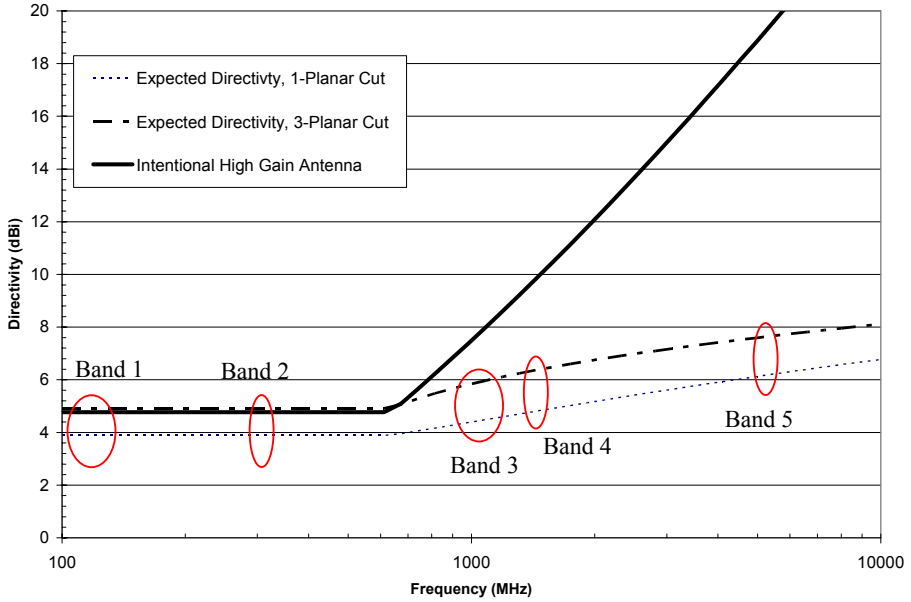

Figure 3.5-2: Expected directivity for a 15 cm (approximately 6 inches) unintentional transmitter.

4 Cargo Bay Interference Path Loss

Addressing IPL is a key element in assessing RFID interference risks to aircraft. IPL is a measurement of propagation loss between the interference source and an aircraft victim system. The victim systems considered include the highly sensitive antenna ports of aircraft communication and navigation equipment.

Unlike the earlier efforts dealing with devices located in the passenger cabin [3][4][5], RFID tags are normally attached to cargos located in the cargo bays. As a result the existing passenger cabin IPL may be inappropriate for the analysis. It is a goal to measure the cargo bay IPL.

Under a joint effort between United Airlines, Eagle Wings Inc., NASA, and the FAA, IPL measurements were performed on several B747-422 and A320-232 aircraft. During two one-week efforts at a United Airlines' facility, IPL for various combinations of aircraft interference source locations and victim aircraft radio antennas were measured. The victim aircraft systems considered include LOC, GS, VHF, DME, ATCRBS and GPS. The interference source locations include passenger cabins, cockpits, avionic bays, and cargo bays. The measured cargo bay data are reported in this section, and are useful for assessing interference risks of RFID devices.

The measurements were performed over the operating frequency bands of the aircraft receivers similar to the earlier efforts reported in [2][3]. The collected data are reported as "narrow-band" IPL data.

"Wide-band" IPL measurements were also conducted by performing wide-band frequency sweeps over the two bands: 100 MHz to 1 GHz, and 1 GHz to 3 GHz. These bands aligned with the frequency ranges of the antenna used. By taking wide-band sweeps the data automatically account for the aircraft radio bands under consideration. In addition, the bands also include many frequencies used by intentional transmitting PEDs such as wireless phones, wireless LAN devices, RFID tags, and others. Knowing the IPL at wireless PEDs frequencies may be useful in assessing the effects PEDs frequency on front door interference.

Care must be taken in analyzing the wide-band IPL data as the measurements normally contain components of strong ambient transmissions. Proper analysis may require careful and selective rejection of undesired ambient signals that typically appear as narrow peaks in the data. The wide-band results are not discussed here as the process is still being evaluated.

The data are available to all participating parties. However, only a part of the data collected are currently processed. Of particular interest to this RFID effort are the cargo bay IPL data reported in this section.

4.1 Measurement Process

Figure 4.1-1 illustrates the representative coupling paths between the cargo doors and a top-mounted antenna. For lower frequencies, earlier studies [3] indicate strong RF leakage through the aircraft doors. There could be additional coupling paths not shown. Since the material separating the passenger cabin and the cargo bays is not completely metal, RF energy could propagate from the cargo bays to the passenger cabin and out the windows to the aircraft antennas. In addition, there are several aircraft antennas located on the bottom of the fuselage. Their locations may be closer to the cargo doors, resulting in stronger coupling with interference sources inside.

Figure 4.1-2 illustrates a typical IPL measurement setup. A known level of RF is radiated from the transmit antenna, while a spectrum analyzer is used to measure the level coupled into the aircraft antenna. The difference between the transmitted power and the measured power, in dB, is the interference path loss between the two locations. Typically, multiple transmit antenna locations and polarizations are used and the minimum loss value of all the measurement represents the minimum IPL for that setup.

In Figure 4.1-2, IPL is defined to be the ratio, or the difference in dB, between the power radiated from the transmit antenna at location (1) to the power received at location (2). For GPS, IPL is defined to be the difference in power between location (1) and (3). Or,

$$IPL = P^{T}_{(1)} - P^{R}_{(2)} \quad \text{for most systems, and} \qquad \text{(Eq. 4.1-1)}$$

$$IPL = P^{T}_{(1)} - P^{R}_{(3)} \quad \text{for GPS,} \qquad \text{(Eq. 4.1-2)}$$

where $P^{T}_{(1)}$ is power transmitted at point (1), and $P^{R}_{(2)}$, and $P^{R}_{(3)}$ are power received at points (2) and (3), in dBm, respectively.

The transmit antennas typically include dipoles for frequencies in the GS band and below, and a dual-ridge horn antenna for the frequencies in the TCAS band and above. In this effort a small and inefficient bi-conical antenna was used for the GS band and below. This antenna was preferable over a dipole antenna due to its wide-band characteristics and small size. However, due to its inefficiency a gain correction factor must be applied to the measurement data for comparability with the dipole measurement. Similar gain correction is applied to the measurement using the dual-ridge horn antenna using the gain data provided by the manufacturer. This process had been demonstrated in previous IPL measurements.

Figures 4.1-3 to 4.1-9 show the measurements conducted for the cargo bay path loss on a B747 and an A320 aircraft. As previously discussed, this measurement was a part of a larger effort between UAL, EWI, NASA and the FAA to address various interference issues. The work of this larger effort is not yet concluded.

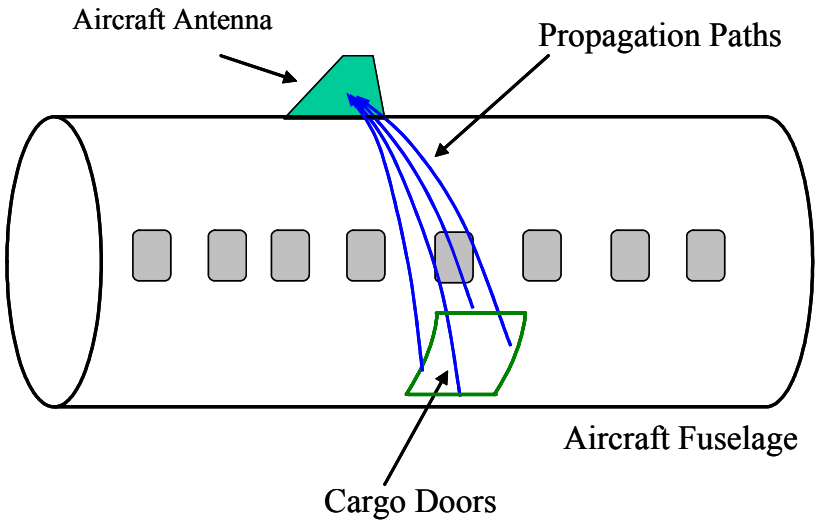

Figure 4.1-1: Representative main IPL coupling paths for a top-mounted aircraft antenna.

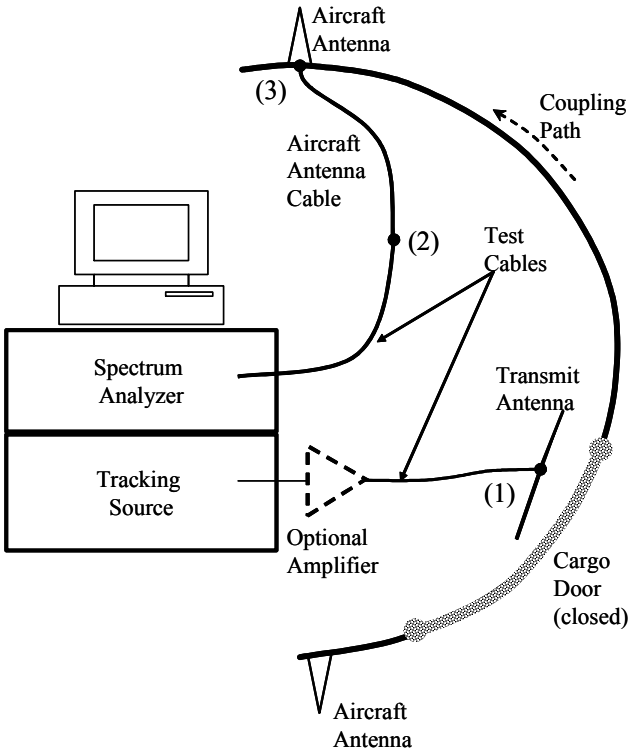

Figure 4.1-2: Typical set-up for cargo-bay excitation and a top-mounted aircraft antenna.

Figure 4.1-3: A B747-422 aircraft used in the IPL measurements.

Figure 4.1-4: B747-422 aircraft front cargo-bay interior.

Figure 4.1-5: Data acquisition instrument and computer.

Figure 4.1-6: Scanning the transmit antenna along cargo door seam of a B747-422 aircraft.

Figure 4.1-7: B747-422 aircraft rear cargo bay.

Figure 4.1-8: An A320-232 aircraft used in the IPL measurements.

Figure 4.1-9: A320-232 aircraft rear cargo door in close proximity to VHF-3 antenna.

4.2 Interference Path Loss Results

In previous passenger cabin IPL measurements [3] coupling paths typically include leakage through the windows and doors seams. The strongest coupling locations are typically near windows and doors, especially those closest to the system antenna in consideration. For cargo bay IPL the most obvious leakage is through the door seam. Thus the IPL measurement typically includes scanning the transmit antenna (simulating a PED source) along the door seam in two polarizations.

It is also important to note that there are other possible leakage locations. RF in the cargo bay may propagate through the mostly non-conducting ceiling into the passenger cabin before leaking through windows and door seams. The passenger seats (and the embedded metal structures) may provide limited

blockage against direct line-of-sight between the cargo bay and the windows. However, it is expected that the energy leaked into the passenger cabin contributes significantly to the IPL value.

The large volumes of the cargo bays were divided into zones for ease of measurement. The forward cargo bay of the B747 aircraft was divided into six zones, whereas the smaller rear cargo bays of a B747 and of the A320 aircraft were divided into four or two zones depending on the volume. IPL measurements were performed with the transmit antenna scanned volumetrically within each of the zones in three polarizations, and the peak coupling values were recorded for each zone. This volumetric scanning ensures coupling paths through the passenger cabin are accounted for. In addition, the transmit antenna was also scanned along the cargo bay doors in two polarizations as previously mentioned.

The data were processed according to Section 4.1. The data were also corrected for the antenna gain of the transmit antennas used, which include a bi-conical antenna for frequencies up to GS, and a dual ridge horn antenna for frequencies above 960 MHz. The antenna gain correction was performed so that the results represent the IPL associated with a half-wave dipole transmit source.

The minimum IPL value for all zone and door scans are reported in the following Table 4.2-1 for different systems and cargo bay combinations. Also reported are the specific aircraft on which the specific measurements were performed. Of the systems measured many have their maximum coupling factors (minimum IPL) through volumetric scans. This indicates that the door may not be the only means to couple interference signals to the aircraft antennas located outside the aircraft. Volumetric scans may be necessary for achieving maximum coupling factors.

Table 4.2-1: Cargo Bay Interference Path Loss in dB

Systems	B747-422 Aircraft		A320-232 Aircraft	
	Forward Cargo Bay	Aft-Cargo Bay	Forward Cargo Bay	Aft-Cargo Bay
LOC	48.7 {c}	55.1 {c}	53.4 {e}	62.5 {e}
VHF-1 (L)	46.5 {a}	45.5 {a}	*	*
VHF-2 (R)	37.2 {b}	51.8 {a}	*	*
VHF-3 (C)	*	28.7 {c}	54.2 {e}	60.6 {e}
GS	59.2 {c}	99.2 {c}	69.9 {d}	73.7 {d}
DME-1	68.8 {b}	67.6 {b}	65.9 {d}	77.6 {d}
ATC-Top	75.6 {a}	72.4 {a}	78.2 {f}	73.4 {f}
ATC-Bottom	*	*	53.7 {f}	71.3 {f}
GPS-1	74.6 {a}	78.6 {a}	67.1 {d}	71.0 {d}

* Data not measured

The following designations relate the data set to the actual aircraft on which the measurements were performed for the specific communication or navigation systems.

{a} B747-N196UA

{b} B747-N198UA

{c} B747-N104UA

{d} A320-N477UA

{e} A320-N493UA

{f} A320-N481UA

5 Receiver Interference Thresholds

The interference thresholds to continuous or noise-like interference signals have been previously reported in RTCA/DO-199 and DO-233. The most recent data were released in RTCA/DO-294. A new revision to DO-294 is planned and should be more complete. As previously discussed, typical interference threshold to a continuous signal may not be appropriate for the bursty RFID signals. A study has been commissioned to address the issue by extending the work reported in DO-294. It is expected that thresholds for continuous interference signal will be modified according to frequency, duty factor, and/or burst length. Many aircraft systems operate such that the low duty factor may not have an effect on normal operations.

6 Summary and Conclusions

Emission measurements were conducted on multiple active RFID devices. The measurements were performed at various aircraft radio bands. The results show that many tags' peak total radiated power exceeded RTCA/DO-160E Categories L and M *EIRP* emission limits, even with assuming unity device directivity. One of the RFID tags exceeded RTCA/DO-160E Categories L and M limits by as much as 35 dB in the GS band. Adding device directivity would make the *EIRP* even higher. However, it is not known if the high emission would cause interference risk. Consideration for the bursty nature of the tags and the effects on receiver operation should be made in determining the interference risk.

Emissions may be different even for the same tags of the same design and make. As a result, it is believed that performing measurements with multiple tags concurrently may provide an upper-bound on results. There is a possibility of having summing effects caused by multiple devices. The probability is small due to the very low duty factor. For two devices contributing equally at the receiver, the multiple equipment factor is only 3 dB. The chance of three or more devices transmitting concurrently and contributing equally at the receiver is much smaller.

Passenger aircraft cargo-bay IPL data were measured for two aircraft, a B747 and an A320 models. Various aircraft radio systems were considered. The data vary depending on the location of the aircraft antenna and whether the front or aft-cargo bays were considered for each aircraft. The highest cargo-bay coupling measurement resulted in 28.7 dB IPL between the aft-cargo bay and VHF-3 antenna for a B747 aircraft.

7 Recommended Future Work

Aircraft radio receiver interference thresholds to intermittent (bursty) interference signals should be addressed. In addition to the reported passenger aircraft's cargo bay, cargo aircraft IPL should be measured. Cargo aircraft are expected to have the greater need in dealing with active RFID devices due to the number of cargo containers they can hold.

This report does not address the possibility that high-level RF signals, such as those emitted from an aircraft TCAS interrogator, DME or VHF radio, may cause non-linear responses from active or passive

RFID tags. The potential for such responses should be considered if RFID tags are to be approved for routine use on-board aircraft.

9 References

[1] RTCA Inc., *http://www.rtca.org/*

[2] RTCA/DO-294, *Guidance on Allowing Transmitting Portable Electronic Devices (T-PEDs) on Aircraft*, October 19, 2004.

[3] Nguyen, T. X.; Koppen, S. V.; Ely, J. J.; Williams R. A.; Smith, L. J., and Salud, M. T.: *Portable Wireless LAN Device and Two-Way Radio Threat Assessment for Aircraft Navigation Radios,* NASA/TP-2003-212438, July 2003.

[4] Ely, J. J.; Nguyen T. X.; Koppen, S. V.; Salud, M. T.; and Beggs J. H.: *Wireless Phone Threat Assessment and New Wireless Technology Concerns for Aircraft Navigation Radios*, NASA/TP-2003-212446, July 2003.

[5] Nguyen, T. X.; Koppen, S. V.; Smith, L. J.; Williams R. A.; and Salud, M. T.: *Third Generation Wireless Phone Threat Assessment for Aircraft Communication and Navigation Radios,* NASA/TP-2005-213537, March 2005.

[6] RTCA/DO-199, *Potential Interference to Aircraft Electronic Equipment from Devices Carried Aboard*, September 16, 1988.

[7] RTCA DO-233, *Portable Electronic Devices Carried On Board Aircraft*, Prepared by SC-177, August 20, 1996.

[8] Hill, David A.: *Electromagnetic Theory of Reverberation Chambers*, Chapter 4, Technical Note 1506, National Institute of Standards and Technology, December 1998.

[9] 47CFR Ch. 1, Part 15, "Radiated Emission Limits", *US Code of Federal Regulations,* Federal Register dated December 19, 2001.

[10] Ladbury, J.; Koepke, G.; and Camell, D.: *Evaluation of the NASA Langley Research Center Mode-Stirred Chamber Facility*, NIST Technical Note 1508, January 1998.

[11] Crawford, M. L.; and Koepke, G. H.: *Design, Evaluation, and Use of a Reverberation Chamber for Performing Electromagnetic Susceptibility/Vulnerability Measurements*, NBS Technical Note 1092, U. S. Department of Commerce/National Bureau of Standards, April 1986.

[12] RTCA/DO-160E, Section 20 "Radio Frequency Susceptibility (Radiated and Conducted)", *Environmental Conditions and Test Procedures for Airborne Equipment*, Prepared by SC-135, December 9, 2004.

[13] International Electrotechnical Commission (IEC) 61000-4-21, 2003 (Draft).

[14] *http://www.aphena.com/softplot.htm*

[15] RTCA/DO-160E, Section 21 "Emission of Radio Frequency Energy", *Environmental Conditions and Test Procedures for Airborne Equipment*, Prepared by SC-135, December 9, 2004.

[16] Koepke, G.; Hill, D.; and Ladbury, J.: "Directivity of the Test Device in EMC Measurements", *2000 IEEE International Symposium on Electromagnetic Compatibility*, Aug. 21-25, 2000.

Appendix A: Baseline Emissions from Standard Laptop Computers and PDA

Emission measurement results from several laptop computers, PDAs and a portable printer (PRN) are used as a baseline for devices currently allowed in the passenger cabin of an aircraft. The measurements were performed and reported in earlier efforts [2][3]. While the emissions from the RFID devices and the laptop computers should not be directly compared due to the different use location, the data presented in this appendix may provide readers with base lines of emissions currently considered acceptable on an aircraft.

Measurements of the PEDs emissions were performed in all five test bands similar to the RFID testing reported in the main section. However, the 105-140 MHz band was divided into two separate bands, called Band 1 and Band 1a. Band 1 covers from 105 to 120 MHz, and the results were reported in [2]. Band 1a covers 116 to 140 MHz, with the results first reported in [2]-[3]. Since this current report combines the old Band 1 and Band 1a into a new band, named Band 1, the PEDs emission data in the new Band 1 are shown in two separate charts.

The PEDs tested are listed in Table A-1. The test modes and the measurement results are described in the following sub-sections.

Table A-1: Laptop Computers, PDA, and Portable Printer Models

Host Designation	Manufacturer	Model
LAP1	Dell	Latitude C640
LAP2	Hewlett Packard	Pavilion n6395
LAP3	Sony Vaio & Dock	PCG-641R PCGA-DSM51
LAP4	Dell	Latitude C800
LAP5	Fujitsu	Lifebook
LAP6	Panasonic	Toughbook CF-47
LAP7	Fujitsu	Lifebook CP109733
LAP8	Gateway	450SX4
PDA1	Palm	m515
PDA2	Toshiba	e740
PRN	Hewlett Packard	DeskJet 350

A.1 Laptop Computer Test Modes

Spurious radiated emissions were recorded for eight laptop computers, each operating in five modes. Operating modes, or processing tasks that may be performed by a laptop, include: idle, screensaver, file transferring, CD playing, and DVD playing. Radiated emissions from the modes were measured separately. The overall maximum emission envelope across the band of all operating modes is termed as the radiated peak envelope of the laptop.

The PED devices were measured using the same facility and instruments. However, the PED emissions were measured with 1) a different pre-amplifier in the receive path, 2) an equipment operator in the chamber, and 3) without measurement path filters. These differences may affect the measurement

noise floor, but should not affect the emission results since they are accounted for in the calibration. Different laptop computer operating modes are explained below:

- Idle: Idle mode testing is conducted as a normal desktop screen is displayed.
- Screensaver: The flowerbox screensaver was selected to be a large, smooth, checkerboard cube pattern that spins and blooms at maximum complexity. This selection is a simple way to simulate computationally intensive operations.
- File Transfer: This mode includes transferring files from the hard drive to the Personal Computer (PC) Card hard drive, which is well shielded with all metal casing.
- CD Playing: The computer plays a music CD, exercising the audio circuitry.
- DVD Playing: The computer plays a movie DVD, exercising the video system.

A.2 PDA and Printer Test Modes

A PDA baseline consisted of the idle and file-transfer modes. File transfer was performing a backup operation to a secure digital or compact flash card. The printer testing consisted of the idle mode with the unit powered on.

A.3 PED Emission Results

The following charts report the PED data envelopes, with each chart containing plots of all individual PED envelopes. Each individual PED envelope was generated from the measured emissions data, including idle mode and all other PED test modes discussed earlier. The charts also show composite maximum envelopes that represent the highest emission level of all devices at any given frequency.

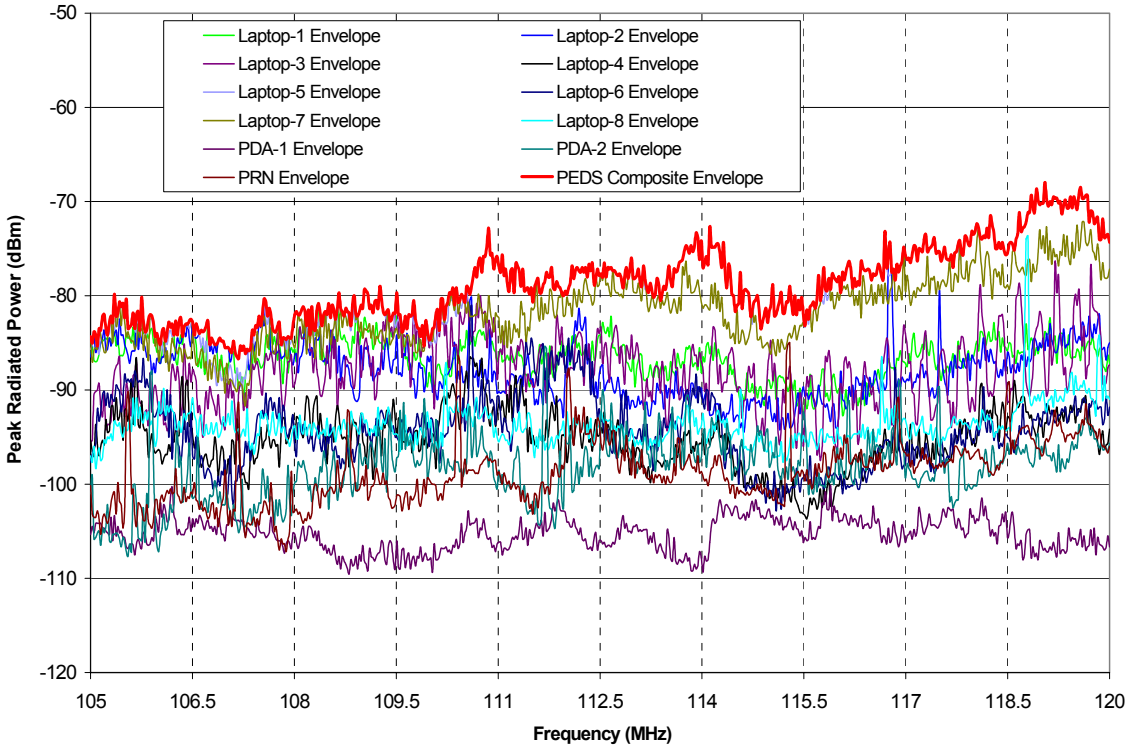

Figure A.3-1: Individual PED Envelopes and PEDS Composite Envelope for Band 1a (105 MHz to 120 MHz).

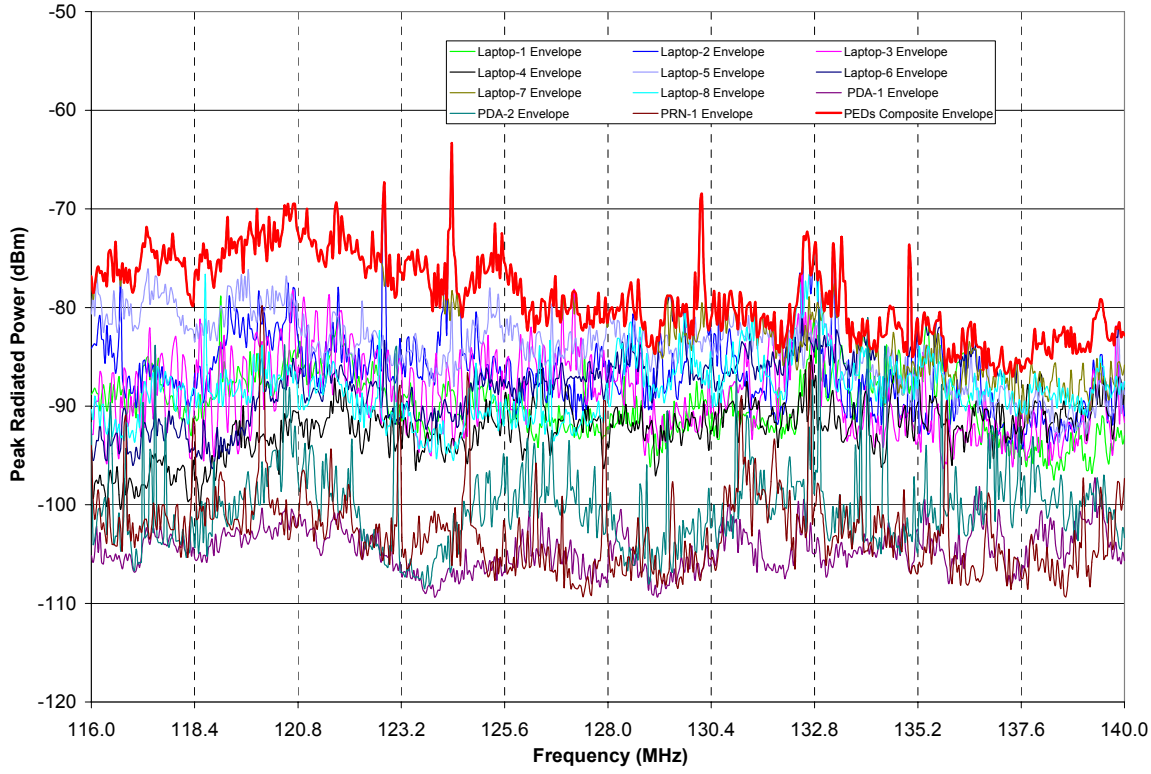

Figure A.3-2: Individual PED Envelopes and PEDs Composite Envelope for Band 1b (116 MHz to 140 MHz).

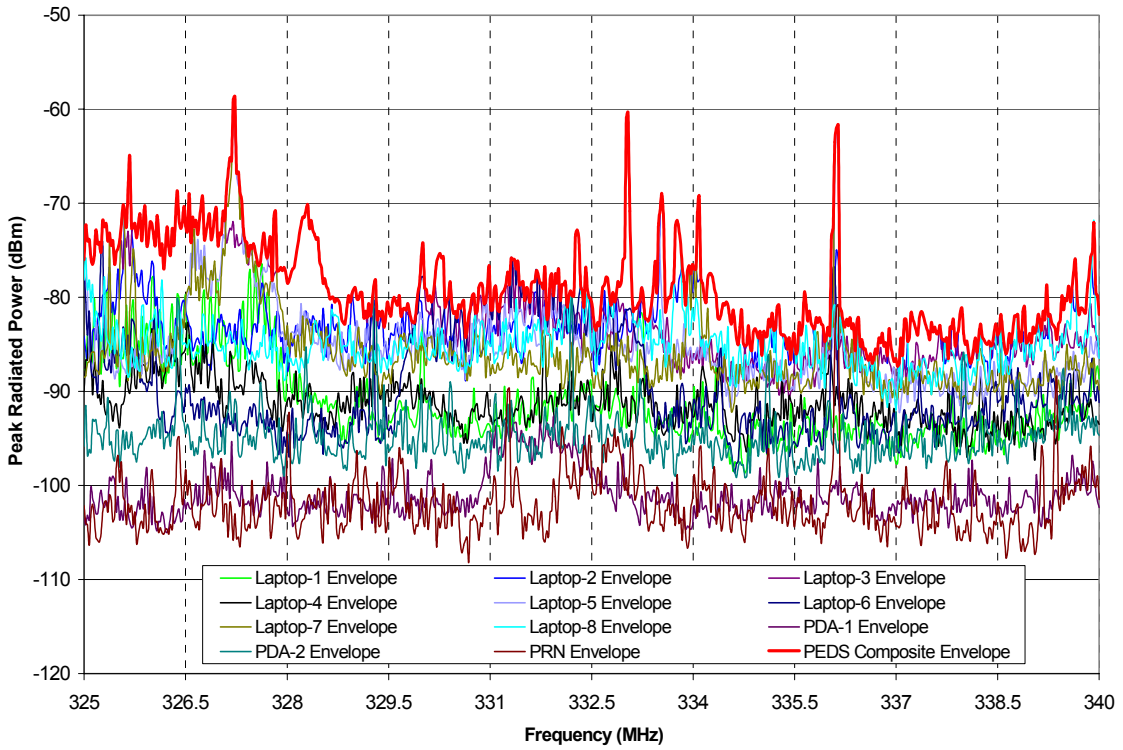

Figure A.3-3: Individual PED Envelopes and PEDS Composite Envelope for Band 2.

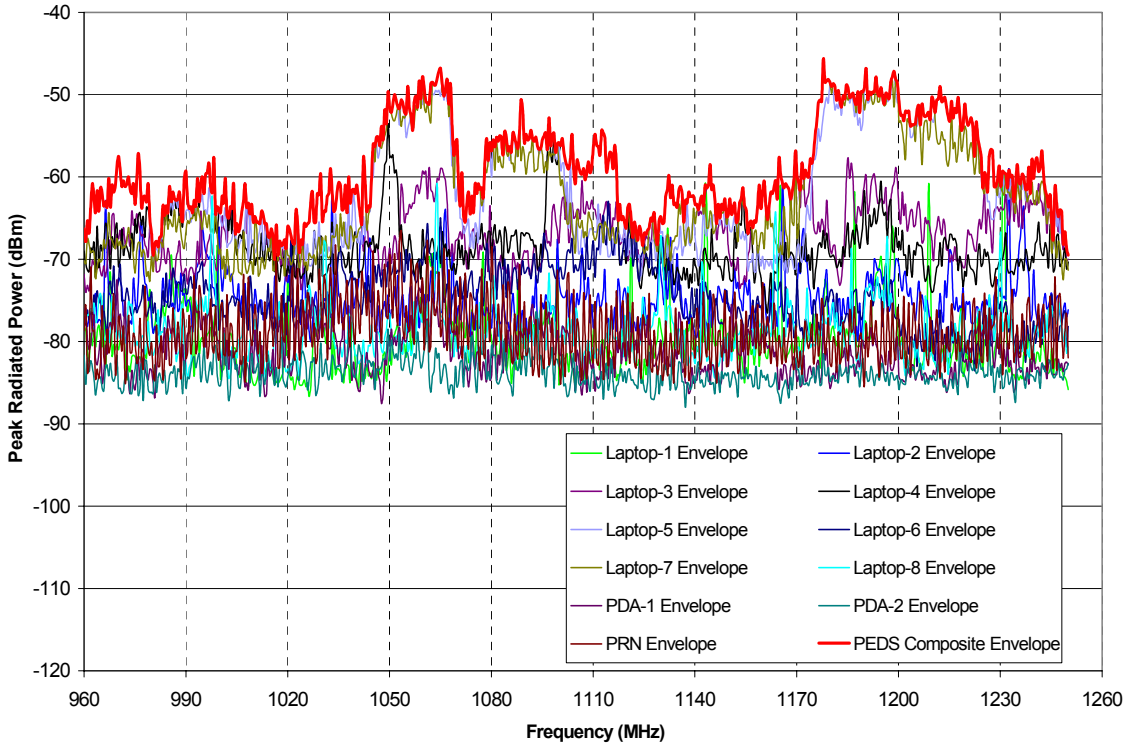

Figure A.3-4: Individual PED Envelopes and PEDS Composite Envelope for Band 3.

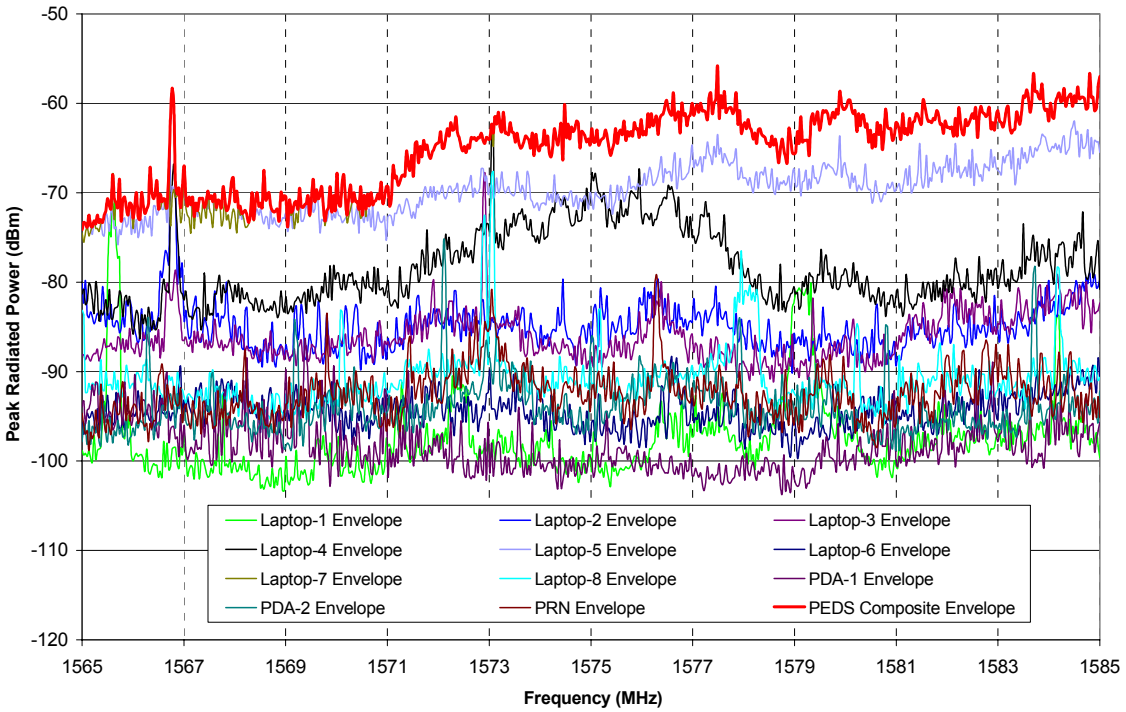

Figure A.3-5: Individual PED Envelopes and PEDS Composite Envelope for Band 4.

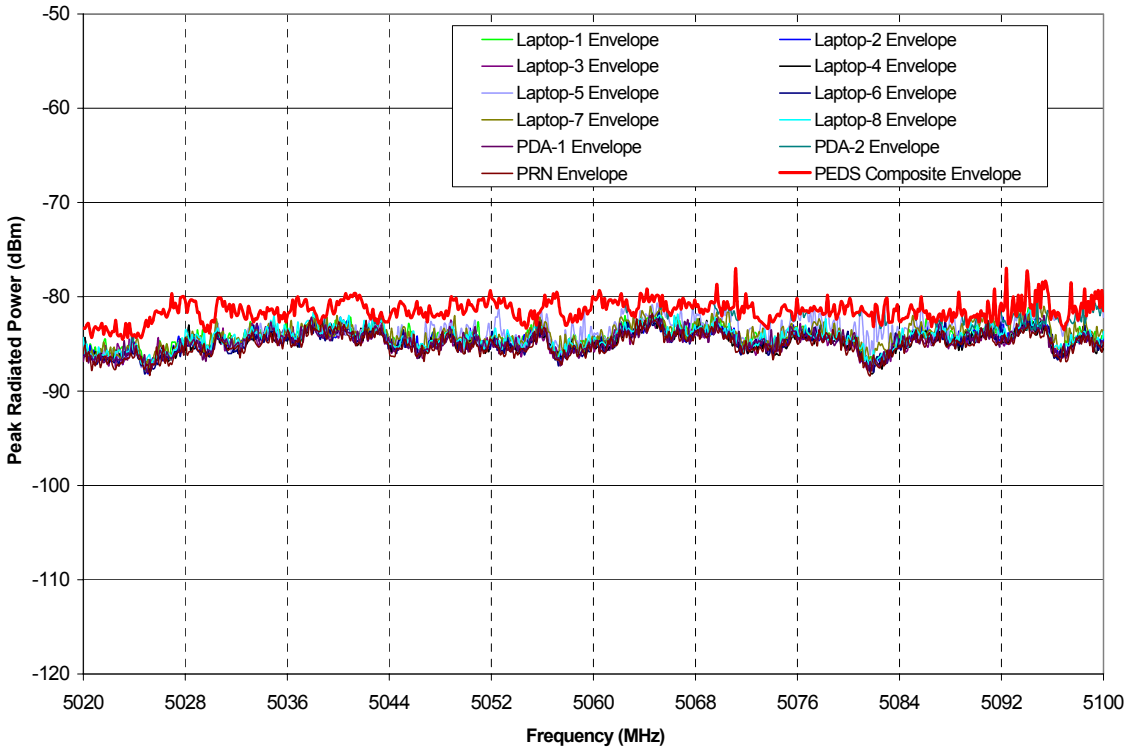

Figure A.3-6: Individual PED Envelopes and PEDS Composite Envelope for Band 5.

A.4 Summary of Maximum Emissions from Laptop Computers and PDAs

Table A.4-1 summarizes maximum emission results reported in the Appendix A, along with the potentially affected aircraft radio bands. Graphical representations of the data are shown in Figure 3.4-8 in the main section.

Table A.4-1: Maximum Emission from Laptop Compupters and PDA in Aircraft Bands (in dBm)

Measurement Band	Frequency (MHz)	Baseline Laptops PDAs Peak Emissions (dBm)	Aircraft Bands
Band 1	105 - 140	-63.3	LOC, VOR, VHF-Com
Band 2	325 - 340	-58.7	GS
Band 3	960 - 1250	-45.7	TCAS, DME, GPS L2
Band 4	1565 -1585	-55.8	GPS L1
Band 5	5020 - 5100	-77.0	MLS

Appendix B: Alternative Test Method for Savi Tags

One back-up approach involves physically moving the tags in and out of the coverage zone of an interrogator. Typically the tags blink upon entering the interrogator coverage area and would not blink again as long as the same interrogator is sensed. Physically moving the tags in and out of the interrogator coverage area simulates leaving and re-entering the coverage zone, thereby causing the tags to blink again.

An apparatus was built to rotate the tags one at a time in and out of the interrogator field. The apparatus incorporated an electrically shielded motor rotating about two dozen non-conducting arms. The tags were attached at the end of each arm as shown in Figure B-1. The tags blinked approximately every 2 seconds at the fastest rate, thus the motor rate was one rotation every two seconds.

Figure B-1 also illustrates multiple tags mounted on the motor assembly for simultaneous testing. Simultaneous testing of multiple tags helps overcome slow blink rate and reduce measurement time.

The back-up approach worked very well. However, it was more complicated than testing beacon tags. The motor assembly must be shielded. The interrogator ferrite rod antennas had to be disassembled to be positioned inside the test chamber. Low pass filters were used between the interrogator and its antenna to block the interrogator's spurious emissions from entering the test chamber. Figure B-2 shows the antenna detached from the interrogator.

In another alternative approach the connection to the interrogator antenna inside the test chamber was electrically switched on/off using a switch or relay driven by a function generator. This set-up simulated the tags entering and exiting the interrogator field. Similar to the previous alternate approach, the interrogator antenna had to be disconnected from the interrogator for installation near the tags inside the test chamber. Low pass filters on the antenna cables were also used to avoid spurious emissions from the interrogator. The shielded motor assembly was not needed in this set up.

The disadvantage of this setup was it may cause multiple tags to blink simultaneously. Simultaneous blinking of many tags may cause power summing at the measurement equipment, resulting in increased uncertainty caused by MEF.

These alternative plans illustrate the increased complication if the programming software were not available. For this testing, the proprietary programming software was supplied by the vendor, greatly improving test efficiency and simplicity.

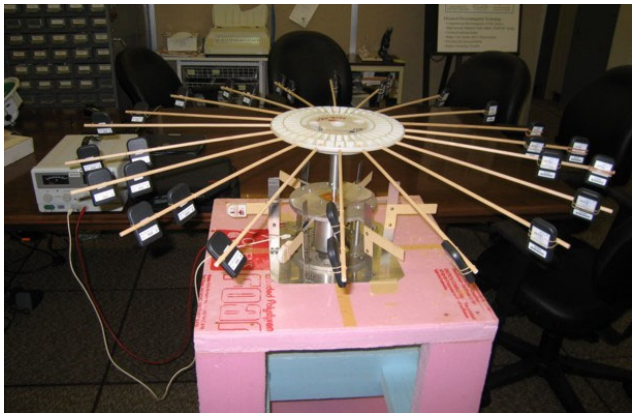

Figure B-1: An apparatus for rotating the tags in and out of the interrogator's field.

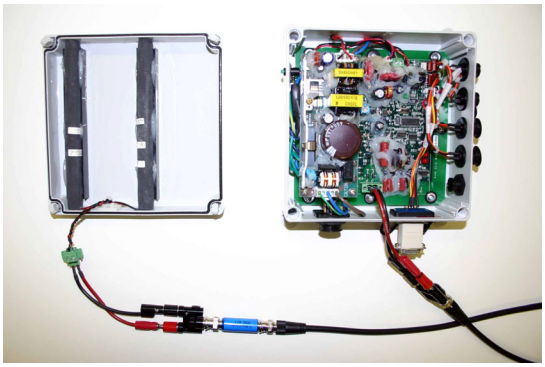

Figure B-2: Ferrite rod antenna attached to inside of lid on the Savi's interrogator

REPORT DOCUMENTATION PAGE

Form Approved
OMB No. 0704-0188

1. REPORT DATE *(DD-MM-YYYY)*	2. REPORT TYPE	3. DATES COVERED *(From - To)*
01- 03 - 2006	Technical Publication	

4. TITLE AND SUBTITLE

RFID Transponders' Radio Frequency Emissions in Aircraft Communication and Navigation Radio Bands

5a. CONTRACT NUMBER

5b. GRANT NUMBER

5c. PROGRAM ELEMENT NUMBER

6. AUTHOR(S)

Nguyen, Truong X; Ely, Jay J.; Williams, Reuben A.; Koppen, Sandra V.; and Salud, Maria Theresa P.

5d. PROJECT NUMBER

5e. TASK NUMBER

5f. WORK UNIT NUMBER

23R-079-30-9D11-01

7. PERFORMING ORGANIZATION NAME(S) AND ADDRESS(ES)

NASA Langley Research Center
Hampton, VA 23681-2199

8. PERFORMING ORGANIZATION REPORT NUMBER

L-19243

9. SPONSORING/MONITORING AGENCY NAME(S) AND ADDRESS(ES)

National Aeronautics and Space Administration
Washington, DC 20546-0001

10. SPONSOR/MONITOR'S ACRONYM(S)

NASA

11. SPONSOR/MONITOR'S REPORT NUMBER(S)

NASA/TP-2006-214295

12. DISTRIBUTION/AVAILABILITY STATEMENT

Unclassified - Unlimited
Subject Category 04
Availability: NASA CASI (301) 621-0390

13. SUPPLEMENTARY NOTES

An electronic version can be found at http://ntrs.nasa.gov

14. ABSTRACT

Radiated emissions in aircraft communication and navigation bands are measured from several active radio frequency identification (RFID) tags. The individual tags are different in design and operations. They may also operate in different frequency bands. The process for measuring the emissions is discussed, and includes tag interrogation, reverberation chamber testing, and instrument settings selection. The measurement results are described and compared against aircraft emission limits. In addition, interference path loss for the cargo bays of passenger aircraft is measured. Cargo bay path loss is more appropriate for RFID tags than passenger cabin path loss. The path loss data are reported for several aircraft radio systems on a Boeing 747 and an Airbus A320.

15. SUBJECT TERMS

Aircraft; Cargo Bay; Communication; Interference; Interference Path Loss; Navigation; RFID; Radiated Emissions; Reverberation Chamber

16. SECURITY CLASSIFICATION OF:			17. LIMITATION OF ABSTRACT	18. NUMBER OF PAGES	19a. NAME OF RESPONSIBLE PERSON
a. REPORT	b. ABSTRACT	c. THIS PAGE			STI Help Desk (email: help@sti.nasa.gov)
					19b. TELEPHONE NUMBER *(Include area code)*
U	U	U	UU	85	(301) 621-0390